Universitat de Girona

DEVELOPMENT OF THREE-DIMENSIONAL ELECTROCHEMICAL SYSTEMS FOR THE DEGRADATION OF PERSISTENT CONTAMINANTS AND DISINFECTION

Giannis-Florjan Norra

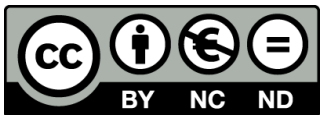

Universitat de Girona

DOCTORAL THESIS

DEVELOPMENT OF THREE-DIMENSIONAL ELECTROCHEMICAL SYSTEMS FOR THE DEGRADATION OF PERSISTENT CONTAMINANTS AND DISINFECTION

Giannis-Florjan Norra

2024

DOCTORAL THESIS

DEVELOPMENT OF THREE-DIMENSIONAL ELECTROCHEMICAL SYSTEMS FOR THE DEGRADATION OF PERSISTENT CONTAMINANTS AND DISINFECTION

Giannis-Florjan Norra

2024

Water Science and Technology Doctoral Programme

School of Doctoral Studies, University of Girona

UdG Code: u1969592

Supervised by: Jelena Radjenovic

Tutor: Joaquim Comas Matas

Presented to obtain the degree of PhD at the University of Girona

Acknowledgments

«Την άνοιξη αν δεν την βρεις την φτιάχνεις»

First, I would like to thank Prof. Jelena Radjenovic for granting me the opportunity to pursue this PhD. I am thankful her for her scientific guidance and support throughout these years, as well as her contribution to the elaboration of the scientific publications and the current thesis. I would also like to thank Prof. Carles Borrego for his contribution to an important part of the thesis as well as Prof. Quim Comas for accepting to be my tutor. I would also like to express my sincere gratitude to Dr. Luis Baptista Pires for his great support and mentorship during his stay in ICRA, without whom I would not be able to finish the thesis. Special appreciation goes out to all the wonderful people of the E4W group, with whom I spend countless hours in the lab and had an excellent collaboration. Their support on both emotional and practical level has been invaluable. Furthermore, I would like to acknowledge all the people at ICRA whom I had the pleasure of crossing paths with. From the technicians, who facilitated our work, to every student, employee, and cleaning staff with whom we shared some moments together. You all contributed to making my experience at ICRA truly enriching. I am not mentioning specific names here to avoid unintentional exclusions, but I trust that these people will recognize themselves in these words. Last but not least, I am deeply grateful to my family for their unconditional support and love throughout these years, and I dedicate this thesis to them.

Tabla de contenido

List of publications

The results of this PhD thesis, presented as chapters herein, have been published in the scientific journals as follows:

Norra, G.F., Radjenovic, J., 2021. Removal of persistent organic contaminants from wastewater using a hybrid electrochemical-granular activated carbon (GAC) system. J. Hazard. Mater. 415, 125557. https://doi.org/10.1016/j.jhazmat.2021.125557

Norra, G.F., Baptista-Pires, L., Cuervo Lumbaque, E., Borrego, C.M., Radjenovic, J., 2022. Chlorine-free electrochemical disinfection using graphene sponge electrodes. Chem. Eng. J. 430, 132772. https://doi.org/10.1016/j.cej.2021.132772

Patent: Method to prepare a graphene coated sponge-based electrode, electrode obtained thereof and use of the electrode for water treatment. J. Radjenovic, L Baptista-Pires, G.F. Norra, N. Duinslaeger, WO2022069621A1.

List of acronyms

2D	Two Dimensional
3D	Three Dimensional
A-C	Anode-Cathode
ADS	Adsorption
AOCl	Adsorbable Organic Chloride
AOI	Adsorbable Organic Iodide
AOX	Adsorbable Organic Halides
BDD	Boron Doped Diamond
BRGO	Boron Doped Reduced Graphene Oxide
C-A	Cathode to Anode
CBZ	Carbamazepine
CDI	Capacitive Deionization
CFU	Colony-Forming Unit
CNT	Carbon NatoTube
COD	Chemical Oxygen Demand
DALY	Disability-Adjusted Life Year
DEET	N,N-Diethyl-meta-toluamide
DFT	Density Functional Theory
DO	Dissolved Oxygen
DOC	Dissolved Organic Carbon
DPD	N,N-diethyl-pphenylenediamine
DSA	Dimensionally Stable Anode
DTR	Diatrizoate
E_{Eo}	Electric Energy Per Order
EIS	Electrochemical Impedance Spectroscopy
ELOX	Electrochemical Oxidation
FAC	Free Available Chlorine
FESEM	Field Emission Scanning Electron Microscope
GAC	Granular Activate Carbon
GG	Graphite Granules
GO	Graphene Oxide
Gr	Graphene

HAA	Haloacetic Acid
HCD	High Current Density
HPIC	High-Pressure Ion Chromatography
HRT	Hydraulic Retention Time
IPM	Iopromide
LB	Luria-Bertani
LCD	Low Current Density
MBR	Membrane Biological Reactor
MW	Molecular Weight
NDMA	N-nitrosodimethylamine
NPOC	Non-Purgeable Organic Carbon
NRGO	Nitrogen Doped Reduced Graphene Oxide
OC	Open Circuit
PB	Phosphate Buffer
PPCPs	Pharmaceuticals and personal care products
PSA	Polar Surface Area
PI	Propidium Iodide
RGO	Reduced Graphene Oxide
SEM	Scanning Electron Microscopy
SHE	Standard Hydrogen Electrode
SRM	Selected Reaction Monitoring
TA	Terepthalic Acid
THM	Trihalomethane
Ti	Titanium
TOC	Total Organic Carbon
TPS	Terra Preta Sanitation
UN	United Nations
UPLC	Ultra-Performance™ liquid chromatograph
WASH	Water, Sanitation and Hygiene
WHO	World Health Organisation
WWAP	World Water Assessment Programme
WWTP	WasteWater Treatment Plant
XPS	X-ray Photoelectron Spectroscopy
XRD	X-Ray Diffraction

List of figures

List of tables

Summary

The challenge of clean water has been present for ages, since water is essential for human life. Lately, the increase in the use of chemical products and the ongoing water scarcity have showed the necessity of inventing new methods for water treatment that are able to treat persistent contaminants. Electrochemical methods can provide a solution since they do not use additional chemicals, they can be used in decentralized systems and could be also operated using renewable energy sources. The aim of this thesis is to evaluate new electrochemical methods for the degradation of persistent organic contaminants and water disinfection.

To begin with, the three-dimensional (3D) electrochemical oxidation was explored. Graphite granules were used as particle electrodes for the conversion of a two-dimensional (2D) electrochemical reactor into a 3D reactor for the degradation of persistent organic contaminants in water. The 3D system proved to be more efficient and with lower energy demand, compared with the 2D one for both anode materials that were tested, namely boron-doped diamond (BDD) and Ti/RuO_2-IrO_2. A synergy between adsorption/electrosorption and electrochemical oxidation was achieved in the 3D process, compared with the adsorption of the granules in the open circuit (i.e., without applying current/potential) and the performance of electrochemical oxidation only, in the 2D reactor, i.e., without the granules. Coating the granules with reduced graphene oxide (RGO) further improved the system, increasing the removal rates of the contaminants and lowering the electric energy per order.

To explore the sustainability of the 3D processes, the regeneration of the particle electrode was also examined. Granular activated carbon (GAC), previously saturated with wastewater, was used as particle electrode in a 3D reactor, equipped with BDD as an anode, for the treatment of real secondary municipal wastewater effluent spiked with persistent organic contaminants during 27 consecutive runs. Application of sufficient current density increased the adsorption ability of the saturated GAC during the consecutive runs., while degradation of the organic contaminants was also achieved. The synergy between adsorption/electrosorption and electrochemical oxidation in terms of the target contaminants removal increased through the successive runs. The GAC packed bed also managed to reduce chlorate and perchlorate and adsorbable organic halides (AOX) generation, thus minimizing the toxicity of the effluent.

In the last chapter of the thesis, we examined the possibility of applying an

electrochemical process for the inactivation of *Escherichia coli* from water. Graphene sponge electrodes, based on the RGO coating, were produced with a low cost, bottom-up synthesis method and were employed as both anodes and cathodes for electrochemical disinfection, which was achieved without the contribution of chlorine species. Nitrogen and boron were examined as dopants for enhancing the performance of graphene sponge anode and cathode. The results indicated that the nitrogen-doped graphene sponge anode was more effective towards *E. coli* inactivation, compared to the boron-doped anode. Two different flow-through reactor configurations, anode-cathode and cathode-anode were examined, with the former achieving higher removal of the bacteria. The main inactivation mechanism proposed is the disruption of the bacterial cell walls due to electroporation and consequent cell lysis. The electrogenerated ozone and hydroxyl radicals also contributed to the bacteria inactivation. Storage experiments confirmed the damaged cell walls, as no regrowth of *E. coli* was observed after treatment. The treatment was examined in both low conductivity phosphate buffer and real tap water, achieving up to 5 log removal in both systems. The energy efficiency of the system was improved by using intermittent current instead of continuous current application, taking the advantage of the capacitance of RGO, without any decrease in the disinfection efficiency.

Overall, the results of this thesis show that 3D electrochemical methods can be efficiently used for both degradation of organic contaminants and disinfection. A 3D system can be achieved by using 3D anode or cathode or by adding a particle electrodes between the two main 2D electrodes. The transformation of a 2D reactor to a 3D reactor increases the electrode surface area and facilitates mass transfer, thus enhancing the removal efficiency and potentially reducing the energy consumption.

Resum

El repte de l'aigua neta és present des de fa temps, ja que l'aigua és essencial per a la vida humana. Últimament, l'augment de l'ús de productes químics i l'escassetat d'aigua actual han demostrat la necessitat d'inventar nous mètodes per al tractament de l'aigua que siguin capaços de tractar contaminants persistents. Els mètodes electroquímics poden proporcionar una solució, ja que no utilitzen productes químics addicionals, poden ser utilitzats en sistemes descentralitzats i també podrien ser operats utilitzant fonts d'energia renovables. L'objectiu d'aquesta tesi és avaluar nous mètodes electroquímics per a la degradació de contaminants orgànics persistents i la desinfecció de l'aigua.

Per començar, es va explorar l'oxidació electroquímica tridimensional (3D). Els grànuls de grafit es van utilitzar com elèctrodes de partícules per a la conversió d'un reactor electroquímic bidimensional (2D) en un reactor 3D per a la degradació de contaminants orgànics persistents en aigua. El sistema 3D va demostrar ser més eficient i amb menor demanda d'energia, en comparació amb el 2D per als dos materials d'ànode que es van provar, i.e., el diamant amb dopatge de bor (BDD) i Ti/RuO_2-IrO_2. Una sinergia entre l'adsorció/electrosorció i l'oxidació electroquímica es va aconseguir en el procés 3D, en comparació amb l'adsorció dels grànuls en el circuit obert (i.e., sense aplicar corrent/potencial) i el rendiment de l'oxidació electroquímica només, en el reactor 2D, i.e., sense els grànuls. Cobrint els grànuls amb òxid de grafè reduït (RGO) va millorar encara més el sistema, augmentant les taxes d'eliminació dels contaminants i baixant l'energia elèctrica per ordre.

Per explorar la sostenibilitat dels processos 3D, també es va examinar la regeneració de l'elèctrode de partícules. El carbó actiu granular (GAC), prèviament saturat amb aigües residuals, es va utilitzar com a elèctrode de partícules en un reactor 3D, equipat amb BDD com a ànode, per al tractament de l'efluent d'aigües residuals municipals secundàries reals empalmat amb contaminants orgànics persistents durant 27 operacions consecutives. L'aplicació de suficient densitat de corrent va augmentar la capacitat d'adsorció del CAG saturat durant les operacions consecutives, mentre que també es va aconseguir la degradació dels contaminants orgànics. La sinergia entre l'adsorció/electrosorció i l'oxidació electroquímica en termes de l'eliminació de contaminants va augmentar a través de les successives operacions. El llit compacte de GAC també va aconseguir reduir la generació de clorat i perclorat i halurs orgànics adsorbibles (AOX), minimitzant així la toxicitat de l'efluent.

En l'últim capítol de la tesi, es va examinar la possibilitat d'aplicar un procés electroquímic per a la inactivació d'*E. coli* en l'aigua. Els elèctrodes d'esponja de grafè, basats en el recobriment RGO, es van produir amb un mètode de síntesi de baix cost i ascendent i es van utilitzar tant com ànodes com càtodes per a la desinfecció electroquímica, que es va aconseguir sense la contribució d'espècies de clor. El nitrogen i el bor van ser examinats com a dopants per millorar el rendiment de l'ànode d'esponja de grafè i el càtode. Els resultats van indicar que l'ànode d'esponja de grafè dopat amb nitrogen era més eficaç cap a la inactivació d'*E. coli*, en comparació amb l'ànode dopat amb bor. Es van examinar dues configuracions diferents de reactors de flux, ànode-càtode i càtode-ànode, i els primers van aconseguir una major eliminació del bacteri. El principal mecanisme d'inactivació proposat és la interrupció de les parets cel·lulars bacterianes a causa de l'electroporació i la consegüent lisi cel·lular. L'ozó electrogenerat i els radicals hidroxil també van contribuir a la inactivació dels bacteris. Els experiments d'emmagatzematge van confirmar les parets cel·lulars danyades, ja que no es va observar cap recreixement d'*E. coli* després del tractament. El tractament es va examinar tant en la memòria intermèdia de fosfats de baixa conductivitat com en l'aigua de l'aixeta real, aconseguint eliminació fins a 5 log en tots dos sistemes. L'eficiència energètica del sistema es va millorar mitjançant l'ús de corrent intermitent en lloc d'aplicació de corrent continu, aprofitant la capacitància de RGO, sense cap disminució en l'eficiència de desinfecció.

En general, els resultats d'aquesta tesi mostren que els mètodes electroquímics 3D es poden utilitzar de manera eficient tant per a la degradació de contaminants orgànics com per a la desinfecció. Un sistema 3D es pot aconseguir mitjançant l'ús d'ànode o càtode 3D o mitjançant l'addició d'elèctrodes de partícules entre els dos elèctrodes 2D principals. La transformació d'un reactor 2D a un reactor 3D augmenta la superfície de l'elèctrode i facilita la transferència de massa, millorant així l'eficiència d'eliminació i reduint potencialment el consum d'energia.

Resumen

El desafío del agua potable ha estado presente desde hace mucho tiempo, ya que el agua es esencial para la vida humana. Últimamente, el aumento del uso de productos químicos y la actual escasez de agua han demostrado la necesidad de inventar nuevos métodos de tratamiento del agua que sean capaces de tratar contaminantes persistentes. Los métodos electroquímicos pueden proporcionar una solución, ya que no utilizan productos químicos adicionales, se pueden usar en sistemas descentralizados y también podrían funcionar con fuentes de energía renovables. El objetivo de esta tesis es evaluar nuevos métodos electroquímicos para la degradación de contaminantes orgánicos persistentes y la desinfección del agua.

Para empezar, se exploró la oxidación electroquímica tridimensional (3D). Se utilizaron gránulos de grafito como electrodos de partículas para la conversión de un reactor electroquímico bidimensional (2D) en un reactor 3D para la degradación de contaminantes orgánicos persistentes en el agua. El sistema 3D demostró ser más eficiente y con menor demanda de energía, en comparación con el 2D, para ambos materiales de ánodo probados, a saber, diamante dopado con boro (BDD) y Ti/RuO_2-IrO_2. Se logró una sinergia entre adsorción/electrosorción y oxidación electroquímica en el proceso 3D, en comparación con la adsorción de los gránulos en el circuito abierto (i.e., sin aplicar corriente/potencial) y la realización de oxidación electroquímica únicamente en el reactor 2D (i.e., sin los gránulos). Recubrir los gránulos con óxido de grafeno reducido (RGO) mejoró aún más el sistema, aumentando las tasas de eliminación de contaminantes y reduciendo la energía eléctrica por pedido.

Para explorar la sostenibilidad de los procesos 3D, también se examinó la regeneración del electrodo de partículas. Se utilizó carbón activado granular (GAC), previamente saturado con aguas residuales, como electrodo de partículas en un reactor 3D, equipado con BDD como ánodo, para el tratamiento de efluentes secundarios reales de aguas residuales municipales enriquecidos con contaminantes orgánicos persistentes durante 27 ejecuciones consecutivas. La aplicación de suficiente densidad de corriente aumentó la capacidad de adsorción del GAC saturado durante las ejecuciones consecutivas, mientras que a la vez se logró la degradación de los contaminantes orgánicos. La sinergia entre la adsorción/electrosorción y la oxidación electroquímica en términos de la eliminación de los contaminantes aumentó a lo largo de las sucesivas ejecuciones. El lecho empacado de

GAC también logró reducir la generación de clorato, perclorato y haluros orgánicos adsorbibles (AOX), minimizando así la toxicidad del efluente.

En el último capítulo de la tesis, examinamos la posibilidad de aplicar un proceso electroquímico para la inactivación de Escherichia coli en el agua. Los electrodos de esponja de grafeno, basados en el recubrimiento RGO, se produjeron con un método de síntesis ascendente y de bajo costo y se emplearon como ánodos y cátodos para la desinfección electroquímica, lo que se logró sin la contribución de especies de cloro. Se examinaron el nitrógeno y el boro como dopantes para mejorar el rendimiento del ánodo y cátodo de esponja de grafeno. Los resultados indicaron que el ánodo de esponja de grafeno dopado con nitrógeno fue más eficaz para la inactivación de E. coli, en comparación con el ánodo dopado con boro. Se examinaron dos configuraciones diferentes de reactor de flujo continuo, ánodo-cátodo y cátodo-ánodo, logrando la primera una mayor eliminación de bacterias. El principal mecanismo de inactivación propuesto es la alteración de las paredes celulares bacterianas debido a la electroporación y la consiguiente lisis celular. El ozono electrogenerado y los radicales hidroxilos también contribuyeron a la inactivación de las bacterias. Los experimentos de almacenamiento confirmaron los daños a las paredes celulares, ya que no se observó ningún nuevo crecimiento de E. coli después del tratamiento. El tratamiento se examinó tanto en tampón de fosfato de baja conductividad como en agua del grifo real, logrando una eliminación de hasta 5 log en ambos sistemas. La eficiencia energética del sistema se mejoró mediante el uso de corriente intermitente en lugar de la aplicación de corriente continua, aprovechando la capacitancia de RGO, sin disminuir la eficiencia de la desinfección.

En general, los resultados de esta tesis muestran que los métodos electroquímicos 3D se pueden utilizar de manera eficiente tanto para la degradación de contaminantes orgánicos como para la desinfección. Se puede lograr un sistema 3D utilizando un ánodo o cátodo 3D o agregando electrodos de partículas entre los dos electrodos 2D principales. La transformación de un reactor 2D en un reactor 3D aumenta la superficie del electrodo y facilita la transferencia de masa, mejorando así la eficiencia de eliminación y reduciendo potencialmente el consumo de energía.

CHAPTER 1 General introduction

The concept that clean water and safe sanitation are essential to health is an intertemporal issue. In 350 B.C., for example, Hippocrates recommended boiling water to inactivate "impurities". One of the most significant public health achievements of the 20th century was the establishment of public water disinfection and treatment. However, nowadays, billions of people, especially in rural communities, continue to be lacking access to safe drinking water and adequate sanitation (WHO/UNICEF, 2017). A large proportion of the overall disease burden, 3.3% of global deaths and 4.6% of global disability-adjusted life years (DALYs), was attributed to quantifiable effects of inadequate water, sanitation, and hygiene (WASH) in 2016. This represents nearly 2 million preventable deaths and 123 million preventable DALYs annually. Children under 5 years of age are disproportionally affected by inadequate WASH: 13% of all deaths and 12% of all DALYs in this age group are related to inadequate WASH (WHO, 2019).

Many of the diseases responsible for these deaths are caused by waterborne pathogenic bacteria and viruses. Efficient water treatment could reduce the number of disease incidents by decreasing pathogen transmission from the environment. A considerable source of pathogens in water treatment is fecal contamination, because of the poorly and unsafely managed sanitation systems. Open defecation or improperly sited sanitation interventions leach wastewater and pathogens into onsite and downstream water supplies (Hand and Cusick, 2021). Another major issue deteriorating living conditions is the extensive use of anthropogenic chemicals in modern society, which has severe consequences for both the environment and human populations. Large amounts of organic contaminants such as industrial chemicals, pesticides, dyes, pharmaceuticals, and personal care products reach freshwaters **Figure 1.1.**

Many of these chemicals are persistent and can cause long term damage to human health. Even at low concentrations, they are known or suspected to be toxic, carcinogenic, and mutagenic and thus they can be categorized as contaminants of emerging concern (or emerging contaminants)**.** Pharmaceuticals and personal care products (PPCPs) are among the most prevalent categories of emerging contaminants found in the environment. They are widely utilized in both human and veterinary medicine, with their usage showing a growing trend These compounds are classified as emerging contaminants due to their recognized or potential negative impacts on ecological systems or human health (Lozano et al., 2022). PPCPs are a category of emerging contaminants distinguished by their unique physicochemical characteristics. Pharmaceuticals are specifically formulated to enhance their biological activity at minimal concentrations and are engineered for

sustained effectiveness. These attributes underscore the potential risks associated with the unintended presence of PPCPs in the environment (Ebele et al., 2017). The main pathway through which PPCPs enter the environment is through human excretion into wastewater systems, where they can persist during treatment and be released into the environment through treated wastewater effluent. Furthermore, PPCPs may also be environmentally exposed through emissions from hospitals, the pharmaceutical industry, and agriculture. The elimination of PPCPs is influenced by factors such as the type of pollutant (e.g. chemical structure, concentration, solubility) and the treatment technology employed for wastewater processing (Adeleye et al., 2022). The elimination of this category of contaminants was chosen to be investigated in the framework of this thesis. Current conventional (waste)water treatment technology is ineffective towards the removal of several of the abovementioned persistent organic contaminants which can pass unmodified through sewage treatment plants. Thus, new treatment methods that can eliminate efficiently these contaminants should be developed (Rizzo et al., 2019).

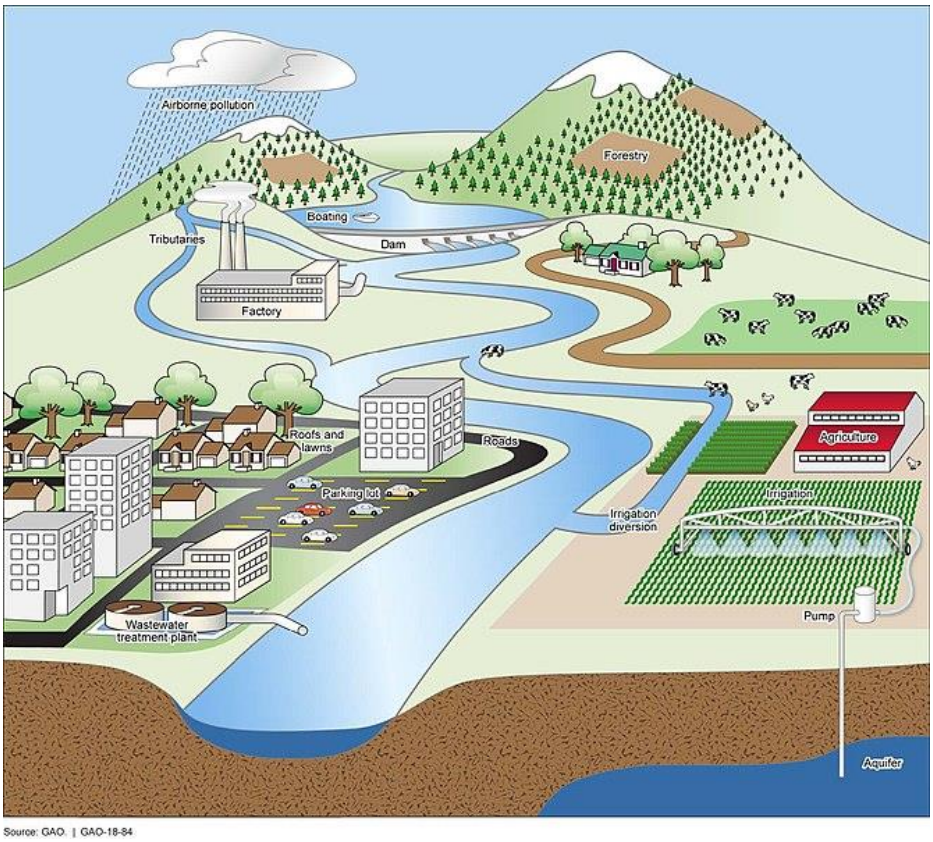

Figure 1.1: Sources of contamination in the hydrologic cycle. Source: Wikimedia Commons

1.1. Decentralized water and wastewater treatment

The United Nations (UN) 2030 Agenda for Sustainable Development includes a dedicated goal on water and sanitation, with "universal and equitable access to safe and affordable drinking water for all" as one of the targets to be reached by 2030 (World Health Organization, 2017). The growing human population in combination with the ongoing water scarcity creates a great challenge for the future. Despite the growing urbanization of the last decades, half of the global population still lives in rural areas. According to the World Water Assessment Programme (WWAP), 80% of the wastewater worldwide is returned to the ecosystems without proper treatment (Unesco and World Water Assessment Programme, 2014). The lack of water and wastewater treatment is more pronounced in rural communities and small settlements (World Health Organization, 2014). These communities usually depend on the on-site water treatment. To accomplish UN´s objective and answer these challenges, decentralized water treatment units should be installed to complement the existing centralized water treatment systems. Reliable and robust technologies that will ensure the quality of the treated water at low cost is required to implement community or household-managed non-networked water treatment systems. Decentralization can be a solution for small communities as it can be based on a holistic approach, promote water reuse and resource recovery and thus form part of the local circular economy. One of the main advantages of decentralized systems is that they can be adapted to the needs of each community, considering local expected population growth pattern, economical capacity for investment, (waste)water quality and quantity, soil, and land properties. In comparison to centralized systems, decentralized ones can be a sustainable and financially sound solution for water treatment, with more efficient land and energy usage, lower capital, maintenance and operational costs, and more specialized application (Khalid and Orozco Garcia, 2019).

Except for rural areas, decentralization can also be implemented in urban centers. Due to the growth of urban and peri-urban areas, the existing treatment plants may not be able to satisfy the treatment requirements of the increased wastewater volume, whereas there are various limitations on their expansion, regarding high maintenance and capital costs as well as large area requirements. Besides, the increasing water scarcity propitiates the consideration of alternative sources of water commodities such as urban and domestic wastewater, and new systems capable of reducing and recycling water resources are necessary. Already existing centralized treatment plants can play an important role, but

additional decentralized systems should be developed to face this issue. An additional benefit of decentralized systems in urban centers is the reduction of the contaminant burden of the nearby areas, since the volume of treated water is lower than in the centralized treatment plants, thus reducing the environmental impact. The implementation of decentralized systems in urban areas requires different planning and design, taking into account the heterogeneity that occurs within a single urban center, where social, environmental, geographic, economic, and technological conditions can vary greatly (Bernal et al., 2021). Decentralization emphasizes a holistic approach, based on the benefits of reducing waste at source and thus avoiding the component of collection and transportation of wastewater. The main cost of these systems is focused on the treatment and disposal of wastewater, improving recycling and reuse on site. An example of decentralized systems application is the wastewater treatment in commercial centers, hospitals, industries, or airports, where the load of contaminants can be very high and needs to be reduced before disposal or transport to a centralized treatment plant. They can also be used for the recovery of bioenergy (from organic material transformation) and nutrients (mainly nitrogen and phosphorus). Separating the different wastewater streams (grey-, brown- and yellow-water) could facilitate the process of resource recovery, like for example ammonia from urine. Another example of an opportunity for decentralized treatment is rainwater and greywater treatment and reuse, which can be applied either at a municipal or household level, and could be a solution to growing water scarcity, as mentioned above (Khalid and Orozco Garcia, 2019).

In rural areas, the main decentralized (waste)water systems that have been used include septic tanks, stabilization ponds, constructed wetlands, up-flow anaerobic sludge blankets (UASB) and membrane biological reactors (MBR) (Muzioreva et al., 2022). In urban areas, where a limitation of available land exists, more advanced technologies have been used for decentralized (waste)water treatment. These include chlorination, sand filtration, adsorption on GAC, zeolite or other clay materials, MBRs and most recently Advanced Oxidation Processes (AOPs). AOPs are based on the in-situ generation of strong oxidants that degrade contaminants. The majority of AOPs are based on hydroxyl radicals ($OH^{\bullet}$) production, but there are also AOPs that utilize other oxidizing species, such as O_3, sulfate or chlorine radicals. Numerous AOPs, particularly those utilizing ozonation and ultraviolet (UV) irradiation, have already been successfully implemented at full-scale in drinking water treatment and water reuse facilities. However, ongoing research conducted by various researchers continues to unveil new studies on emerging AOPs for water

treatment. These include Fenton and photo-Fenton processes, plasma, electron beam, ultrasound and microwave-based AOP (Miklos et al., 2018). In practice, using a single AOP alone may not be ideal for effectively treating complex organic wastewater systems, as it has limitations in terms of operating parameters. To overcome these limitations and enhance the generation of ROS, different AOPs can be combined taking in advantage the synergistic effects of these different substances. Combined AOPs can significantly improve the oxidation efficiency of contaminants and expand the range of operating parameters, compared to individual treatment technologies (D. Ma et al., 2021)

Ideally, the technologies used for decentralized systems should fulfill some requirements. They need to be easily operated, economically affordable, environmentally friendly, independent from the power grid or tap pressure, robust, socially acceptable, have a compact design and flexible operation conditions. They should also be able to remove emerging organic contaminants that are persistent and cannot be treated efficiently by the current centralized wastewater treatment systems. Among the available physico-chemical technologies that can be used in point of entry and point of use treatment devices (e.g., chemical disinfection, membrane filtration, heat and UV-based disinfection and others), no single small-scale system meets all the performance criteria needed. Electrochemical systems fulfill several of the abovementioned requirements and are well-suited to be implemented for the decentralized on-site treatment of contaminated water because they do not use chemical reagents, thus avoiding the costs associated to the production, transport, storage and handling of chemicals; they do not form a residual waste stream, they operate at ambient temperature and pressure, are robust, versatile, and can be combined with other water treatment technologies; finally, electrochemical treatment systems can be easily automatized and have a small carbon footprint. Combining them with the renewable energy sources could reduce their environmental impact even more and tackle one of their biggest drawback, which is the high energy consumption (Garcia-Segura et al., 2018; Radjenovic and Sedlak, 2015).

1.1.1. Electrochemical systems for decentralized treatment of contaminated water

Electrochemical systems consist of two main electrodes, anode and cathode, and the electrolyte. Oxidation takes place at the anode and reduction at the cathode. The reaction rate can be affected by the applied current density, mass transfer, electron transfer, surface

reactions (e.g., adsorption/desorption) and possible chemical reactions that can occur before or after the electrochemical reaction. At current densities typically applied in electrochemical water treatment (i.e., ≥50 A m^{-2}), water electrolysis occurs as well. Due to the complex composition and highly contaminated water streams, where proper treatment could not be achieved using only one method, electrochemical technologies show potential to become excellent candidates for combination with other methods in an integrated sequential process. This way, the advantages of each individual methods are combined and numerous wastewater streams with different characteristics can be treated. Electrochemical processes have been combined with other processes for the treatment of (waste)water, such as aerobic and anaerobic processes, membrane processes, photocatalysis, adsorption and ozonation. Electrochemical methods have demonstrated good versatility for the treatment of diverse wastewaters, containing high or low concentrations of various organic pollutants and other chemicals. These include industrial effluents with high chemical oxygen demand (COD) concentration, brackish effluents (e.g. reversed osmosis concentrates), solutions contaminated with a mixture of organic and inorganic contaminants (e.g. leachate), effluents with rheological complexity and effluents with low pollutant and high COD load (Garcia-Rodriguez et al., 2022). The most common electrochemical processes for wastewater treatment include electrocoagulation, electroflotation, electrochemical precipitation, electro-Fenton and electrochemical oxidation (Muddemann et al., 2019)..

There are several examples of the use of electrochemical systems for decentralized water and wastewater treatment in the state-of-the-art. For example, Butkovskyi et al. used batch electrochemical oxidation reactors to post-treat effluent from the greywater treatment system of the DeSaR (Decentralised Sanitation and Reuse) plant at Sneek (The Netherlands) to remove micropollutants that are frequently found in personal care and household products. They used Ti sheet anodes coated with Ru/Ir mixed metal oxide (MMO), Pt/Ir MMO, or Pt. The micropollutants were successfully removed in the system with low energy consumption, but the presence of halogenated compounds and free chlorine in the effluent made the utilized system inappropriate as a sole post treatment of greywater effluent (Butkovskyi et al., 2014). Cho et al. investigated electrochemical treatment of real domestic wastewater, powered by a photovoltaic panel. The 20 L prototype electrolysis cell reactor was able to remove up to 95% of COD and eliminate coliform bacteria in less than 4 h of treatment, resulting in an effluent water quality suitable for non-potable purposes (Cho et al., 2014). Another electrochemical cell reactor,

equipped with a boron doped diamond (BDD) anode, was used for the disinfection of biologically treated wastewater for direct recycling of domestic wastewater. The process successfully inactivated the bacteria present in the effluent, while the adsorbable organic halides (AOX) formation could be limited by applying low electric charge, making it eligible for reuse (Schmalz et al., 2009). Haaken et. al utilized a UV/electrolysis hybrid technology to address the drawbacks associated with UV radiation and electrolysis for the same purpose. A reliable, sustained bacterial reduction was achieved (up to 5.6 log removal), while reactivation and reversible damage of the bacteria was prevented by the synergistic effect of the combined methods (Haaken et al., 2014). In order to mitigate disinfection by-products (DBPs) and enable water reuse, Drennan et al. suggested the use of a divided cell configuration for the treatment of greywater, which was able to electrochemically remove COD, while haloacetic acids (HAAs), trihalomethanes (THMs) and perchlorate formation was reduced. HAAs and THMs were generated anodically, but were removed on the cathode in the divided cell that was also equipped with a ion exchange membrane (Drennan et al., 2019).

Electro-Fenton has been also used for decentralized treatment. A stacked flow-through electro-Fenton reactor was used for the treatment of domestic sewage, removing COD, total phosphorus, ammonia nitrogen, suspended solids and bacteria, while the DBPs formation was limited, due to the quenching effect of active chlorine by the electrogenerated H_2O_2. The effluent met China's urban water quality standards and could be reused for road cleaning or flushing toilets (Ren et al., 2020). The advantages of electro-Fenton are the continuous regeneration of Fe^{2+} on the cathode and the in-situ production of H_2O_2. The disadvantages include the difficulty of eliminating Fe^{3+} at the end of the process, the fact that electro-Fenton is more efficient in acidic conditions and thus requires a final neutralization step as well as the low H_2O_2 yield (Ebba et al., 2022; Nidheesh et al., 2023).

Another electrochemical method suitable for decentralized treatment is electrocoagulation. For example, an electrocoagulation process with a sacrificial Al electrode was used for the treatment of wastewater generated from a hospital, removing COD, color, and turbidity with low energy consumption (Ebba et al., 2022). Cotillas et al. suggested a combined electrodisinfection-electrocoagulation method for the treatment of actual urban wastewater, collected at the secondary clarifier of the WWTP of Ciudad Real. The influent of the plant originates from domestic activities. The pilot scale system was equipped with BDD anodes and iron bipolar electrodes and was operated in

continuous mode, achieving simultaneous disinfection and turbidity removal, while the formation of hazardous chlorates and perchlorates was avoided (Cotillas et al., 2020). Electrocoagulation is a relatively fast process that can be performed in continuous mode, it can treat large volumes of contaminated water with high organic load, it has good removal efficiency for ionic and colloidal matter and the electrode cost is low. Its advantages include simplicity of equipment, low energy requirements, the fact that no additional chemicals are needed and the low initial installation and maintenance cost. In contrast, the process may require periodic replacement of sacrificial anodes, may lead to cathode passivation, and may result in the production of sludge (Ebba et al., 2022)

Another opportunity for decentralized treatment is the source separation of urine, which can help reduce the nutrient load of municipal wastewater. Electrochemical oxidation of urine using Pt/Ir, anodes was able to reduce its unpleasant odor, which is caused by the formation of ammonia. This facilitated the storage of urine for its reuse as flush water in the toilets (Ikematsu et al., 2007). Except for the odor, organic contaminants and pathogen bacteria, that many cause potential threat to the environmental and human health, must be removed from urine prior to its safe reuse,. Electrochemical oxidation is one method that has been extensively used for urine treatment. Recovery of nutrients from source-separated urine can be achieved via different on-site electrochemical treatments in the form of liquid, solid and gaseous products (Liu et al., 2022).

1.2. Electrochemical oxidation processes

Electrochemical oxidation is an emerging technology for (waste)water treatment that has gained increasing interest in the last years due to its versatility to degrade or completely mineralize a wide spectrum of organic contaminants, such as pharmaceuticals, pesticides, dyes and carboxylic acids. Many of these contaminants are persistent and difficult to remove with conventional wastewater treatment technologies, thus highlighting the need for the development of alternative and efficient technologies for their removal. Electrochemical oxidation systems offer several advantages : (i) modular and compact design, (ii) they do not produce secondary waste streams that require further treatment, (iii) they can be easily controlled and automatized, (iv) the treatment operates under ambient temperature and pressure, and (v) no additional chemical is needed for the process, thus eliminating the need of their transportation and storage (Garcia-Segura et

al., 2018; Qiao and Xiong, 2021). Electrochemical oxidation systems have been used for the treatment of different effluents, including textile dyeing, petrochemical, petroleum and petroleum derivatives, paper industry, diaries, landfill leachates tannery and pharmaceutical industry effluents (Radha and Sirisha, 2018; Radjenovic and Sedlak, 2015).

1.2.1. Mechanisms of electrochemical oxidation

Electrochemical process consists of the redox reactions occurring at the anode and cathode, which lead to the oxidation and reduction of contaminants, respectively. Oxidation of organic contaminants can occur via two different pathways, direct and indirect oxidation. Direct oxidation involves the diffusion of the contaminants from the bulk solution to the anode surface and the subsequent electron transfer between the anode surface and the contaminant, leading to the partial degradation of the contaminants or their mineralization, i.e. transformation to water, carbon dioxide and other inorganic components (Anglada et al., 2009). Indirect oxidation occurs because of the in-situ generated oxidant species on the electrode surface, either the anode or the cathode, such as $OH^{\bullet}$, active chlorine species, hydrogen peroxide, O_3, peroxodisulfate, peroxodiphosphate, and peroxodicarbonate. $OH^{\bullet}$ are highly reactive and short-lived, thus their chemical activity is limited near the vicinity of the anode, whereas the other oxidants can be active in the bulk as well (Garcia-Segura et al., 2018; Groenen-Serrano et al., 2013).

$OH^{\bullet}$ are electrogenerated at the anode surface by the following reaction (Comninellis, 1994) :

$$M + H_2O \rightarrow M(OH^{\bullet}) + H^+ + e^- \quad \text{(eq. 1)}$$

Where M refers to the anode and $M(OH^{\bullet})$ to the adsorbed hydroxyl radical.
Nevertheless, there are competitive reactions, which can consume the radical species leading to oxygen evolution, that also occur:

$$M(OH^{\bullet}) + H_2O \rightarrow M + O_2 + 3\,H^+ + 3\,e^- \quad \text{(eq. 2)}$$

$$2M(OH^{\bullet}) \rightarrow 2\,M + O_2 + 2\,H^+ + 2\,e^- \quad \text{(eq. 3)}$$

Reaction 1, and thus the $OH^{\bullet}$ generation, can be enhanced when anodes with high overpotential for oxygen evolution reaction (OER) are used. These usually include the non-active anodes, with BDD presenting the one with the highest oxidizing power anodes among the commonly used electrodes (Groenen Serrano, 2018)

Chlorine species are generated by the oxidation of chloride anions on the anode. Active anode materials such as Ti/RuO_2, Ti/IrO_2 present better performances than the non-active anode materials considering the electrogeneration of active chlorine species.

$$2Cl^- \rightarrow Cl_2(aq) + 2e^- \quad \text{(eq. 4)}$$

$$Cl_2(aq) + H_2O \rightarrow HClO + Cl^- + H^+ \quad \text{(eq. 5)}$$

$$HClO \leftrightarrow H^+ + ClO^- \quad \text{(eq. 6)}$$

On the other hand, at non-active anodes, $OH^{\bullet}$ do not interact with the surface of the electrode, making them available to react with $HClO/ClO^-$ and resulting in undesired perchlorates, according to the following reactions (Isidro et al., 2020) :

$$ClO^- + 2\ OH^{\bullet} \rightarrow ClO_3^- + 2\ H^+ + 2e^- \quad \text{(eq. 7)}$$

$$ClO_3^- + OH^{\bullet} \rightarrow ClO_4^- + H^+ + e- \quad \text{(eq. 8)}$$

The oxidation of organic pollutants is considerably faster when active chlorine species are present, compared to their oxidation only by $OH^{\bullet}$. However, the presence of the active chlorine species can cause the formation of undesirable organo-chlorinated by-products (e.g. HAAs, THMs, etc) and toxic ionic species, such as chlorate and perchlorate, as seen in the equations above (Garcia-Segura et al., 2018).

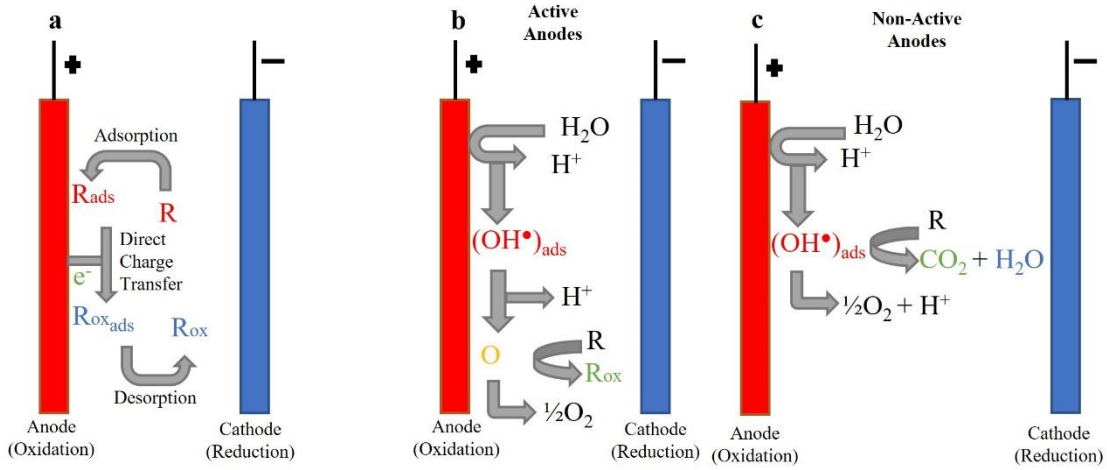

Figure 1.2: Scheme of a) direct and b,c) indirect electrolysis process in electrochemical oxidation. Source: (Garcia-Segura et al., 2018)

1.2.2. Impact of the electrode material on electrochemical oxidation process

Non-active anodes do not change the oxidation state during electrochemical reactions, while active anodes continuously cycle oxidation states during electrochemical oxidation. Active anodes, such as dimensionally stable anodes (DSA) of ruthenium (IV) oxide (RuO_2), iridium (IV) oxide (IrO_2) and other mixtures of metal oxides, have low oxidation potential. The formation of $OH^{\bullet}$ is low at active anodes, because $OH^{\bullet}$ remain chemisorbed on the anode, and the organic contaminants are converted to other transformation products but are not completely mineralized. On the other hand, non-active anodes, such as lead (IV) oxide (PbO_2), tin (IV) oxide (SnO_2) and boron-doped diamond (BDD), exhibit higher oxidation potential, resulting in an increased production of $OH^{\bullet}$ radicals, which remain physiosorbed at the anode surface and can completely mineralize contaminants (Chaplin, 2014; Garcia-Segura et al., 2018; Kapałka et al., 2008).

Among the non-active anodes, the most efficient are SnO_2, PbO_2, BDD and sub-stoichiometric and doped TiO_2. For instance, SnO_2 and PbO_2-based anodes have demonstrated high performance, due to the advantages of high oxygen evolution potential, strong oxidation ability, excellent electrical conductivity, and low cost, but they have the disadvantage of short life and possible leaching of the catalytic oxide (like the toxic Pb). Modifying the synthesis method, incorporating dopants, introducing interlayers, or even altering the substrates can help overcome the disadvantages (Salazar-Banda et al., 2021). The suboxides of TiO_2 are called collectively as Magnéli phases, with Ti_4O_7 and Ti_5O_9 being the most conductive and thus most widely used. Ti_4O_7 has gained

recently more attention, due to its ability of generating weakly adsorbed $OH^{\bullet}$, its corrosion resistance and electrochemical stability. The weak interaction of the $OH^{\bullet}$ with the electrode surface enables them to remain available for substrate oxidation in the vicinity of the anode surface. The $OH^{\bullet}$ produced on the commercial anode named Ebonex®, consisting of Ti_4O_7, are less abundant but can be more reactive than those formed on BDD (Bejan et al., 2012). Besides, BDD is regarded as the most efficient and widely used anode material in electrochemical oxidation processes due to its excellent properties. It exhibits an extremely wide potential window in both aqueous and non-aqueous solutions, it has great stability and strong corrosion resistance even in acidic media, an inert surface with low adsorption properties and a tendency to resist deactivation and low double-layer capacitance and background current. However, the main disadvantage of BDD electrodes, as far as scaling up is concerned, is their high production cost (Chaplin, 2014; Hu et al., 2021; Panizza and Cerisola, 2005; Salazar-Banda et al., 2021).

Active anodes have been less investigated compared with the non-active anodes, as they exhibit inferior performance in contaminant removal (Pointer Malpass and de Jesus Motheo, 2021). Among them, RuO_2 is the most common material used due to its excellent electrocatalytic activity. However, it has been reported to show low stability due to corrosion during electrolysis in acidic environments and thus ways of improving its stability need to be found, such as the addition of a second material like SbO_2, IrO_2 or TiO_2 (Salazar-Banda et al., 2021).

The activity of the different anodes depends on their value of overpotential of OER. For the anodes with low OER overpotential values, when the current densities are high, current efficiency is reduced due to oxygen formation. At the anodes with high OER overpotential values, anodic oxidation can occur at high current densities and oxygen evolution side reactions are reduced (Jiang et al., 2021). **Table 1.1** summarizes the overpotentials of OER for the most common anode materials.

Table 1.1: Overpotentials of oxygen evolution (vs SHE) for several anode materials

Anode	Value (*V*)	Conditions
Pt	1.3	0.5 M H_2SO_4
IrO_2	1.6	0.5 M H_2SO_4
PbO_2	1.9	1 M $HClO_4$
SnO_2	1.9	0.5 M H_2SO_4
Pb–Sn (93:7)	2.5	0.5 M H_2SO_4
Ebonex® (titanium oxides)	2.2	1 M H_2SO_4
Si/BDD	2.3	0.5 M H_2SO_4
Ti/BDD	2.7	0.5 M H_2SO_4
Nb/BDD (DiaChem®)	2.8	0.5 M H_2SO_4

1.2.3. Electrochemical degradation of trace organic contaminants

As mentioned before, trace organic contaminants such as pharmaceuticals and personal care products (PPCP), pesticides, surfactants, and industrial chemicals are persistent and cannot be effectively removed in conventional wastewater treatment plants. AOPs and more recently electrochemical advances oxidation processes (EAOPs) can be used for the degradation of such contaminants, but EAOPs have the advantage of not requiring additional chemicals as well as the ability to degrade contaminants that are unreactive with $OH^{\bullet}$, such as fluorinated organics, via direct electron transfer reactions (Chaplin, 2014). Electrochemical oxidation has also emerged as a technology for the treatment of trace organic contaminants recently. In electrochemical oxidation, the direct oxidation of the contaminants at the electrode surface via direct electron transfer yields poor degradation. Contaminants are mainly degraded by the $OH^{\bullet}$ near the vicinity of the anode or other electrogenerated oxidants. The limitation of the $OH^{\bullet}$ reaction with contaminants to a narrow zone near the electrode surface, in combination with the rapid electron transfer step, results in the overall process being limited by mass transfer. Thus, the reaction rates are dependent on the diffusion of contaminants to the electrode surface (Brillas and Martínez-Huitle, 2015).

The low concentration of trace contaminants in real wastewater, in combination with the high concentration of natural organic matter (NOM), can lead to decreased reaction rates, and thus increase in the energy consumption of the process (Chaplin, 2014). Pérez et al. investigated the electrooxidation of ten emerging contaminants, contained in low concentrations in reversed osmosis concentrates generated in tertiary WWTP, using a BDD anode. Removals higher than 92% were achieved for all ten contaminants. It was

reported that the overall removal kinetics were influenced by the mass transfer resistance caused by the diffusion of contaminants from the bulk to the anode, primarily due to their very low initial concentration (lower than 50 μg L^{-1}) (Pérez et al., 2010). Garcia-Segura et al. achieved the removal of 29 pharmaceuticals and pesticides at trace level concentrations (80–118 μg L^{-1}), from secondary effluent from a municipal sewage treatment plant, by anodic oxidation using BDD anode. $OH^{\bullet}$ formed at the BDD surface were reported as the main oxidants that caused the contaminants oxidation (Garcia-Segura et al., 2015). RuO_2/IrO_2-coated titanium anodes have been also reported for the electrochemical oxidation of 29 pharmaceuticals and pesticides, present in trace concentrations (8-37 μg L^{-1}) in reverse osmosis concentrate. Their removal was attributed to electro-chlorination (Radjenovic et al., 2011).

During the oxidation of organic contaminants in various wastewaters, toxic halogenated organic compounds (HOCs) can be formed, due to the reaction of the in-situ formed active chlorine species (Cl_2, OCl^-, HOCl) and chloride radicals ($Cl^{\bullet}$, Cl_2^{-}). The treatment of organic contaminants in realistic conditions of wastewater, where low conductivity is also expected, has not been reported extensively in the literature. In one of the few studies reported, Ma et al. investigated the treatment of real wastewater, with low conductivity, by anodic oxidation using BDD. They achieved total organic carbon (TOC) removal ranging from 50 to 84%, applying different current densities, but increased current densities and thus increased energy consumption was required, due to the large ohmic drops as a result of the low conductivity (Ma et al., 2018). Similar results were reported by Martínez-Huitle et al., who used a BDD anode for the treatment of real textile effluent. Long times and high current density were required for the complete COD removal, due to the low conductivity and the presence of organic matter dissolved in the effluent. Consequently, a higher charge was required for complete mineralization, since an amount of $OH^{\bullet}$ is wasted in parasitic non-oxidizing reactions such as oxygen evolution. The efficiency of the process was drastically improved with the addition of Na_2SO_4 in the system, due to the increase in the conductivity of the effluent (Martínez-Huitle et al., 2012).

1.2.4. Electrochemical disinfection

The most common disinfection methods used nowadays are chlorination, UV radiation and ozonation. Due to their various limitations, attention has been driven towards new disinfection methods, such as electrochemical disinfection. The main disadvantage of

chlorination is the generation of toxic DBPs, which can be carcinogenic (Li and Mitch, 2018). Furthermore, the corrosiveness and toxicity of the additional chemicals used can cause problems with their transportation and operation. Unfavorable taste and odor, as well as ineffectiveness against resistant microorganisms are also drawbacks of using this method (Martínez-Huitle and Brillas, 2008).UV does not lead to the production of harmful by-products, but it cannot cause a residual effect, thus recontamination or regrowth of damaged bacteria can occur during distribution and storage. Also, UV is limited towards the damage of antibiotic resistance genes and antibiotic resistant microbes (Singh et al., 2021). Ozonation can be applied in-situ and O_3 has high oxidizing power and reactivity, but it is highly unstable, toxic and has very short lifetime. An additional problem regarding ozonation is the formation of assimilable organic carbon (AOC), which permits the microbe regrowth. Also, it can produce DBPs, such as bromate (in waters containing bromide), which is considered carcinogenic (Singh et al., 2021; Von Gunten, 2003).

Electrochemical disinfection can be defined as the inactivation of microorganisms by the application of electric current (Kraft, 2008). Compared to the conventional methods, electrochemical disinfection is more sustainable, cost effective and is known to be effective towards the inactivation of a wide variety of microorganisms, from bacteria to viruses. It is mainly based on the in-situ generation of oxidants via redox reactions at the surface of the electrodes. Like conventional disinfection methods, these oxidants include active chlorine species, H_2O_2, O_3 and $OH^{\bullet}$. Chlorine species are the most commonly used electrochemically generated disinfectants due to their low redox potential (E^o $[Cl_2]/[Cl^-]$ = +1.36 V vs SHE (Huang et al., 2016)), high reactivity and prevalence of chloride precursors in most waters. Cl_2 is electrogenerated on the electrode surface and then is diffused into the solution and hydrolyses to hydrochloric acid and hypochlorous acid (Hand and Cusick, 2021; Palmas et al., 2018). It can also react with ammonia to form chloramines, which are disinfectants with great stability and low DBPs production. Due to the relatively low standard oxidation potential of Cl_2, electrochlorination systems require less energy compared to the systems relying on $OH^{\bullet}$ generation. On the other hand, addition of Cl^- may be required in water matrices with insufficient Cl^- concentration to produce Cl_2. $OH^{\bullet}$ are the strongest oxidants (standard redox potential E^o = +2.8 V vs SHE), but require more energy to be produced and have short lifetime (Hand and Cusick, 2021). Although chlorine is a very efficient disinfectant, it rapidly reacts with the organic matter to form THMs, HAAs and other chlorinated organic byproducts (Palmas et al.,

2018). At the highly oxidizing anodes such as BDD, Ti/SnO_2-based anodes, and Magnéli phase titanium suboxide (Ti_4O_7) electrodes, chloride is oxidized to chlorate and perchlorate, thus further compromising the quality of the treated water (Radjenovic et al., 2020).

Studies have shown that in the presence of chloride, bacteria inactivation can be faster or higher compared to when chloride is absent (Bruguera-Casamada et al., 2017; Kerwick et al., 2005; Long et al., 2015). On the other hand, relatively high removal, ranging from 4 to 7 log removal, was reported using chloride-free electrolytes, like phosphate (Kerwick et al., 2005; Long et al., 2015) , sulfate (Bruguera-Casamada et al., 2017; Kerwick et al., 2005; Li et al., 2010; Liang et al., 2018; Long et al., 2015) or fluoride (Liu et al., 2020, 2019; X.-Y. Ni et al., 2020) with different anode materials (including BDD, Ti_4O_7 and 3D carbon fiber felt) proving that efficient disinfection is possible, even in the absence of active chlorine. In the above systems, the inactivation of the bacteria was achieved by the reactive oxygen species (ROS) generated in the systems and direct disinfection on the electrodes surface. Nevertheless, given that chloride is in virtually all contaminated water, the real challenge is to develop new low-cost electrode materials, that can efficiently remove bacteria from water without producing chlorine or other toxic by-products. In **Table 1.2** the main studies of chlorine-free electrochemical disinfection examples are summarized.

Table 1.2: Examples of electrochemical disinfection treatments without the presence of chloride

Anode	Experimental Conditions	Removal	Energy consumption	Reference
Carbon fiber felt	10^6–10^7 CFU mL^{-1}, 10 mM NaF, 4.6 mA cm^{-2}, flow-through	6.5 log *E. coli*	0.05 kWh m^{-3}	(Liu et al., 2019)
Ti_4O_7	10^6 CFU mL^{-1} E. coli/ 10^{11} PFU MS2, 50 M Na_2SO_4, 10 mA cm^{-2}, REM reactor	6 log *E. coli* 6.7 log *bacteriophage MS2*	3.18 kWh m^{-3}	(Liang et al., 2018)
BDD, Ti/IrO_2, Ti/RuO_2	10^6 CFU mL^{-1}, 7 mM Na_2SO_4, 33.3 mA cm^{-2}, batch	7 log *P. aeruginosa*	0.44 kWh m^{-3}	(Bruguera-Casamada et al., 2017)
BDD	10^7 CFU mL^{-1}, 200 mM Na_2SO_4, 20 mA cm^{-2}, batch	4 log *E. coli*	0.78 kWh m^{-3}	(Li et al., 2010)
Zappi™ cell (platinum clad niobium mesh)	10^8 CFU mL^{-1}, 30 mM Na_2SO_4, 32 mA cm^{-2}/ 24 mA cm^{-2}, continuous flow recycling	4 log *E. coli* 6 log *bacteriophage MS2*	6.3 kWh m^{-3} 7.8 kWh m^{-3}	(Kerwick et al., 2005)

Another way of the inactivation of pathogens is direct oxidation, which involves electron

transfer between the electrode and cell membrane, and is affected mainly by mass transfer limitations, electrode surface area, and anode potential (Liu et al., 2019). Direct oxidation is a two-step process, which includes the electrosorption of the microorganism at the electrode surface and subsequent electron transfer, which triggers cellular oxidative stress (Y. Chen et al., 2021). Electrosorption on the electrode surface does not ensure the death of the microorganisms since the bacteria can remain active at the electrodes surface as long as the current is on but can get released back to the treated water once the electric field is off.

The inactivation mechanisms of microorganisms include oxidative stress and cell death due to the electrochemically produced oxidants, but also irreversible permeabilization of the cell membranes by the applied electric field and electrochemical oxidation of vital cellular constituents during the current application (Ghernaout and Ghernaout, 2010). The cell death can become evident by the morphological changes of the cells. Cellular walls can break, which results in the release of the intracellular material and its subsequent degradation by the electrogenerated oxidants. The subcellular inactivation mechanism can vary according to the anode material, the microorganism and the electrolyte which is present. Depending on them, different parameters, such as proteins, K^+ leakage, membrane potential, lipid peroxidation, permeability, intracellular enzymes, cellular adenosine triphosphate (ATP) level or even the DNA can be altered and thus lead to cell death (Martínez-Huitle and Brillas, 2021).

When cells are exposed to a sufficiently strong electric field, a fast and large increase in cell permeability occurs. This phenomenon is called electroporation. If the strength of the field is high enough, the cell damage is irreversible and can lead to cell death. Inactivation via electroporation is feasible for bacteria, protozoa and viruses (Huo et al., 2018, 2019; C. Liu et al., 2013). The exact mechanism of electroporation is believed to be related to nanoscale pore formation in the cell membrane. It is assumed that hydrophobic pores are randomly generated due to the thermal motion of the phospholipid molecules. If the radius of these pores is bigger that a critical radius (0.3 to 0.5 nM), they overcome the energy barrier and turn into hydrophilic pores, which are believed to be responsible for the electroporation phenomenon (Golberg and Rubinsky, 2013). If the pores are big enough, ions can pass through them, which could mean that in the presence of oxidant species, the microorganisms could be disactivated even in the case of reversible electroporation (Haas and Aturaliye, 1999; Xie et al., 2020).

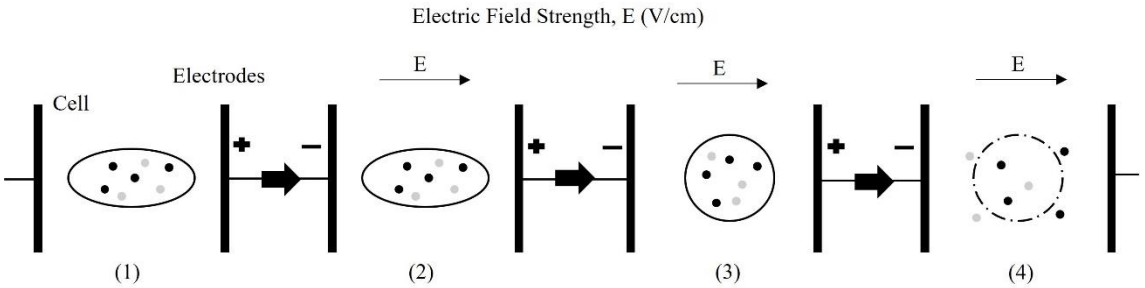

Figure 1.3: Electroporation mechanism of a cell membrane: (1) At zero potential, (2) Osmotic imbalance, (3) Swelling, (4) Membrane ruptures. Source: (Joannes et al., 2015)

Electroporation has been recently studied for electrochemical disinfection using nanostructured electrode materials. Among the materials that have been reported are carbon nanotube (CNT) sponges, that were used as 3D electrodes for the inactivation of bacteria and viruses, taking advantage of the electric field enhancement near the sharp edges of CNTs at the electrode surface (Huo et al., 2017). The phenomenon of the enhancement of the electric field using one-dimensional (1D) nanostructures to induce the inactivation of the bacteria through electroporation has been studied by other groups as well. Some of the electrodes used are copper foams equipped with copper oxide nanowires (Huo et al., 2018, 2016) or hierarchical Cu_7S_4 nanowires covered by N-doped carbon film (Cui et al., 2021) and polyurethane sponges coated with CNTs and silver nanowires (C. Liu et al., 2013). Recently, graphite felt electrodes equipped with Co_3O_4 nanowires were also reported for the inactivation of gram-positive and gram-negative bacteria (Pi et al., 2022). Due to the local enhancement of the electric field near the electrode, low voltages are sufficient to achieve disinfection and thus energy demand and potential formation of DBPs is reduced (Huo et al., 2020).

The electrode materials play a crucial role in the electrochemical water/wastewater disinfection process. Anode materials that have been investigated for electrochemical disinfection include SnO_2, PbO_2, RuO_2, doped TiO_2, glassy carbon and BDD (Y. Chen et al., 2021). Some common cathodes include stainless steel, copper, graphite, carbon cloth and reticulated vitreous carbon (RVC) (Ghernaout and Ghernaout, 2010). Among them, BDD electrodes are considered the most effective towards the degradation of waterborne pathogens (Martínez-Huitle and Brillas, 2021). However, the use of these commercially available electrodes has some disadvantages. One of them is the low current efficiency, which impacts both the electro-generation of oxidant species and the electrocatalytic activity of the electrode. Another issue is the low overpotential for OER observed in

certain electrodes, resulting in a decreased production rate of oxidant species. Moreover, the electrocatalytic activity towards chloride oxidation is high, whereas some of these electrodes have a high cost as well. BDD anodes cost, for example, is estimated around 4,200 € per m^2 (Wenderich et al., 2021). To overcome these issues, new electrode materials need to be developed. Carbon fiber-based flow-through electrodes have been recently utilized in electrochemical water disinfection. These electrodes were specifically employed for the purpose of inactivating *E. coli*. (Liu et al., 2019). The same electrodes were tested for the inactivation of gram-negative and gram-positive bacteria and provided effective inactivation of both at low applied voltages, with direct oxidation reported as the main mechanism, while the production of free chlorine was negligible (X. Y. Ni et al., 2020). These systems were further improved by combining different stackable multi-cathode units (Liu et al., 2020) or using alternating pulse current (Ni et al., 2021), leading to the reduction of the energy demand and increase in the bacteria removal (Singh et al., 2021).

1.3. Three-dimensional electrochemical systems

Electrochemical water treatment is typically performed using conventional two-dimensional (2D) reactors. Given that electrochemical degradation of contaminants is a surface-based reaction, 2D reactor design results in high mass transfer limitations and thus high energy consumption. A promising solution to improve the efficiency of water treatment processes is to use three-dimensional (3D) reactors. In 3D systems, the specific surface area of the electrode is increased, whereas the mass transfer limitations are decreased (Zhang et al., 2013). More efficient degradation of contaminants can also lower the formation of their unwanted by-products. The transformation of a 2D to a 3D system is possible by either introducing a third electrode, called particle or bed electrode in between the two main electrodes or by using 3D anodes or cathodes (Cañizares et al., 2004; Zhang et al., 2013).

1.3.1. 3D electrochemical systems based on particle electrodes.

With the addition of a material between the two main electrodes, named particle electrode, 2D electrochemical processes can be converted into 3D ones. When the 3D reactor functions in open circuit, i.e. without current application, the particles function only as

adsorbents. Upon the application of an external electric field, they get polarized, resulting in the formation of charged microelectrodes with one anodic and one cathodic side. Thus, electrosorption also occurs, due to the Coulombic force between the charged ions and the oppositely charged sides of the particle electrode (J. Ma et al., 2021; Zhang et al., 2013). The particles can also be polarized when they are not in direct contact with the main electrodes, if the electric field applied is large enough to induce charge separation on their surface, according to the microconductor principle (Narbaitz and Karimi-Jashni, 2009). In Figure 1.4 different configurations of 3D reactors are illustrated, according to the particle electrode position.

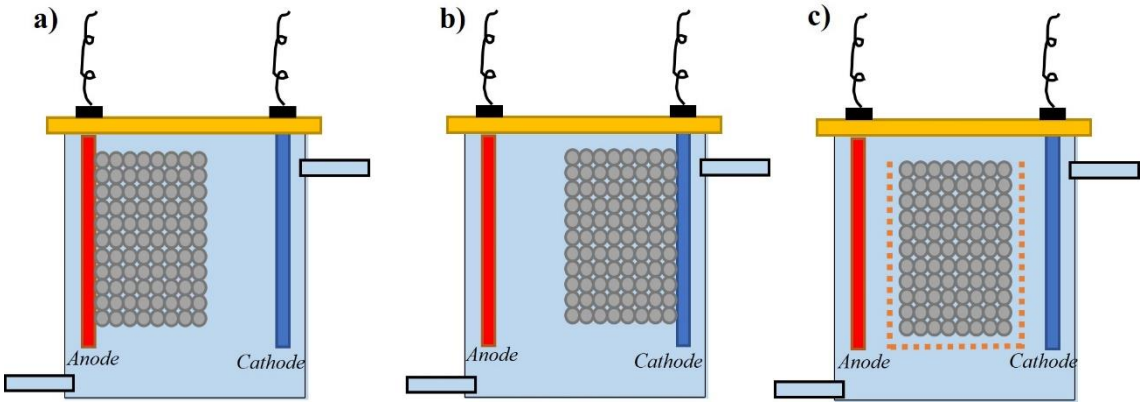

Figure 1.4: Different Configuration of 3D reactors according to the place of particle electrodes a) in contact with the anode, b) in contact with the cathode, c) no contact with the main electrodes

Besides adsorption and electrosorption, direct and indirect electro-oxidation are contributing to the removal of the contaminants. Direct oxidation occurs via direct electron transfer at the surface of the particle electrodes, whereas indirect oxidation is due to the in-situ generation of strong oxidants like $OH^{\bullet}$, H_2O_2, Cl_2, HClO (J. Ma et al., 2021; Zhang et al., 2013). Direct oxidation is also enhanced due to the adsorption ability of the particles since contaminants are concentrated near the surface of the adsorbent. Some particle electrodes, such as activated carbon (Sowmiya et al., 2016) or nickel foam (Liu et al., 2012) have been reported to reduce O_2 to H_2O_2 on their surface and can also act as catalysts for the decomposition of H_2O_2 to $OH^{\bullet}$. The $OH^{\bullet}$ are generated on the external surface boundary layer of the particle electrode and then reacts with the contaminants (J. Ma et al., 2021). **Figure 1.5** illustrates the main reactions that take place in a 3D electrochemical system.

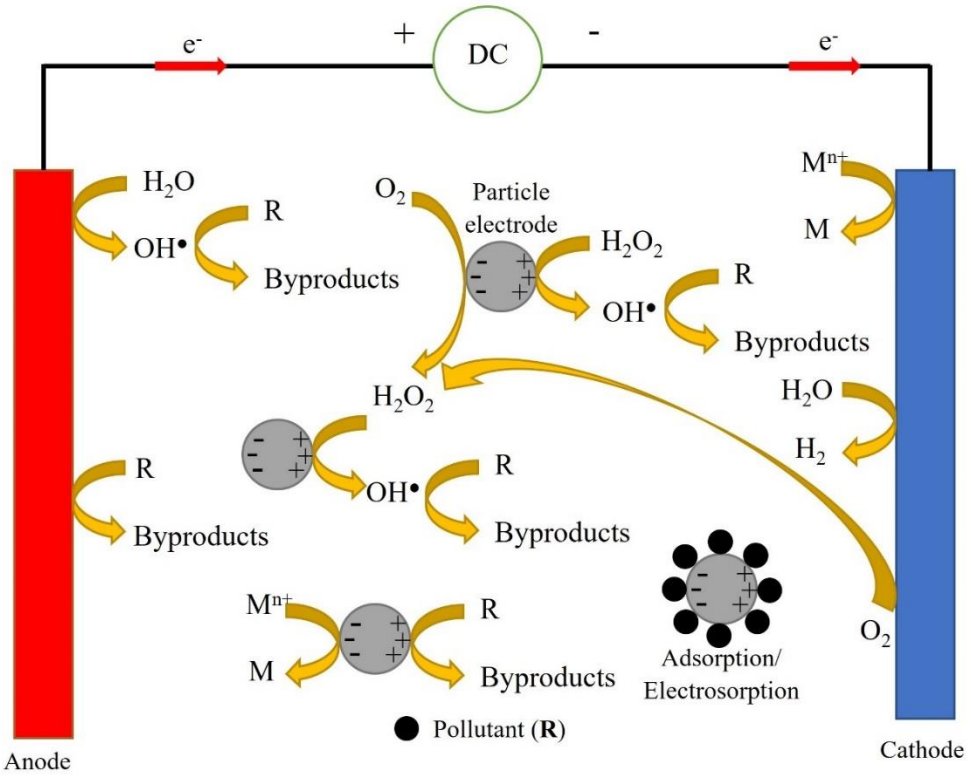

Figure 1.5: Mechanistic scheme of the reactions in the 3D electrochemical system. Source (J. Ma et al., 2021)

1.3.1.1. Reactor configuration and impact of operating parameters

3D electrochemical reactors can be classified into two main categories, according to the position of the particle electrode, fixed bed electrode and fluidized bed electrode. In the case of fixed bed, the particle electrodes are fixed between the two main electrodes. The advantage of these reactors is the high space-time yield. On the other hand, the particle electrode may get easily saturated with contaminants, thus requiring regeneration. In the case of fluidized bed electrode reactors, the main advantage is the enhanced mass transfer due to the continuous mixing and larger surface area in contact with the contaminants. However, the system can be more unstable and more difficult to control because of the non-uniform current distribution and electrical contact. **Figure 1.6** illustrates an example of a fixed and fluidized bed electrode reactor (Zhang et al., 2013).

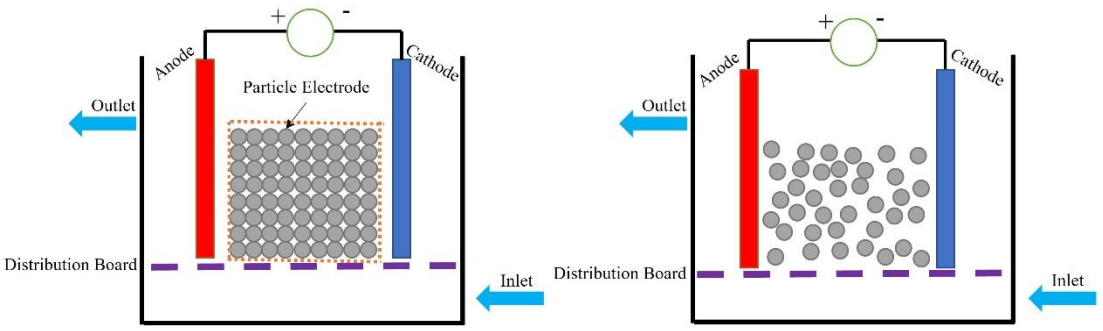

Figure 1.6: Typical 3D reactor types, fixed bed (left) and fluidized bed (right). Source (Li et al., 2021)

There are several operating parameters that can influence the efficiency of 3D systems. One of the most important is the current density applied in the system, as it can influence both the degradation of contaminants and polarization of the particle electrode. A sufficient current density can polarize the particles so that they form microelectrodes, with an anodic and cathodic side. On the other hand, higher current density can also lead to higher energy consumption, thus it is crucial for the system to find the optimized current density for contaminants degradation (GracePavithra et al., 2020; Zhang et al., 2013)

The energy consumption does not depend only on the current density applied and total cell potential, but also on the treatment time of the process. For batch processes, the treatment time should be sufficient to ensure the required extent of contaminants degradation and can also affect the particle electrode regeneration. In the case of continuous flow reactors, the hydraulic retention time (HRT), which is defined as the ratio between the reactor volume and the feed flowrate, is the crucial parameter (GracePavithra et al., 2020; Zhang et al., 2013).

1.3.1.2. Particle/Bed electrode types

The material of the particle electrode can play a crucial role in the 3D electrochemical system efficiency and can also determine its cost. Ideally, an electrode material should have a large surface area and high porosity to promote direct electrochemical oxidation, electrosorption and adsorption on its surface. Furthermore, it should meet other requirements such as low cost, high electrical conductivity, good catalytic activity and

enhanced mechanical and chemical stability, to avoid its attrition or corrosion. Activated carbon, either in powder or granules, carbon aerogel, carbon fiber, CNTs, biochar, graphite, metal particles, metal oxides, slags, metal foams, kaolin, ceramics, zeolite, γ-Al_2O_3 particle, glass balls are among the material that have been used as particle electrodes in 3D electrochemical reactors (Li et al., 2021; J. Ma et al., 2021; Zhang et al., 2013).

The most widely used particle electrodes are carbon-based materials, with granular activated carbon (GAC) being the most common, due to its high surface area, porosity, oxygen containing surface functional groups, good electrical conductivity, high chemical stability, and low price. These characteristics ensure its adsorption ability (Zhang et al., 2013) and allow the electrosorption of contaminants and their direct electrocatalytic oxidation on its surface (McQuillan et al., 2018). Furthermore, GAC is known to increase the production of $OH^{\bullet}$ through formation of H_2O_2 at cathodically polarized particles (Bañuelos et al., 2014) and its decomposition to $OH^{\bullet}$ (Fortuny et al., 1998). It has also been reported to catalytically decompose O_3 to $OH^{\bullet}$, when O_3 is present in the system (Zhan et al., 2019).

GAC has been used as particle electrode in 3D processes for different effluent types and contaminants, improving their efficiency and lowering the energy consumption, compared to 2D processes. Xiong et al. studied the removal of formic acid from wastewater by a 3D electrochemical reactor equipped with a GAC packed bed, working in batch mode (Xiong et al., 2003). COD removal was found to be 13.7 times higher in the 3D process in comparison to the 2D one (Xiong et al., 2003). Wang et al. used a 3D reactor in batch mode, equipped with a GAC packed bed, to treat paper-mil wastewater, reaching up to 86% COD removal, compared to 46% when GAC was not used (B. Wang et al., 2007). The energy consumption of the 3D process was 650 kWh kg^{-1}_{COD}, lower than that of the 2D process, which was 900 kWh kg^{-1}_{COD}. GAC has been also used in a 3D batch reactor for the treatment of landfill leachate. The 3D process achieved a 78% COD removal compared to 28% of the 2D process. The COD removal was further increased, up to 80%, when GAC with higher surface area was used (Nageswara Rao et al., 2009). Wei et al. utilized a 3D batch reactor for the treatment of oil refinery wastewater (Wei et al., 2010). The 3D process, with GAC as a bed electrode, achieved up to 86% COD removal, significantly higher than in the 2D process (36% removal), and by the adsorption on the GAC alone (41% removal) (Wei et al., 2010). GAC was also used as a particle electrode for the treatment of reactive black B in a batch reactor (Sowmiya

et al., 2016). Decolorization reached about 27% without GAC addition and increased to 40% with 5 g of GAC, while the energy consumption was 22% higher without the GAC (Sowmiya et al., 2016). Andrés Garcia et al. employed a 3D flow-through reactor, with a GAC packed bed, for the treatment of synthetic greywater. They observed a synergy between adsorption/electrosorption and electrochemical oxidation the 3D process. Positive synergy indicates that the removal rates using the 3D system are greater than the sum of rates obtained by the adsorption and electrooxidation processes performed individually. The removal of COD and TOC were 21% and 23% higher, respectively, in the 3D process compared to the combined performances of GAC adsorption and the 2D process. Besides, the energy consumption was lowered from 46 kWh kg COD^{-1} in the 2D system to 30 kWh kg COD^{-1} in the 3D system (Andrés García et al., 2018).

Graphite is a material with low electrical resistivity and low cost, which make it eligible for use as a particle electrode (Li et al., 2021; J. Ma et al., 2021) and has indeed been used before as such, improving the efficiency of 3D systems, but not as widely as GAC. Shen et al. used graphite granules in combination with glass beads in a 3D electrochemical reactor for the removal of estriol. The 3D process achieved 100% estriol removal, while the 2D one removed only 35%, whereas the energy consumption in the 3D process was 80% lower in comparison with the 2D process (Shen et al., 2017).

Lately, some examples of bed electrodes that have been developed more recently and attracted attention are multiwalled carbon nanotubes (MWCNTs), offering high surface area, high electrical conductivity, mechanical and chemical stability, as well as excellent electrocatalytic activity (J. Ma et al., 2021). Pourzamani et al. used a batch 3D reactor with MWCNTs as particles electrodes, resulting in higher removal efficiencies of diclofenac compared to the 2D process, while the MWCNTs showed excellent stability and reusability as well (Pourzamani et al., 2018). Although CNTs seem promising, worries have been expressed about their manufacturing costs, as well as their toxicity and hazards. A reduction in the cost and the development of solid regulatory guidelines should be developed before the extended application of CNTs in water treatment. Nano zero-valent iron (nZVI) is another example of a particle electrode that has gained attention lately due to its has high conductivity and large surface area. It is a strong electron donor that has strong reducing ability and thus, contaminants can be adsorbed on it and get reduced. It has also a strong catalytic activity for the production of $OH^{\bullet}$, through the electro-Fenton reaction. First, nZVI is oxidized by O_2 to Fe^{2+}, which subsequently reacts with the electrogenerated H_2O_2 to produce $OH^{\bullet}$ (J. Ma et al., 2021). Chi et al. used

bentonite-lignin nano zero-valent iron (BL-nZVI) as particle electrode in a batch 3D reactor for the treatment of pulp and paper wastewater, managing to increase the removal efficiencies of COD and color from 52% and 55% to 88% and 93%, respectively, compared to the 2D process (Chi et al., 2018). The disadvantage of using nZVI is that it can be corroded, and iron precipitation can occur. What is more, excessive Fe^{2+} can also consume $OH^{\bullet}$, resulting in a decrease of $OH^{\bullet}$ utilizations, and can lead to the formation of sludge, causing secondary pollution. Thus, optimization of nZVI amount used is required (Xue et al., 2023). A summary of the studies mentioned above can be found in **Table 1.3**.

Table 1.3: Summary of 3D electrochemical reactors studies with different particle electrodes

Anode	Particle electrode	Reactor setup	Effluent	Removal	Energy consumption	Reference
Stainless steel	GAC	batch	Simulated organic wastewater	76% COD	-	(Xiong et al., 2003)
Ti/Co/SnO_2-Sb_2O_5	GAC	batch	Paper mill wastewater	75% Color	650 kWh kg^{-1}_{COD}	(Wang et al., 2007)
Carbon plate	GAC	batch	Landfill leachate	80% COD 85% TOC	1.3 kWh kg^{-1}_{COD}	Nageswara Rao et al., 2009
Ti/SnO_2+Sb_2O_3 DSA®	GAC	batch	Heavy oil refinery wastewater	86% COD	58 kWh kg^{-1}_{COD}	(Wei et al., 2010)
Graphite plate	GAC	batch	Synthetic dye solution	100% Reactive black B 75% TOC	30 kWh kg^{-1}_{COD}	(Sowmiya et al., 2016)
BDD	GAC	flow-through	Synthetic greywater	86% COD 86% TOC 100% Color	30 kWh kg^{-1}_{COD}	(Andrés García et al., 2018)
Ti/IrO_2-RuO_2	Graphite	batch	0.1 M Na_2SO_4	100% Estriol	700 kWh kg^{-1}_{E3}	(Shen et al., 2017)
Ti/RuO_2–TiO_2	Multiwalled carbon nanotubes (MWCNTs)	batch	0.05 M Na_2SO_4	99% Diclofenac	-	(Pourzamani et al., 2018)
Ti/IrO_2-RuO_2	Nano zero-valent iron (nZVI)	batch	Pulp and paper secondary wastewater	88% COD 93% Color	10 kWh kg^{-1}_{COD}	(Chi et al., 2018)

1.3.1.3. Regeneration of particle electrode

One important factor that can lower the cost and make the 3D processes more sustainable is the ability of the particle electrode to get regenerated and allow its reuse. After being used several times, the contaminants adsorbed on the particle electrode surface cause the blockage of its pores. Once reached its adsorption capacity, the saturated particle is not very efficient for adsorption. In addition, its ability to trap and degrade the pollutant

deteriorates as well. Conventional regeneration processes include thermal, chemical, and microbial (when microorganisms are used for the regeneration) methods. The drawback of these methods is the high energy consumption, particle attrition and possible pore blockage, that can affect the adsorption capacity. An alternative to these methods is electrochemical regeneration, where the saturated particle electrode is placed between the anode and the cathode of a reactor. Upon the application of the electric current, enhanced desorption of the adsorbed contaminants occurs at the particle electrode surface, followed by their degradation via direct oxidation on the granules´ surface or anode and indirect oxidation due to the generated oxidant species (McQuillan et al., 2018). Enhanced desorption and electrodesorption is induced by local pH changes, local salinity concentration changes and electrostatic repulsion. There are several electrochemical regeneration methods, including anodic, cathodic, combined anodic and cathodic, electro-Fenton regeneration and electro-peroxone regeneration, as seen in **Figure 1.7** (Zhou et al., 2021).

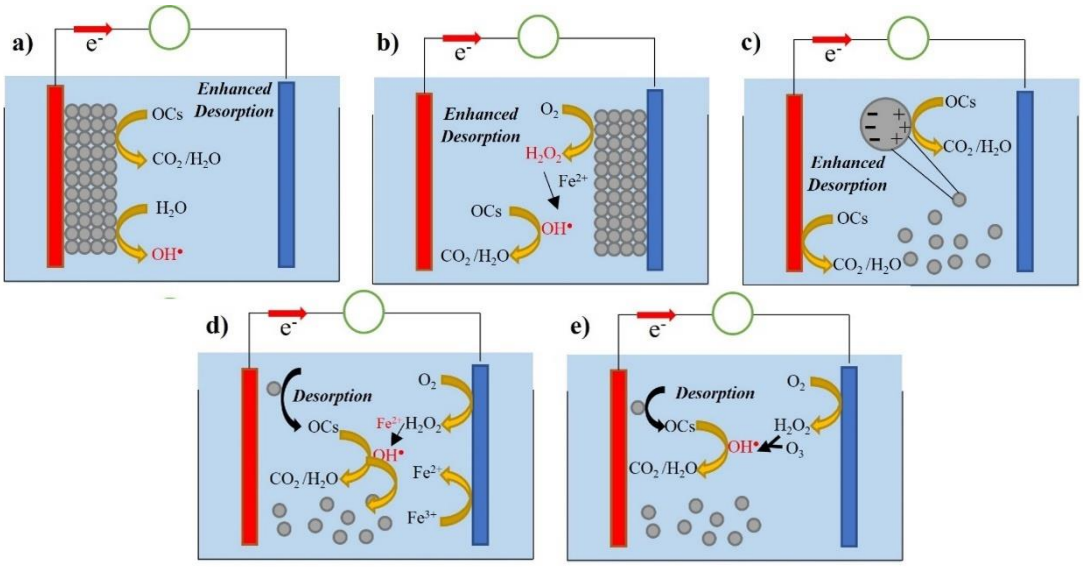

Figure 1.7: Schematic illustration of the various electrochemical regeneration methods of exhausted carbon adsorbents and their mechanisms: (a) anodic regeneration, (b) cathodic regeneration, (c) combined anodic and cathodic regeneration, (d) electro-Fenton regeneration and (e) electro-peroxone regeneration. Source: (Zhou et al., 2021)

Electrochemical regeneration efficiency depends on the utilized reactor configuration and on the operating parameters such as pH, electrolyte type and concentration, applied current density and treatment time. The advantages of the method compared to the conventional ones is that no additional chemicals are used, it can be performed in ambient

conditions, the structural properties of the particles are not significantly altered and the adsorbed contaminants can be simultaneously degraded during the process (McQuillan et al., 2018). It can thus be environmentally compatible, safer, selective and more efficient energetically and economically (Zhou et al., 2021). Another important advantage of electrochemical regeneration, in the case of 3D electrochemical systems, is the potential of in-situ regeneration of the particle electrode, without the need to remove it from the reactor. This can reduce the capital cost as well as the energy consumption, avoiding the steps of transportation and a separate regeneration operation. For example, Shi. et al. reported a study where GAC was regenerated in-situ while functioning as a particle electrode, packed between anode and cathode, for the degradation of amoxicillin in a 3D electrochemical system, where amoxicillin and TOC removal efficiencies reached 99% and 48%, respectively (Shi et al., 2020). Nyex™, a graphite intercalation compound, is another material that has been reported for the simultaneous adsorption and electrochemical degradation of trace organic pollutants. Acid violet 17 (AV17) dye was removed up to 98%, while regeneration of the material was also achieved (Mohammed et al., 2011). Nyex™ is a non-porous material, which can make the adsorption and desorption process of the contaminants faster, although its adsorption capacity is lower than porous materials. During the process, the wastewater passes through the electrochemical reactor containing the Nyex™ bed and once the adsorbent is saturated, voltage is applied, leading to the desorption and oxidation of the contaminants and thus regeneration of adsorbent (McQuillan et al., 2018).

To obtain more information of the possible lifetime of each particle electrode, the physicochemical changes on the surface of the particle electrode should be also considered during their regeneration. The surface of the materials can be oxidized directly by the applied current or indirectly by the produced active species. This oxidation may lead to the creation of additional adsorption sites for subsequent adsorption steps, but on the other hand, it can have a negative impact on the adsorbent lifetime (Mohammad et al., 2020). Sometimes, the loss of micropores after electrochemical regeneration can be compensated by an increase in the mesopore regions and thus maintenance of adsorption/electro-regeneration efficiency over several consecutive cycles. Organic contaminant properties such as carbon chain length, ring structure), functional groups, hydrophobicity and molecular size are also important factors affecting regeneration (Ersan et al., 2023). Ideally, combination of two or more different contaminants should be used for the study of the adsorption and regeneration capacity of the different particle

electrodes. Operating parameters, reactor configurations and regeneration kinetics are the last parameters to be investigated before scaling up a process (Zhou et al., 2021).

1.3.2. 3D electrochemical systems based on 3D-structured anode and/or cathode

An alternative way of constructing 3D reactors is by using electrodes with 3D geometries. Recent focus has been given to 3D, monolithic, porous flow through electrodes (Chaplin, 2018). The advantages of 3D structured electrodes compared to 2D plates include the large surface area that enhances adsorption, better catalytic activity due to the increased number of exposed catalytic sites, improved mass transfer, enhanced electrical conductivity and the reduced cost, due to the potential use of cheap materials for their construction. On the other hand, what needs to be carefully evaluated about 3D electrodes is their stability and the current distribution, which may be uneven for high specific surface area electrodes. The stability is a very important factor determining the practical application of 3D electrodes. Due to the increased surface area, 3D electrodes are susceptible to fouling and aging, which may lead to the decrease of the catalytic activity and changes of the structure and morphology of the electrode (Li et al., 2023). Coating or doping the surface of the electrodes could provide solutions to increase their stability, whereas a standard life cycle analysis is necessary to be applied before their scale-up. The uneven current distribution can be caused because of the low conductivity of the electrode material and can lead to the reduction of energy efficiency due to electrocatalytic "dead" zones (Li et al., 2023)

Similar to 2D electrodes, 3D electrodes can be used for anodic oxidation or cathodic reduction processes. Considering anodic oxidation, a 3D BDD film material on a foamed Cu/W surface was used as an anode for the removal of tetracycline and it was more efficient than the planar BDD electrode, consuming 8 times less energy (Miao et al., 2022). Another example is the 3D microporous foam BDD electrode that was used for the electrochemical oxidation of RB-19 dye, with a removal rate 350 times higher than that of the 2D BDD (Mei et al., 2019). Recently, there has been growing interest in utilizing Magnéli phase, especially Ti_4O_7, 3D electrodes as reactive electrochemical membranes (REMs). Ti_4O_7 offers several advantages, including its high OER overpotential resulting in a significant yield of $OH^{\bullet}$, high conductivity and chemical stability (Villanueva Martinez et al., 2023). For example, a 3D Ti_4O_7 tubular ceramic electrode, operated in cross-flow filtration mode, was used for the oxidation of p-

methoxyphenol, yielding up to 99% removal (Zaky and Chaplin, 2013). Another example of a 3D structured electrode is SnO_2-Sb, with macro-pores, that was fabricated and used in an electrochemical cell for the degradation of antibiotics in real wastewater. The 3D anode proved to perform better that the conventional 2D Ti/SnO_2-Sb anode, due to the increased electro-active surface area. Notably, the electrode exhibited remarkable stability as well, even after 200 test cycles (Yang et al., 2021) In another research, 3D porous Ti/Sb-SnO2-graphene electrode was employed as anode in a continuous flow reactor for the removal of 2,4–dichlorophenol, with up to 99% removal efficiency, having excellent stability as well (Asim et al., 2017). In the process of cathodic reduction, the most crucial parameter is the H_2O_2 generation and thus electrodes with high power for H_2O_2 generation are required. Carbon-felt and graphite-felt have traditionally been the preferred choices for cathodes. However, advancements in material development have led to the emergence of new options such as carbon sponges or carbon aerogels. Ganiyu et. al, for example, developed and employed a biomass derived carbon foam as a cathode in an electro-Fenton process for the degradation of antibiotics in different water matrices. The cathode exhibited excellent H_2O_2 production and antibiotic removal, while it also showed stability and reusability for ten cycles (Ganiyu et al., 2021). In addition to the development of new materials, the coating of conventional materials can be employed to enhance the production of H_2O_2 and improve the efficiency of cathodes. For example, both activated carbon cloth (Yu et al., 2015) and graphite felt (Jiao et al., 2020) were modified with carbon black and polytetrafluoroethylene (PTFE) and had their efficiency increased significantly during electro-Fenton processes. The cathodes demonstrated excellent stability as well. A summary of studies with 3D-structured electrodes can be found in **Table 1.4**. The above examples prove the great potential of 3D structured electrodes in electrochemical water treatment and their superiority to 2D electrodes. Future research should focus on some key issues for the scale up and application of these electrodes, such as their stability and low-cost and simple fabrication. Another key issue that needs to be considered is generation of toxic halogenated organic by-products and chlorinated by- products.

Table 1.4: Summary of 3D-structured electrochemical electrode systems.

3D electrode	Experimental Conditions	Removal	Energy consumption	Reference
3D BDD film material on foamed Cu/W surface (anode)	0.01 M Na_2SO_4, 30 mA cm^{-2}, batch	99% tetracycline hydrochloride 83% TOC	0.4 kWh g^{-1} TOC E_{Eo} 3.4 kWh m^{-3}	(Miao et al., 2022)
3D-BDD nickel foam substrate (anode)	0.1 M Na_2SO_4, 50 mA cm^{-2}, batch	100% Reactive blue 19 87% TOC	0.5 kWh g^{-1} TOC	(Mei et al., 2019)
3D porous (Ti_4O_7) tubular, ceramic electrode (anode)	0.01 M $NaClO_4$, 1.0 mA cm^{-2}, continuous mode recycled	100% p-methoxyphenol	-	(Zaky and Chaplin, 2013)
3D macro-porous SnO_2-Sb (anode)	Synthetic wastewater, 5 mA cm^{-2}, batch	100% ciprofloxacin 90% TOC	E_{Eo} 1.1 kWh m^{-3}	(Yang et al., 2021)
3D–porous Ti/Sb–SnO_2–Gr (anode)	0.5 M Na_2SO_4, 30 mA cm^{-2}, continuous flow	100% 2, 4–dichlorophenol 100% TOC	0.5 kWh g^{-1} TOC	(Asim et al., 2017)
Carbon foam (cathode)	0.05 M Na_2SO_4, 10 mA cm^{-2}, continuous flow	100% COD	0.03 kWh g^{-1} COD	(Ganiyu et al., 2021)
Carbon cloth modified with carbon black and polytetrafluoroethylene (cathode)	0.05 M Na_2SO_4, 5 mA cm^{-2}, flow-through E-Fenton	100% methyl orange 96% TOC	E_{Eo} 1.3 kWh/m^3	(Yu et al., 2015)
Graphite felt modified with carbon black and polytetrafluoroethylene (cathode)	0.05 M Na_2SO_4, 14 mA cm^{-2}, flow-through E-Fenton	96% Orange II	-	(Jiao et al., 2020)

1.3.3. 3D electrochemical systems applications

3D reactors have been employed for the treatment of a wide range of wastewaters, including chemical industry production wastewater, petroleum refinery wastewater, printing and dyeing wastewater, landfill leachate, coking wastewater, pig raising wastewater, papermaking wastewater, brown copper waste liquid from circuit board factories, coal chemical industry wastewater, and pesticide chemical production wastewater (Li et al., 2021; Zhang et al., 2013). The wastewaters mentioned above contain various organic contaminants, such as hydrocarbons, organic acids, phenolic

compounds, dyes, anionic surfactants and antibiotics, as well as inorganic contaminants, such as heavy metals, cyanide and nitrate, have been also treated with 3D electrochemical reactors (Li et al., 2021; Zhang et al., 2013). 3D electrodes of copper nets, porous RVC, graphite particles and graphite felt are among the electrodes that have been used in the treatment processes. 3D processes have been also combined with other conventional treatment methods in order to overcome the limitations of each treatment´s individual application and achieve higher degradation efficiencies. They have been used, for example, as a pretreatment method before the biological treatment of wastewater, in order to degrade organic components to more biodegradable ones by the following biochemical method. The two methods can be combined and work simultaneously, either by using a 3D anode or adding a biofilm on the particle electrode. A third electrode can be also introduced in the electro-Fenton system. This particle electrode could be a matrix to support heterogenous ferriferous oxide and thus provide the Fe^{2+} necessary for the Fenton reaction and function like a third electrode at the same time (Li et al., 2021). 3D electrolysis can be also combined with ozonation, where the added particle electrode could contribute to the system enhancement via several pathways. Zhan et al. claimed for example that O_2 can undergo two-electron electrochemical reduction at the GAC particle electrodes to form H_2O_2, which enhances the rate of O_3 reduction to $OH^{\bullet}$. Furthermore, O_3 may be electrochemically reduced to $O_3^{\bullet-}$ at the GAC particle electrodes, thus leading to the formation of $OH^{\bullet}$ (Zhan et al., 2019).

1.4. Reduced Graphene Oxide-based electrodes

Graphene (GR) is a single atom plane of graphite, that was discovered by mechanical exfoliation of graphite, back in 2004 (Novoselov et al., 2004). Graphene oxide (GO) is the oxidized form of a graphene molecule made from oxidation of graphite and in contrast with graphene (GR), it contains oxygen functional groups (hydroxyl, carboxyl, carbonyl and epoxy). GO is a hydrophilic and amorphous material with many defects and has weaker mechanical characteristics compared to graphene (Mohammed et al., 2020). Moreover, GO is an isolator, but can become electrically conductive reducing it, e.g., through thermal or chemical reduction, to reduced graphene oxide (RGO), which is also anti-corrosive (Chen et al., 2011; Mao et al., 2014; Morimoto et al., 2016; Zhang et al., 2020). RGO is characterized by its reduced number of functional groups, increased number of electroactive groups and structure similar to graphene. It combines properties

from both GO and graphene (Mohammed et al., 2020). RGO can be used as coating for conventional materials (metals, zeolite, graphite, carbon felt, GAC etc.) to enhance their conductivity, specific surface area and adsorption capacity and thus contaminants´ removal (Gao et al., 2011; Y. Liu et al., 2013).

There are several ways of coating RGO or GO on other materials. The reduction of GO can happen before or after the coating. One of the coating methods is electrophoretic deposition, where RGO particles can be deposited on an electrode of the opposite charge, under the effect of an electric field in a two-electrode cell. Another method is ink-coating, where an ink of the RGO has to be produced, using a binder, and then the electrode is immersed in the ink. Spin coating and spray coating are other common methods that are used. In spin coating, the prepared dispersion or solution is drop casted on rotating flat surfaces while spray coating includes the nebulization of RGO dispersions through a nozzle on 3D objects. Recently, hydrothermal methods have also been used for the simultaneous reduction of GO and its coating to other materials (Du et al., 2021; Garg et al., 2017).

An attractive characteristic of graphene-based materials is the possibility of fine-tuning of their electrical, physico-chemical and mechanical properties via introduction of dopants into the graphene network. N-doping of graphene has been reported to enhance the cathodic production of H_2O_2 (Su et al., 2019), while pyrrolic-N is considered to enhance the oxygen reduction to H_2O_2 (Li et al., 2020) and pyridinic-N groups are correlated with in-situ activation of H_2O_2 to $OH^{\bullet}$ (Su et al., 2019). Furthermore, a synergy between N and B dopants was reported for B,N co-doped materials for the anodic generation of O_3 at a carbon electrode (Baptista-Pires et al., 2021). In another study it was shown that doping of graphene sponge electrodes with hexagonal boron nitride (hBN) improved the adsorption of more hydrophobic organic contaminants via van der Waals and π-π interactions (Cuervo Lumbaque et al., 2022). On the other hand, doping with borophene promoted the higher generation of oxidants species such as H_2O_2, O_3 and $OH^{\bullet}$ (Cuervo Lumbaque et al., 2022). Furthermore, modification of RGO hydrogel with polydopamine can significantly improve the adsorption capacity for Pb^{2+} and Cd^{2+}, whereas N-doped graphene aerogel has been reported as an anode material for microbial fuel cells, enhancing power density (Yang et al., 2016).

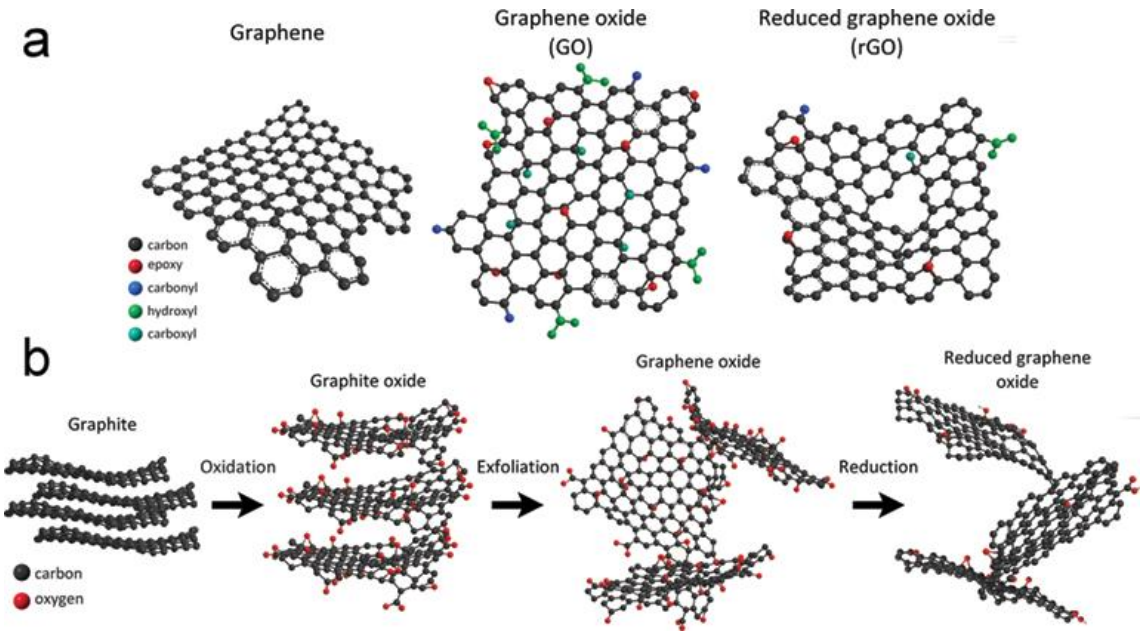

Figure 1.8: (a) Schematic chemical structures of graphene, GO, and GO. (b) Route of graphite to RGO. Source: (Jimenez-Cervantes et al., 2016)

Graphene-based materials have been applied for the removal of dyes, heavy metals, radionuclides and other contaminants from wastewater via adsorption (Ali et al., 2019; Wang et al., 2020). Graphene-based materials have been also reported for their ability to get their adsorption capacity restored via electrochemical regeneration. Pan et al. reported the in-situ electrochemical regeneration of graphene aerogel saturated with methylene blue. A column consisted of graphene aerogel was placed in close contact with the anode and water was pumped in the reactor, with a simultaneous voltage application, resulting in the simultaneous adsorption, desorption and degradation of methylene blue (Pan et al., 2018). RGO-iron oxide nanocomposites loaded with methylene blue were also regenerated electrochemically (Sharif et al., 2017). RGO/Fe_3O_4 composite was also reported to have its adsorption ability restored by Fenton-like catalytic oxidation (Shan et al., 2018).

Except for adsorption, RGO materials have been used for electrochemical oxidation applications as well. For example, they have been used as coating for cathodes, to enhance the generation and activation of H_2O_2. Some of the materials that have been coated with RGO are graphite and carbon felt, since these 3D materials have low cost, high surface area, high conductivity and porosity (Kim et al., 2018; Le et al., 2015; Mousset et al., 2016). For example, Le et al. modified carbon felt electrodes with RGO and used it as a cathode in an electro-Fenton process for the removal of dyes. RGO was electrodeposited

on the surface of the carbon felt and enhanced significantly the production of H_2O_2. The cathode showed good stability as well, since the mineralization ratio was maintained above 64% even after 10 cycles (Le et al., 2015). In another case, RGO/CNT/Fe_3O_4 hybrid aerogel has been utilized as cathode in an electro-Fenton system for efficient degradation of methylene blue, where the H_2O_2 generation was enhanced due to the ample porosity and high surface area of the cathode material (Chen et al., 2016).RGO coated graphite anode was able to efficiently decolorize Reactive Turquoise Blue 21, in a electrochemical cell with graphite as the cathode (Vaghela and Nath, 2020). Besides, our group recently reported RGO based sponges that were used as 3D electrodes, both anode and cathode, for the removal of persistent contaminants from water, using a one-pass flow through reactor (Baptista-Pires et al., 2021)

Fewer are the reports of graphene-based materials as particle electrodes in 3D electrochemical systems. Nitrogen-doped aerogel particle electrodes were used for the electro-catalytic oxidation of bisphenol A (Chen et al., 2017), while graphene/polyurethane particle electrodes were used for the electrochemical removal of levofloxacin (Guo et al., 2020). Polypyrrole/reduced GO aerogel particle electrodes were reported for the simultaneous reduction of hexavalent chromium (Cr(VI)) and oxidation of bisphenol A (Zhang et al., 2018). The reason for the combination of GO/RGO aerogels with other materials, such as polymers, is to increase the structural stability of the composite aerogel (Wang et al., 2023).

1.4.1. Antimicrobial properties of RGO coating

Graphene-based materials have also exhibited strong antibacterial activity. This activity can be attributed to the membrane stress induced by the sharp edges of graphene nanosheets, which can physically damage the cell membranes of the bacteria and thus their inactivation, due to the leakage of intracellular substrates. The functional groups present on these materials can induce interaction with bacterial cells and consecutive cell deposition (Liu et al., 2011). Another mechanism of bacteria inactivation is the oxidative stress which can disrupt the cellular functions and mechanisms, resulting in cellular inactivation and death. Oxidative stress can be caused from the ROS that are produced by graphene-based materials or the charge transfer between the cell membrane and the graphene-based materials (Mohammed et al., 2020). Also, lipid extraction from the bacterial cell membrane may occur, due to the strong van der Waals interaction between

graphene-based materials and the outer and inner bacterial membranes (Díez-Pascual, 2020).

GO and RGO have been used in dispersions showing high antibacterial activity (Liu et al., 2011). The antibacterial activity can be affected by the physicochemical properties and the surface functional groups of GO and RGO nanomaterials. For example, it was shown that larger GO nanosheets showed better inactivation performance towards inactivation of *E. coli* when in suspension, but smaller nanosheets were more effective as GO-based surface coatings (Zeng et al., 2017). This can be explained because the interaction between GO sheets, that are immobilized on some surface, and bacterial cells can be different than in GO suspensions (Perreault et al., 2015). Oxidative stress mediated by ROS and physicochemical properties, such as the porosity and surface roughness, of the GO-coated substrate can also affect bacteria inactivation (Yadav et al., 2017). Li et al. coated hydrated GO (hGO) on glass and silicone surfaces and showed that the coating was effective towards the killing of antibiotic-resistant *E. coli*. The coating showed great stability and durability as well (Li et al., 2016). The antimicrobial activity of GO coating was also proved for GO coated nitinol, that was developed for biomedical implants (Zhao et al., 2016). Hu et al. fabricated freestanding GO and RGO paper and demonstrated that its antibacterial activity was similar to GO and RGO dispersions (Hu et al., 2010). Choudhary and Das reported that the antimicrobial activity of GO and RGO in dispersion is higher than the activity of GO and RGO coated on aluminum plates. They claimed that after binding on the cell wall, GO and RGO in dispersion could penetrate into the cells and cause damage to the intracellular organelles, apart from the physical disruption, in contrast with the immobilized GO and RGO on the plates where penetration was restricted. Additionally, the surface of GO and RGO that could interact with bacteria is higher in dispersion than on the coated plate, as only one part of the plate is exposed to the bacteria and direct contact is required for the bacteria disruption. They also found that contact with GO and RGO-coated plates triggered intracellular ROS production. The RGO antimicrobial activity proved to be higher than GO, both in dispersion and immobilized, while lower number of cells adhered on the RGO-coated surface (Choudhary and Das, 2019). GO and RGO antibacterial activity has also been compared in other studies. Chen et al. reported that GO dispersions had higher antibacterial activity from RGO, considering membranes and oxidation stress, but conductive RGO had higher oxidation capacity that insulating GO (Liu et al., 2011). Akhavan and Ghaderi showed that RGO nanowalls had stronger antimicrobial activity from GO nanowalls, due to the

sharper edges and better charge transfer of RGO that resulted in more extensive membrane damage of the bacteria (Akhavan and Ghaderi, 2010). RGO dispersion was also reported to show enhanced antibacterial activity in the presence of an electric field by BDD in a 3D electrochemical system, which was maintained after the power cut as well, for an extended period of time, due to the capacitance of RGO (Qi et al., 2015).

Single component graphene-based nanomaterials have shown certain antibacterial activity, but the inactivation process is slow. To accelerate the process, various nanomaterials are functionalized on graphene-based materials enhance and induce tailor-made antimicrobial functionality (Zeng et al., 2017). Some examples of GO and RGO combined with other materials and have been reported to show antibacterial activity are RGO nanocomposites, decorated with iron oxide (Fe_2O_3) nanorods (Jana et al., 2020), starch-reduced GO-polyiodide nanocomposites (Narayanan et al., 2021), silver modified GO nanosheets (Ma et al., 2011), protamine-RGO paper (Feng et al., 2021) as well as RGO-Zn nanocomposites (Zhang et al., 2019). Graphene-based materials have been also used as electrodes in electrochemical processes. RGO–silver nanostructure coated carbon foam (rGO-Ag-CF) was fabricated and used as an electrode for the complete inactivation of *E. coli* and *Staphylococcus aureus*, using an electrochemical device powered up by a 1.5 V battery (Kumar et al., 2013). Wang et al. performed capacitive deionization disinfection utilizing an activated carbon electrode coated with cationic nanohybrids of GO-graft-quaternized chitosan for the inactivation of *E. coli* in a continuous flow cell, achieving up to 6 log bacterial removal (Yilei Wang et al., 2015). Besides, El-Deen et al. used asymmetric nanoporous graphene-based electrodes for the inactivation of E. coli in brackish water, achieving 98% bacterial removal (El-Deen et al., 2016).

CHAPTER 2 Objectives

The general objective of this doctoral thesis is to develop and optimize innovative electrochemical technologies based on 3D reactor and/or electrode geometries for (waste)water treatment.

More specifically, the objectives are:

1. To evaluate the performance of RGO-coated particle electrodes in a 3D electrochemical reactor for enhancing the removal of persistent organic contaminants:

   -To evaluate the effect of RGO coating on the performance of particle electrodes in terms of contaminants removal and energy consumption.

   -To explore methods of improving RGO coating in terms of stability, conductivity, and contaminants removal.

   -To examine the effect of the anode material on the 3D electrochemical reactor equipped with particle electrodes.

2. To evaluate the synergy between adsorption/electrosorption and electrochemical oxidation of persistent organic contaminants in a GAC-based 3D electrochemical reactor:

   - To compare a 2D and a 3D electrochemical process for the removal of persistent organic contaminants.

   -To investigate the simultaneous degradation of persistent organic contaminants and the regeneration of the adsorption ability of GAC.

   -To evaluate the effect of the electric field on the polarization of GAC and its performance in the system.

   -To examine the effect of GAC on the formation of adsorbable organic halides (AOX) and other chlorinated toxic byproducts (ClO^-_3, ClO^-_4).

3. To investigate the performance of 3D electrochemical reactor based on functionalized 3D graphene sponge electrodes for electrochemical disinfection:

. -To employ graphene-based sponge electrodes for the removal of *E. coli* from water.

-To examine the effect of atomic doping on the electrode's performance.

-To explore the inactivation mechanism of bacteria in the absence of chlorine species.

-To explore new strategies for decreasing the energy consumption of the system.

-To evaluate the application of the disinfection treatment in realistic conditions, using real tap water as a water matrix.

CHAPTER 3 Material and methods

3.1.1 Materials

Analytical standards for diatrizoate (DTR), carbamazepine (CBZ), DEET and iopromide (IPM) were purchased from Sigma-Aldrich. Sodium sulfate (Na_2SO_4) was also purchased from Sigma-Aldrich. All solutions were prepared using analytical grade reagents and Milli-Q water. Chemical structures and physicochemical properties of the above chemicals can be found in **Table 3.1.**

Table 3.1: Chemical structures and physico-chemical properties of target contaminants; molecular weight (MW), pKa, octanol-water distribution coefficient calculated based on chemical structure at pH 7.4 (CX LogD), polar surface area (PSA) and polarizability, i.e., ability to form instantaneous dipoles. Calculated CX logD values were collected by ChEMBL database. Polar surface areas and polarizability were collected from Chemspider.com database.

Organic compound (MW, g mol^{-1})	**Chemical structure**	**pKa**	**PSA, Å^2**	**Polarizability, Å^3**	**logD**
Iopromide (791.1)	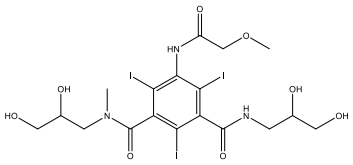	9.9[1]	169	56.4	-0.44
Carbamazepine (236.3)	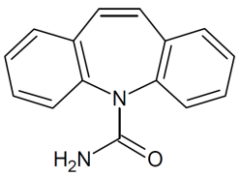	13.9[2]	47	28	2.77
Diatrizoate (613.9)	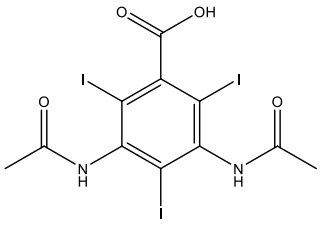	3.4[3]	96	39.8	-0.63
DEET (191.3)	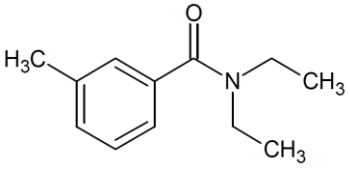	0.67[4]	20	23.3	2.50

Graphene oxide (GO) was provided as a GO water dispersion (0.4 wt%) from Graphenea S.L. (Spain). Boric acid, urea and Live/Dead BacLightTM bacterial viability kits were purchased as ACS reagents from Sigma Aldrich (Spain). Mineral wool template was purchased from Diaterm (Spain). Autoclave reactor was purchased from Techinstro. Stainless steel 316 was purchased from Wire Weaving Company (the Netherlands). Chromocult® Coliform agar and the cellulose ester filters (0.45 μm) were purchased from Merck (Spain). Luria-Bertani (LB) broth and Ringer solution were purchased from Sharlab (Spain).

3.1.2 Graphite granules coating

The graphite granules (GG) were coated with GO of 1 g L^{-1} concentration which was further reduced using a hydrothermal reactor at 170 ^{o}C for 16 h. More specifically, 50 g of the GG were added in a volumetric cylinder which was filled with GO up to 70 mL. After, the granules with the GO were moved to the hydrothermal reactor. For the nitrogen doped (NRGO) granules, urea was added to the GO solution, in concentration of 40 g L^{-1}. For the Mn_xO_y-NRGO granules, the method described from Wang et al. was followed (Yan Wang et al., 2015).

3.1.3 Chemical Analysis

Target organic contaminants were analyzed using a 5500 QTRAP hybrid triple quadrupole-linear ion trap mass spectrometer (Applied Biosystems, Foster City, CA, USA) in selected reaction monitoring (SRM) mode, equipped with a turbo Ion Spray source, coupled to a Waters Acquity Ultra-Performance™ liquid chromatograph (UPLC) (Milford, MA, USA). They were analyzed in electrospray (ESI) positive mode using an Acquity ultraperformance liquid chromatography (UPLC) HSS T3 column (2.1×50 mm, 1.8 μm, Waters) run at 30°C. The eluents employed were acetonitrile with 0.1% formic acid (eluent A), and milli-Q (LC-MS grade) water with 0.1% formic acid (eluent B) at a flow rate of 0.5 mL min^{-1}. The gradient was started at 2% of eluent A that was increased to 20% A by 3 min, further increased to 50% A by 6 min and further increased to 95% A by 7 min. It was kept constant for 2.5 min, before returning to the initial condition of 2% A by 9.5 min. The total run time was 11 min. The target organic contaminants were analyzed in a multiple reaction monitoring (MRM). The settings for the compound-

dependent parameters of each transition are summarized in **Table 3.2.**

Table 3.2: The optimized compound-dependent MS parameters: declustering potential (DP), collision energy (CE) and cell exit potential (CXP)) for each compound and each transition of the negative and positive mode.

Organic compound	Q1 Mass (Da)	Q3 Mass (Da)	DP	CE	CXP
Iopromide	791.72	572.9	156	35	20
	791.72	300	156	83	10
Carbamazepine	237.01	194.1	156	47	10
	237.01	193	156	47	10
DEET	193.05	120	176	23	14
	193.05	91.6	176	39	12
Diatrizoate	614.9	361	80	30	10
	614.9	233.1	85	33	10

Dissolved organic carbon (DOC) was determined as non-purgeable organic carbon (NPOC) using a total organic carbon analyzer (TOC-V CSH, Shimadzu, Kyoto, Japan). COD was measured using COD cuvette test kits (15-150 mg/L O_2 LCK 314) provided by Hach using a spectrophotometric method (APHA, 2017).

Free available chlorine (FAC), total chlorine (sum of FAC and combined chlorine) and ozone were measured with the N,N-diethyl-p-phenylenediamine (DPD) ferrous titrimetric method (APHA, 2017) using LCK 310 cuvette tests provided by Hach Lange Spain Sl (Barcelona), immediately after sampling.

The concentrations of chloride, chlorate and perchlorate were determined using high-pressure ion chromatography (HPIC) system (Dionex ICS-5000). The quantification limits for the measurements of Cl^-, ClO_3^- and ClO_4^- were 0.025 mg L^{-1}, 0.015 mg L^{-1} and 0.004 mg L^{-1}, respectively.

Hydrogen peroxide was determined using a spectrophotometric method using 0.01 M copper (II) sulphate solution and 0.1% w/v 2,9-dimethyl-1,10-phenanthroline (DMP) solution, based on the formation of Cu $(DMP)^+_2$ cation, which shows an absorption maximum at 454 nm (Baga et al., 1988).

Halogen-specific AOX analyses, i.e. adsorbable organic chlorine (AOCl), adsorbable organic bromine (AOBr) and adsorbable organic iodine (AOI) were conducted according to the previously published methodology (von Abercron et al., 2019). 20 mL samples

were quenched with 40 μL of 40 g L^{-1} Na_2SO_3 per 3 mg L^{-1} of free chlorine, acidified to pH 2 and extracted on two activated carbon cartridges using a TXA-04 AOX Adsorption Unit. Afterwards, the cartridges were washed with 10 mL of 10 mM $NaNO_3$ solution to remove the inorganic halides. The cartridges were then combusted at 1000ºC in a horizontal furnace AQF-2100H equipped with GA-210 Gas adsorption unit (COSA-Mitsubishi). The halides formed were analyzed using a Dionex Integrion HPIC system.

To analyze the surface of GAC granules, scanning electron microscopy (SEM) analyses were performed on a FEI Quanta FEG (pressure: 70Pa; HV: 20kV; and spot: four).

The Langmuir surface area and pore size distribution were determined by N_2 adsorption-desorption at 77K using Micromeritics ASAP® 2420 Accelerated Surface Area and Porosimetry System.

3.1.4 3D sponge electrode material characterization

Zeta potential of BRGO and NRGO was measured using Zetasizer Nano ZS (Malvern Panalytical Ltd) operating with a 633 nm laser and using an aqueous solution at pH 7.
A FEI Quanta FEG (pressure: 70Pa; HV: 20kV; and spot: 4) was used for the SEM analysis of the morphology of the sponges.
XPS analysis was carried out in ultra-high vacuum (base pressure 1-10 mbar) using a Phoibos 150 analyzer (SPECS GmbH, Germany) with a monochromatic aluminium Kalpha x-ray source (1486.74 eV). The energy resolution of a sputtered silver foil was 0.58 eV, as determined by the FWHM of the Ag 3d5/2 peak.
XRD analysis was performed with a X'pert multipurpose diffractometer using a Cu Kα radiation (l = 1.540 Å), at room temperature. It was equipped with a vertical θ–θ goniometer (240 mm radius) with fixed sample stages that do not rotate around the Ω axis as in the case of Ω–2θ diffractometers. An X'Celerator detector was utilized, which is an ultrafast X-ray detector based on real- time multiple strip technology. The diffraction pattern was recorded with a step size of 0.03 °C and a time per step of 1,000 seconds, between 4 °C and 30 ºC.

3.1.5 Microbiological analysis

Preparation of stock cultures: An overnight culture of *E. coli* (ATCC 700078) in LB broth was used for the experiments at a concentration of ca. 10^8–10^9 CFU mL^{-1}. Working concentrations were adjusted to approximately 10^5–10^6 CFU mL^{-1} by diluting the overnight culture in sterile Ringer solution for all experiments except those where the effect of the initial cell concentration was investigated. In the latter case, the initial *E. coli* concentration was adjusted to ~10^7 CFU mL^{-1} by centrifuging the overnight culture for 10 min at 3,500 rpm (Eppendorf 5804R) and discarding the supernatant to remove chloride from the LB medium to avoid its impact on the conductivity of the supporting electrolyte. In the experiments conducted at 10^5–10^6 CFU mL^{-1}, the initial chloride concentration was ~30 mg L^{-1}, derived from the LB broth. Nevertheless, analysis of chlorine formation at significantly higher chloride concentrations (i.e., 20 mM NaCl) was conducted to exclude any contribution of chlorine species in the disinfection, in accordance with our previous study (Baptista-Pires et al., 2021). The samples from electrochemical disinfection experiments were immediately preserved at 4 ºC.

Determination of cell concentration: The abundance of *E. coli* was determined using the membrane filtration technique and serial dilutions of collected samples and Chromocult® Coliform Agar medium (Merck). Briefly, samples were serially diluted 1:10 in sterile Ringer solution followed by filtration of 1 mL of the correspondent dilutions through 0.45 µm pore size cellulose filters (Merck) that were then placed in Chromocult agar plates and incubated overnight at 37 ºC. After this period, dark-blue colonies (i.e., *E. coli*) were counted and the bacterial concentration was calculated *i)* before, *ii)* immediately after treatment, and *iii)* after 16 h of storage in the dark and at 37 ºC to assess potential regrowth of electrochemically damaged *E. coli*. The regrowth experiment was conducted at 37 ºC, which is the optimal temperature for the growth of *E. coli* according to previous studies (Doyle and Schoeni, 1984; Gorito et al., 2021; Noor et al., 2013).

Cell viability: The viability of treated *E. coli* cells was estimated by epifluorescence microscope (Nikon, 80i) after staining with the Live/Dead bacterial viability kit (Invitrogen Molecular Probes, Inc.). 50 mL of treated water samples were centrifuged at 4,500 rpm for 20 min (Eppendorf 5804R). After removing the supernatant, they were resuspended in 5 mL of Ringer and 1 mL of resuspended sample was exposed to a mix of

SYTO® 9 and Propidium Iodide (PI) mixture solution and incubated for 15 min in the dark at room temperature. Stained samples were then prepared-on slides and images were randomly captured using an image analysis software (NIS-Elements BR).

Cell morphology: To assess the effect of the electrochemical treatment on the morphology of *E. coli* cells, treated samples were fixed and visualized under a field emission scanning electron microscope (FESEM). Briefly, samples were fixed with a 2.5% glutaraldehyde solution buffered with 0.1M sodium cacodylate, pH 7.4, at 4ºC for 2 h. Fixed samples were then washed and progressively dehydrated with ethanol (50%, 75%, 80%, 90%, 90%, 95% and absolute ethanol × 3) at 20 minute intervals. Dehydrated samples were then dried by the critical point method (Emitech, Germany, model K 850 CPD) and finally coated with carbon in an evaporator (Emitech, Germany, model K950 Turbo Evaporator). Observations were carried out in a field emission scanning electron microscope (model S4100, HITACHI, Japan). Images were digitally recorded and processed with the Quartz PCI program (Quartz Imaging Corporation, Canada) with a resolution of 2516 × 1937 pixels.

CHAPTER 4 RGO-coated graphite granules as particle electrodes in 3D electrochemical reactor for the reduction of persistent contaminants

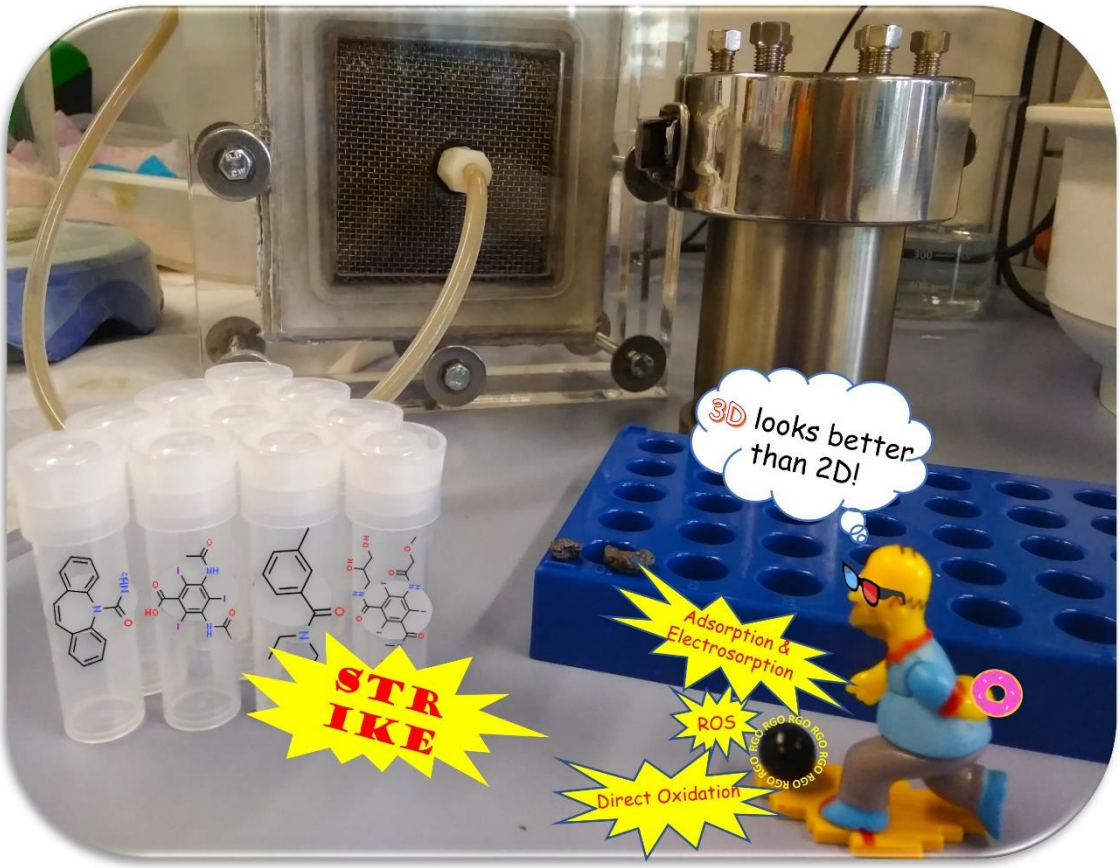

4.1 Framework

Increasing consumption of anthropogenic chemicals in the modern society has severe consequences for both the environment and human populations. Many of these chemicals are persistent and hazardous for both human health and ecosystems. Current conventional wastewater treatment technology is ineffective towards their removal, and they can pass unmodified through sewage treatment plants (Rizzo et al., 2019). Novel technologies that can effectively eliminate these contaminants and are better suited for small scale application and decentralization will be required. Electrochemical systems are well-suited to be implemented for the on-site treatment of contaminated water because they do not use chemical reagents, do not form a residual waste stream, operate at ambient temperature and pressure, are robust, versatile and have a small footprint (Radjenovic and Sedlak, 2015).

Electrochemical water treatment is typically performed using conventional two-dimensional (2D) reactors. Given that electrochemical degradation of contaminants is a surface-based reaction, 2D reactor design results in higher mass transfer limitations and thus higher energy consumption. This energy consumption of electrochemical systems can be significantly reduced using three-dimensional (3D) reactors due to the great increase of surface area available for electrochemical reactions and lower mass transfer limitations. More efficient degradation of contaminants would also lower the formation of their by-products and the energy consumption (Cañizares et al., 2004; Zhang et al., 2013). With the addition of a material between the two main electrodes, named particle electrode, 2D electrochemical processes can be converted into a 3D one. When the 3D reactor functions in open circuit (OC), the particles function as adsorbents, due to their large surface area and porosity. Upon the application of an external electric field, they get polarized resulting in the formation of charged microelectrodes with one anodic and one cathodic side. Thus, electrosorption also occurs. Besides adsorption and electrosorption, direct and indirect (due to the in-situ generation of strong oxidants like, $OH^{\bullet}$, H_2O_2, Cl_2/HOCl/OCl^-) electro-oxidation occurs on the surface of the polarized particles, contributing to the degradation of the contaminants (J. Ma et al., 2021; Zhang et al., 2013). Graphite is a material with low electrical resistivity, chemical stability and low cost, which make it eligible for use as a particle electrode (Li et al., 2021; J. Ma et al., 2021) and has indeed been used before as such, improving the efficiency of the 3D systems (Huang et al., 2018; Li et al., 2021; Shen et al., 2017). Graphene oxide (GO) is made from

oxidation of graphite and in contrast with graphene (GR), it contains oxygen functional groups. GO is nonconductive, but it can become conductive when it gets reduced to reduced graphene oxide (RGO), which is also anti-corrosive (Chen et al., 2011; Mao et al., 2014; Morimoto et al., 2016; Zhang et al., 2020). RGO can be used as coating for conventional materials (metals, zeolite, graphite, carbon felt, granular activated carbon (GAC) etc.) to enhance their conductivity, specific surface area and adsorption capacity and thus contaminants removal (Gao et al., 2011; Y. Liu et al., 2013). Due to the oxygen functional surface species of RGO, when polarized by an electric field, coated materials can promote the charge transfer with the contaminants, which leads to their degradation (Radjenovic and Sedlak, 2015).

This work aims to increase the performance and energy efficiency of 2D electrochemical processes by introducing graphite granules with RGO-based nanostructured coatings between the terminal electrodes, that function as particle electrodes. Two different anode materials are tested, a highly oxidizing boron-doped diamond (BDD) anode capable of producing hydroxyl radicals ($OH^{\bullet}$), and low oxidizing power anode, Ti/RuO_2-IrO_2.

4.2 Experimental set-up

A flow-through electrochemical reactor equipped with a mesh anode (80 × 80 × 1.3 mm) and a stainless-steel cathode of the same dimensions was used for the experiments. One of the anodes tested was Nb/BDD (DIACHEM® electrode, Condias, Germany), both sides of the niobium substrate coated with 4 µm of BDD thin film, whereas the other one was Ti/RuO_2-IrO_2. The total volume of the 2D reactor was 250 mL, while the 3D packed bed of graphite granules comprised approximately 65 mL, 26% of the total reactor volume. The granules were not in direct contact with the main electrodes and were separated from them with a plastic mesh. The anode was positioned at the bottom of the reactor, and water was circulated in the direction from anode to cathode. The interelectrode distance was 3.5 cm. The experiments were conducted in batch mode using 1 L of 20 mM Na_2SO_4, in Milli-Q water, spiked with the target contaminants at 2 µM initial concentration. The flowrate of recirculation was 475 mL min^{-1}. The experiments duration was 6 h. Chronopotentiometric experiments were conducted at 640 mA of applied anodic current (i.e., current density calculated versus the projected anode surface area of 100 A m^{-2}) using a BioLogic multi-channel potentiostat/galvanostat VMP-300 and a leak-free 1 mm diameter Ag/AgCl reference electrode (Harvard Apparatus) placed in the proximity of

the anode. All potentials in this manuscript are expressed versus Standard Hydrogen Electrode (V/SHE). Experiments in the OC mode, i.e., without the application of current to investigate the adsorption of pollutants (ADS), and in an electrochemical system without the addition of the graphite granules packed bed (2D) were also performed. All samples were quenched with methanol and frozen immediately after sampling. The scheme of the experimental set-up can be seen in **Figure 4.1**.

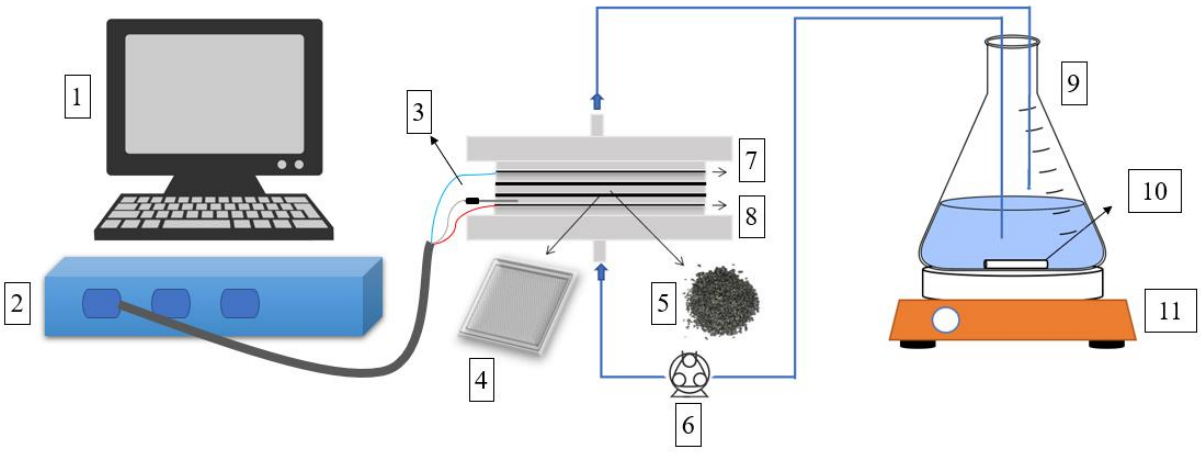

Figure 4.1: Scheme of the experimental set-up used in adsorption (ADS), two-dimensional electrooxidation (2D ELOX) and three-dimensional electrooxidation (3D ELOX) experiments. (1) computer for control of current and data acquisition, (2) potentiostat, (3) reference electrode, (4) inert mesh holder, (5) graphite granueles packed bed, (6) peristaltic pump, (7) stainless steel cathode, (8) boron-doped diamond (BDD) anode, (9) secondary effluent reservoir, (10) magnet, (11) magnetic stirrer.

The experiments were performed in duplicates and average values, with standard deviations, were used for the graphs.

The coating method of the graphite granules as well as chemical analysis are described in Chapter 3.

4.3 Results and discussion

The apparent removal rate constants (k, h^{-1}) of the contaminant removal were expressed in h^{-1} and estimated using the linear regression first-order decay model fit to the data, with coefficient $R^2 \geq 0.9$. The synergy between adsorption (ADS) on the granules and the electrochemical oxidation/electrosorption in the 3D system can be calculated using the following equation:

$$Synergy\ (\%) = \frac{k_{3D} - k_{2D} - k_{ADS}}{k_{3D}} \qquad \text{(eq. 1.1)}$$

The electric energy per order ($E_{EO,}$ kWh m^{-3}) was calculated using the following equation, where I (A) is the applied current, U (V) the total cell voltage, V (L) the volume, c_o and c (μM) the initial and final concentration and t (h) the reaction time required to achieve one order of magnitude of removal.

$$E_{EO} = \frac{U \cdot I \cdot t}{V \cdot log\frac{c_o}{c}} \qquad \text{(eq. 1.2)}$$

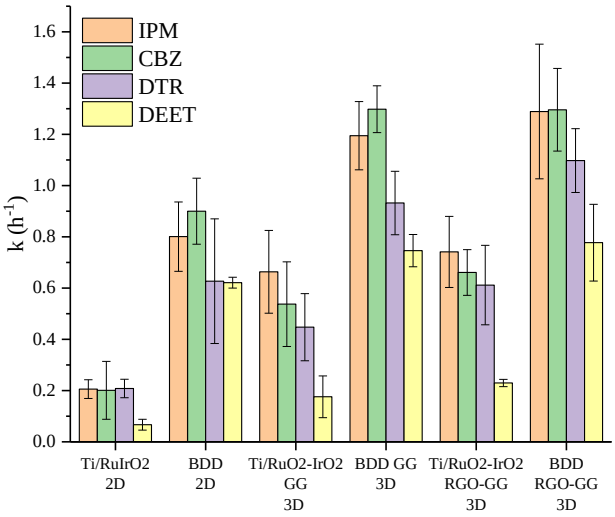

Figure 4.2: Apparent first-order removal rate constants (k, h^{-1}) for: iopromide (IPM) carbamazepine (CBZ), diatrizoate (DTR) and N,N-diethyl-meta-toluamide (DEET) in the different experiments. Ti/IrRuO$_2$ and BDD were the anode materials. 2D stands for the process without particle electrode; 3D is the process with particle electrodes; GG: graphite granules; RGO-GG: RGO coated graphite granules.

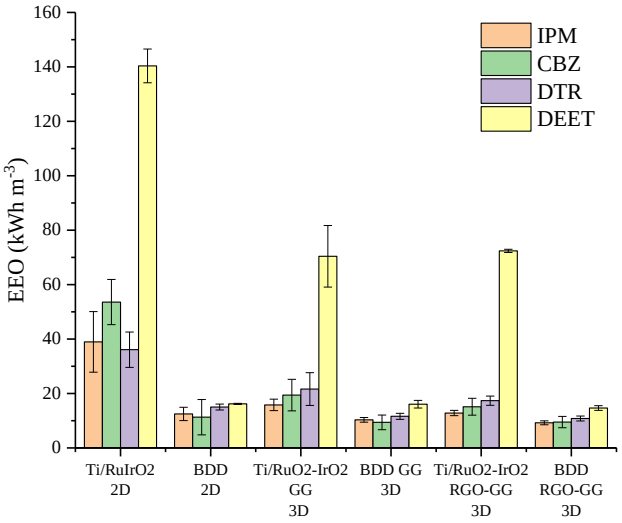

Figure 4.3: Electric energy per order (E_{EO}, kWh m^{-3}) for: IPM, CBZ, DTR and DEET in the different experiments. Ti/RuO_2-IrO_2 and BDD were the anode materials. 2D stands for the process without particle electrode; 3D is the process with particle electrodes; GG: graphite granules; RGO-GG: RGO coated graphite granules.

Table 4.1: Synergies between electrochemical oxidation and adsorption/electrosorption in the 3D system with graphite granules (GG) and RGO coated graphite granules (RGO-GG) for the who anode materials, BDD and Ti/RuO_2-IrO_2.

	Iopromide	**Carbamazepine**	**Diatrizoate**	**DEET**
Ti/$IrRuO_2$ 3D GG	37.9%	-3.6%	39.1%	-21.3%
BDD 3D GG	17.8%	17.6%	28.4%	0.5%
Ti/$IrRuO_2$ 3D RGO-GG	60.5%	58.2%	64.7%	10.7%
BDD 3D ELOX RGO-GG	27.7%	28.4%	22.3%	20.7%

In **Figure 4.3,** the removal rates of the contaminants for the various experiments conducted can be seen. The removal rates are higher in the experiments where BDD was used as anode, in comparison with the experiments in which Ti/RuO_2-IrO_2 was used as anode. BDD has higher overpotential for oxygen evolution and thus the oxidation of the contaminants on its surface is more efficient. Correia-Sá et al. also compared a Ti/RuO_2-IrO_2 anode with a BDD anode for the degradation of carbamazepine and found that

although both could reach 100% carbamazepine removal, BDD removal rates were faster in their case as well (Correia-sá et al., 2021). Similar results were reported in other studies comparing Ti/RuO_2-IrO_2 and BDD anodes (Đuričić et al., 2023; Okur et al., 2022). By adding graphite granules as particle electrodes (3D GG), the removal rate increased e.g., for IPM, from 0.21 h^{-1} to 0.66 h^{-1} and from 0.80 h^{-1} to 1.19 h^{-1} for Ti/$IrRuO_2$ and BDD anodes, respectively. Coating the granules with RGO (RGO-GG) further increased the removal rates to 0.74 h^{-1}, for Ti/$IrRuO_2$ and 1.29 h^{-1} for BDD. The synergy increased from 37.86% (GG) to 60.49% (RGO-GG) for Ti/RuO_2-IrO_2 and from 17.78% (GG) to 27.69% (RGO-GG) for BDD (**Table 4.1**).

Higher synergies in the case of Ti/$IrRuO_2$ can be attributed to the lower kinetic rates of the 2D process when using this anode. This can be explained by the difference in the production of oxidant species. BDD promotes the extensive production of $OH^{\bullet}$ and sulfate radicals, which contribute to the removal of organic contaminants (Farhat et al., 2015; Radjenovic and Sedlak, 2015; Sopaj et al., 2015). Furthermore, O_3 and H_2O_2 can be generated on BDD anodes (Michaud et al., 2003). Considering the low adsorption capacity of the granules (Hussain et al., 2013), the synergy can be attributed mainly to the electrosorption and direct/indirect oxidation on the graphite granules.

The E_{EO} in the system with BDD as anode was lower than in the system with Ti/RuO_2-IrO_2 as anode (**Figure 4.3**). Introducing the graphite granules in the Ti/RuO_2-IrO_2 system achieved to decrease the E_{EO} e.g., for IPM from 38.9 kWh m^{-3} to 15.8 kWh m^{-3}, while coating the graphite granules with RGO further reduced the E_{EO} to 12.8 kWh m^{-3}. In the BDD system, the E_{EO} was 12.5 kWh m^{-3} in the 2D system, and it was reduced to 10.3 kWh m^{-3} and 9.2 kWh m^{-3} when graphite granules and RGO-coated graphite granules were used as particle electrodes, respectively.

The coated graphite granules performed better overall in comparison with the uncoated ones. RGO can enhance conductivity, the specific surface area and the adsorption capacity of the granules (Gao et al., 2011). Chen et al. also enhanced the removal rate of bisphenol A (BPA) to 88% using nitrogen-doped graphene aerogel as particle electrodes, in comparison with 83% removal when activated carbon was used as particle electrode and 76% when the 2D system was used. They attributed the difference in the performance of the particle electrode to the higher specific surface area and more abundant porosity of RGO aerogels compared to activated carbons. Also, the 3D interconnected structure of the nitrogen-doped graphene aerogels was beneficial for electron transfer and their higher

conductivity facilitated their polarization, thus making them more effective as particle electrodes (Chen et al., 2017). Zhang et al. combined the RGO aerogels with polypyrrole (Ppy) for the removal of both Bisphenol A and chromium (Cr(VI)). Removal efficiency of BPA reached 99%, higher than the system with RGO aerogels without polypyrrole, activated carbon (AC) particle electrode and the 2D system, that were 94%, 90% and 87% respectively. For Cr (VI) the removal rates were 98% (Ppy+RGO), 92% (RGO), 90% (AC) and 88% (2D) respectively. Polypyrrole further improved the conductivity of the particles, thus enhancing the removal of the contaminants (Zhang et al., 2018). Besides, a color change was observed in the effluent, which could be because of the corrosion of the graphite granules from the oxidant species produced (Liu et al., 2017). When the RGO-coated granules were used, the color formation was less noticeable, which means that the RGO coating could also protect the granules from corrosion.

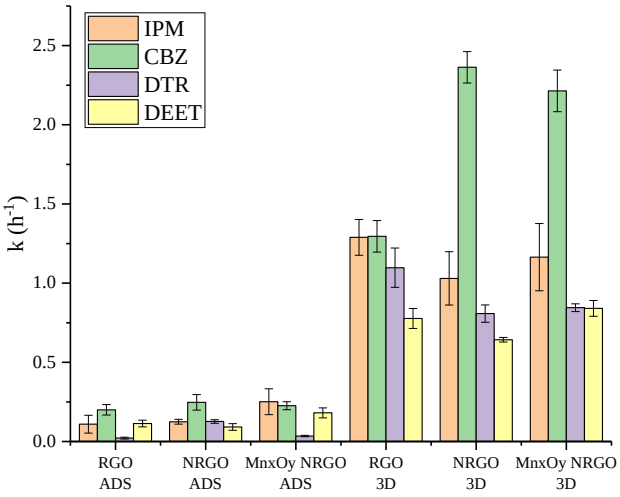

Figure 4.4: Apparent first-order removal rate constants (k, h^{-1}) for iopromide (IPM) carbamazepine (CBZ), diatrizoate (DTR) and DEET for adsorption (ADS) and 3D system using RGO coated granules (RGO), nitrogen-doped RGO coated granules (NRGO) and manganese oxide and nitrogen co-doped RGO coated granules (Mn_xO_y-NRGO).

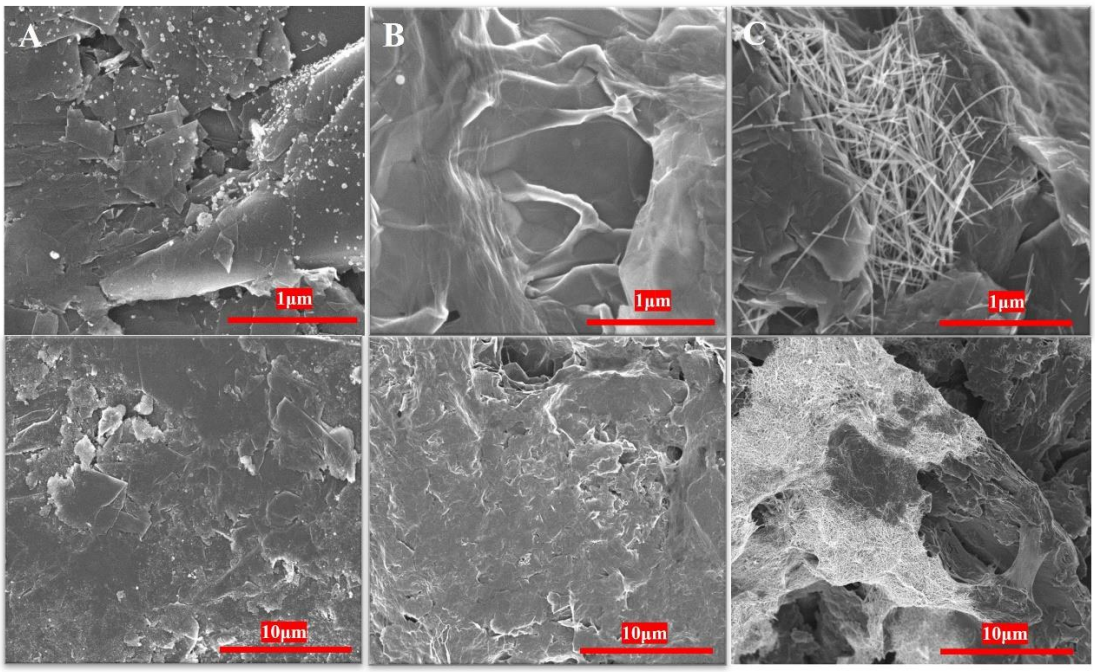

Figure 4.5: SEM images of the (A) graphite granules, (B) NRGO coated granules and (C) Manganese Oxide-NRGO coated granules (Mn_xO_y-NRGO)

As it can be seen in
Figure 4.4, doping the RGO-coated graphite granules with nitrogen or/and manganese oxide managed to increase the adsorption rate of the target organic contaminants. More specifically, the apparent removal rate of IPM increased from 0.11 h^{-1} to 0.13^{-1} and 0.25^{-1} when the granules were doped with nitrogen and nitrogen-Mn_xO_y respectively. The trend was the same for the rest of the contaminants. In the 3D process, doping the RGO-coated granules with nitrogen and co-doping with nitrogen and Mn_xO_y did not have a significant impact in the removal rates. Only in the case of CBZ, the rates showed a considerable increase from 1.29 h^{-1} (RGO) to 2.36 h^{-1} (NRGO) and 2.21 h^{-1} (Mn_xO_y -NRGO) respectively. This can be attributed to the positive charge of CBZ (pKa = 13.9) in the pH that the experiment was conducted, while manganese oxide is expected to have a negative charge (Sergienko et al., 2023). In the case of IPM, the removal rate slightly decreased, from 1.29 h^{-1}, for RGO, to 1.03 h^{-1} and 1.16 h^{-1} for NRGO and Mn_xO_y-NRGO respectively. For DTR, the rate decreased from 1.09 h^{-1} (RGO) to 0.81 h^{-1} (NRGO) and 0.85 h^{-1} (Mn_xO_y -NRGO). Finally, for DEET the rate decreased from 0.77 h^{-1} (RGO) to 0.64 h^{-1} (NRGO) but increased to 0.84 h^{-1} when Mn_xO_y was added (Mn_xO_y -NRGO). The difference in the impact can be attributed to the properties of each contaminant. The enhancement of the removal rate was achieved for the contaminants with higher logD values and lower polarizability, CBZ and DEET. The higher hydrophobicity and lower

polarity of these compounds benefit Van der Waals and π-π interactions between them and the N-doped RGO granules. Using different dopants could functionalize the surface and tailor the electrocatalytic activity of the RGO coated granules for the removal of specific groups of contaminants, as it was seen previous studies as well (Baptista-Pires et al., 2021; Cuervo Lumbaque et al., 2022).

Manganese oxides have large surface areas and microporous structures. There are few studies reporting the application of manganese oxide in water treatment. For example, manganese oxide nanostructures have been reported for the electrooxidation of aniline, formaldehyde, phenol, organic acids and volatile organic contaminants. Moreover, its characteristics allow the efficient adsorption of metals from wastewater, by retaining ions inside the 3D network (Sergienko and Radjenovic, 2020). Manganese oxide electrodeposited on metallic titanium (Ti) and titania nanotubes (TiO_2-NTs) enhanced the degradation of phenol and COD, due to the production of $OH^{\bullet}$ and enhanced charge transfer (Massa et al., 2017). Manganese oxide coating has been also reported to improve metal adsorption on materials such as sand (Han et al., 2006b), GAC (Fan and Anderson, 2005), zeolites (Han et al., 2006a), carbon nanotubes (CNTs) (S. G. Wang et al., 2007) and graphene oxide (GO) suspension (Li et al., 2013), by increasing their specific surface area.

Figure 4.5 shows SEM images of the graphite granules, with and without the RGO coating. Graphite (Figure 1.3A) tends to exhibit compact stacks with well-defined sharp edges and smooth surface. On the other hand, RGO (Figure 1.3B) exhibits smoother edges and wrinkled structure. Due to thinner layers of RGO, SEM images are displayed more transparent (Aradhana et al., 2018). In Figure 1.3C, the rods-like shapes may represent the manganese oxide, as reported also by Wang et al., whose reported method was followed for the coating (Yan Wang et al., 2015). Similar SEM images of Mn_xO_y-RGO were reported in other studies as well (Z. Li et al., 2017; Xavier and Vinodhini, 2023).

.

4.4 Concluding remarks

Converting a 2D electrochemical system to a 3D, by adding graphite granules as particle electrodes, was able to improve its removal efficiency and reduce the energy demand for the removal of persistent organic contaminants. Even when a low oxidizing power anode (Ti/RuO_2-IrO_2) was used, a synergy between adsorption and electrochemical

oxidation/electrosorption was observed. Coating the graphite granules with RGO further increased this synergy as well as the removal rates of the contaminants and decreased the energy consumption. Co-doping of the RGO coating with nitrogen and manganese oxide improved the adsorption of the granules.

As shown in another study with GAC (Norra and Radjenovic, 2021), the particle electrode material can be also regenerated in-situ while it can also limit chlorine by-products and adsorbable organic halogens (AOX) produced during electrochemical processes. Coating the graphite granules with RGO does not only increase its conductivity but could also protect it from corrosion. Thus, optimizing the coating and coupling RGO with other materials could increase the removal efficiency and decrease the energy demand of conventional methods.

This study opens a new horizon on the evolution of the conventional systems used in electrochemistry, which could be applied with a low cost and could tackle one of the main drawbacks of electrochemical treatment systems, which is the high energy demand. It also shows the possibility of tailoring the coated granules using different materials.

CHAPTER 5

Removal of persistent organic contaminants from wastewater using a hybrid electrochemical-granular activated carbon (GAC) system.

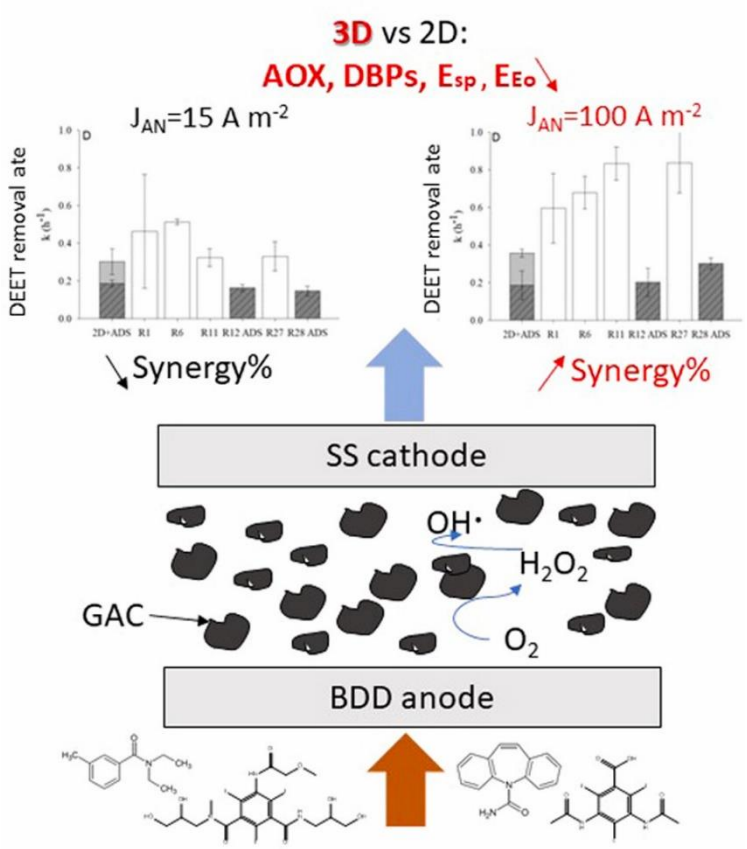

Chapter 5

5.1 Framework

Electrochemical processes are among the most promising and emerging technologies in the field of (waste)water treatment, presenting various advantages, such as no addition of chemicals, versatility and robustness of operation when treating contaminated water of different origin, and compact design, which makes them very well suited for decentralized and distributed treatment systems (Radjenovic and Sedlak, 2015). Nevertheless, the main drawback of conventional, two-dimensional (2D) electrochemical reactors are high mass transfer limitations governing the oxidation or reduction of the contaminants at the electrode surface, resulting in high energy consumption and operational costs(Cañizares et al., 2004; Zhang et al., 2013). In addition, anodic oxidation of chloride that is present in virtually any water source and wastewater leads to the formation of chlorine (i.e., Cl_2, $HOCl/OCl^-$), a long-lived oxidant species that reacts with the organic matter to form persistent and toxic chlorinated byproducts (Bagastyo et al., 2011; Radjenovic and Sedlak, 2015). The removal of organochlorine byproducts, both chlorinated aromatics and low molecular-weight compounds (e.g., trihalomethanes, THMs) is typically achieved using granular activated carbon (GAC) (Cuthbertson et al., 2019; Jiang et al., 2017). Bench-scale studies demonstrated a successful reduction of chlorinated byproducts formed in electrochemical treatment by a GAC post- treatment (Rajkumar et al., 2005), as well as overall enhanced performance of electrochemical treatment by adding GAC as both pre- and post-treatment (Rogers et al., 2018).

Due to its good electrical conductivity and high specific surface area, GAC was also employed as a particle electrode to construct three-dimensional (3D) electrochemical systems, resulting in a higher electroactive surface area and shorter distances for mass transfer of trace contaminants (Zhang et al., 2013). Great majority of studies on hybrid GAC-electrochemical systems was based on GAC bed placed between the vertically positioned anode and cathode and in direct contact with one or both terminal electrodes, typically cathode (Kılıç et al., 2007; Zhan et al., 2019). However, direct polarization of GAC at higher currents and potentials can cause its attrition and compromise the treatment performance(Gedam and Neti, 2014; Kılıç et al., 2007). If the applied electric field is large enough, conductive GAC particles do not need to be in contact with the terminal electrodes and are polarized due to the shift in their electric charge, converting each GAC particle into a charged microelectrode, with one anodic and one cathodic side

(Zhang et al., 2013). Charged GAC particles can thus induce electrosorption/desorption of contaminants and their Faradaic reactions, thus enabling electrolytic degradation of the adsorbed organics (McQuillan et al., 2018). In addition, GAC can enhance the system performance and increase the production of hydroxyl radicals ($HO^{\bullet}$) through the formation of H_2O_2 at cathodically polarized particles (Bañuelos et al., 2014) and its decomposition by GAC to $HO^{\bullet}$ (Fortuny et al., 1998). The amount of H_2O_2 formed at the activated carbon cathode was found to increase linearly with the increase in dissolved oxygen (DO) content (Bañuelos et al., 2014). The anode-cathode flow direction is often the preferred configuration for 3D flow-through reactors as it minimizes the impact of undesirable side reaction (e.g., H_2 evolution) and reduces the risk of re-oxidation of the already reduced products (e.g., NO_2^-, NO) (Garcia-Segura et al., 2020b) Previously, addition of GAC packed bed decreased the energy consumption of electrochemical greywater treatment from 46 kWh kg^{-1} in a conventional 2D system to 30 kWh kg^{-1} removed in the 3D electrochemical system (Andrés García et al., 2018).

In this study, we have investigated for the first time the performance of the flow-through 3D electrochemical reactor equipped with GAC packed bed polarized by the electric field, in removing persistent organic contaminants from real sewage effluent. To promote the in-situ formation of H_2O_2, we used a flow-through reactor with boron-doped diamond (BDD) mesh anode and stainless-steel mesh cathode orientated in anode-cathode flow direction, and influent feed from the bottom of the reactor, thus enabling a continuous supply of DO to the GAC packed bed. As model contaminants, we selected compounds known to be persistent to oxidative degradation, such as iodinated contrast media diatrizoate and iopromide, anti- epileptic drug carbamazepine and insecticide N,N-diethyl-meta-toluamide (DEET) (Dickenson et al., 2009). The experiments were conducted using saturated GAC over multiple subsequent cycles and at low and high applied currents, to study its impact on the process performance and GAC surface characteristics. To gain insight into the potential of the GAC packed bed to minimize the presence of chlorinated byproducts in the system, we analyzed adsorbable organic halogen (AOX) in both 2D and 3D electrochemical systems. We also evaluated the formation of inorganic chlorinated byproducts chlorate (ClO_3^-) and perchlorate (ClO_4^-). This study provides new insights into the fate of organic pollutants in a hybrid electrochemical-GAC system when working with real wastewater, impact of the applied current on their removal, GAC surface characteristics and presence of organic and

inorganic chlorinated byproducts.

5.2 Experimental set-up

All solutions were prepared using analytical grade reagents and Milli-Q water. Secondary treated sewage effluent was collected from local municipal wastewater treatment plant (WWTP) in Girona, Spain. Characteristics of the sewage effluent are summarized in **Table 5.1**.

Table 5.1: Characteristics of the secondary treated sewage effluent.

Parameter	**pH**	**Electric conductivity ($\mu S\ cm^{-1}$)**	**COD ($mg\ L^{-1}$)**	**TOC ($mg\ L^{-1}$)**	**Chloride ($mg\ L^{-1}$)**
Value	8.0±0.04	1154±18	55.7±9.6	13.6±0.5	177.5±0.5

Experiments were conducted in a flow-through electrochemical reactor equipped with a mesh Nb/BDD anode (80×80×1.3 mm, DIACHEM® electrode, Condias, Germany), both sides of the niobium substrate coated with 4 μm of BDD thin film, and a stainless-steel cathode of the same dimensions. The GAC used was CG 1000, provided by ChiemiVall, S.L. (Spain) with granule diameter 2.4—4.8 mm and apparent density of 500±30 kg m^{-3}. Prior to the experiments, GAC was saturated using sewage effluent until its adsorption capacity for the removal of chemical oxygen demand (COD) was reduced to ≤15% of COD removal obtained. In the case of 3D electrochemical oxidation (3D ELOX) reactor, a packed bed of GAC was placed in between anode and cathode. The total volume of 2D electrochemical system was 250 mL, whereas 3D packed bed comprised approximately 65 mL, i.e., 26% of the total volume. BDD anode was positioned at the bottom of the reactor, and wastewater was circulated in the direction from anode to cathode. The experiments were conducted in batch mode using 2 L of secondary sewage effluent amended with the target contaminants at 2 μM initial concentration, and with the recirculation flowrate of 475 mL min^{-1}. The duration of each experiment was 6 h. Chronopotentiometric experiments were conducted at 96 and 640 mA of applied anodic

current (i.e., current densities calculated versus the projected anode surface area of 15 and 100 A m^{-2}, respectively) using a BioLogic multi-channel potentiostat/galvanostat VMP-300 and a leak-free 1 mm diameter Ag/AgCl reference electrode (Harvard Apparatus) placed in the proximity of the anode. A scheme of the experimental set-up used is illustrated in **Figure 5.1**.

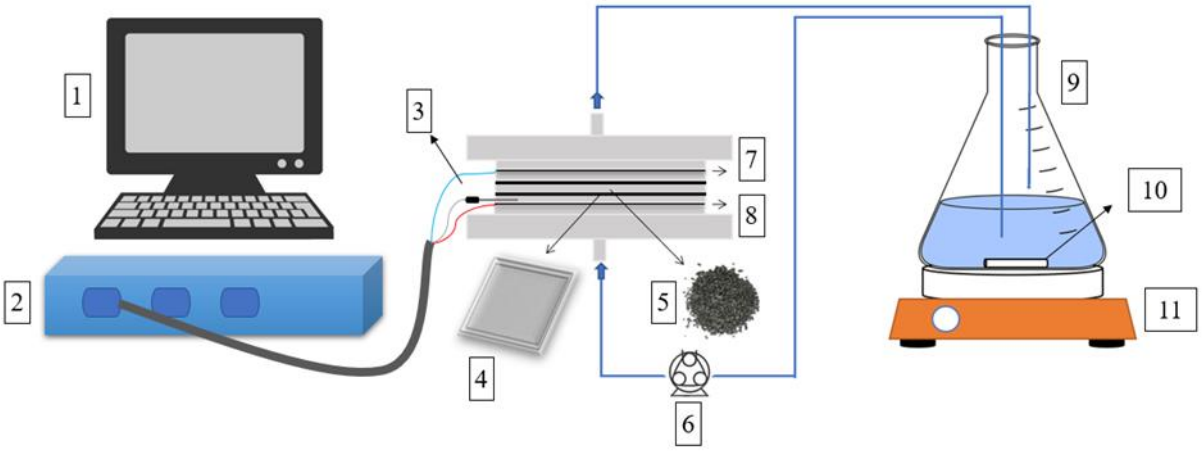

Figure 5.1: Scheme of the experimental set-up used in adsorption (ADS), two-dimensional electrooxidation (2D ELOX) and three-dimensional electrooxidation (3D ELOX) experiments. (1) computer for control of current and data acquisition, (2) potentiostat, (3) reference electrode, (4) inert mesh holder, (5) granules of the granular activated carbon (GAC) packed bed, (6) peristaltic pump, (7) stainless steel cathode, (8) boron-doped diamond (BDD) anode, (9) secondary effluent reservoir, (10) magnet, (11) magnetic stirrer.

All potentials are expressed versus Standard Hydrogen Electrode (V/SHE). To examine the synergy between adsorption on GAC and electrooxidation/electrosorption, experiments were performed in the open circuit (OC) mode, i.e., without the application of current (ADS), and in an electrochemical system without the addition of the GAC bed (2D ELOX). All samples were quenched with methanol and frozen immediately after sampling. The performance of 3D ELOX system was evaluated in 27 consecutive runs applying low current density (LCD) of 15 A m^{-2} and high current density (HCD) of 100 A m^{-2}, to evaluate the impact of anodic current density and electric field strength on the process performance. Runs 12 and 28 were conducted in the open circuit to determine the evolution of the adsorption capacity and regeneration efficiency of GAC. To prevent the growth of the biomass at the surface of the GAC particles, secondary effluent was previously autoclaved, whereas GAC was autoclaved once per week (121°C, 10 min). All experiments were performed in duplicate and the results are expressed as mean values with their standard deviations. Chemical analysis is described in Chapter 3.

5.3 Results and Discussion

The apparent removal rate constants of the contaminant, COD and DOC removal in 2D ELOX (k_{2D}), 3D ELOX (k_{3D}) and ADS system (k_{ADS}) were expressed in h^{-1} and estimated using the linear regression first-order decay model fit to the data, with coefficient $R^2 \geq 0.9$. For a limited number of experiments in the ADS system, first-order rate constants were calculated using the initial stages of adsorption (i.e., first 2 h) instead of the data obtained during the entire 6 h of the experiments, to allow the comparison between different experiments. Good fits obtained for the removal of target contaminants on the saturated GAC in flow-through mode suggest that their adsorption was controlled by the diffusion at the boundary layer, similar to the previously reported data for pilot- and full-scale GAC (Golovko et al., 2020). The synergy between adsorption (ADS) and electrochemical oxidation (2D ELOX) in the 3D system (3D ELOX) can be calculated using the following equation:

$$Synergy\ (\%) = \frac{k_{3D} - k_{2D} - k_{ADS}}{k_{3D}} \qquad \text{(eq. 2.1)}$$

5.3.1 Impact of electric field on the structural properties of GAC

To study the impact of electrochemical polarization of GAC on its surface properties, specific surface area and porosity of the initial (i.e., saturated GAC) and GAC used in the LCD and HCD experiments were investigated. In the LCD experiment, Langmuir surface area of the granules decreased from 1129 to 998 $m^2\ g^{-1}$ (**Table 5.2**). This decrease was more pronounced in the HCD experiment, with the Langmuir surface area of the GAC after 27 runs lowered to 570 $m^2\ g^{-1}$. The T-plot Micropore area, which corresponds to the part of Langmuir Area that is microporous, decreased from 1108 $m^2\ g^{-1}$ for the initial GAC to 978 $m^2\ g^{-1}$ and 557 $m^2\ g^{-1}$ after the LCD and HCD experiments, respectively, indicating a significantly larger decrease in microporosity of GAC when higher currents are applied. The determined Barrett-Joyner- Halenda (BJH) average pore diameters were similar for the saturated GAC (36.5 Å), and GAC after the LCD (35.8 Å) and the HCD experiments (36.3 Å). The density functional theory (DFT) pore size analysis demonstrated that there was an increase in the area of larger pores (i.e., ≥22 Å), which was again more pronounced in the HCD experiment (i.e., from 3 to 11 $m^2\ g^{-1}$) compared

with the LCD experiment (from 3 to 6 m^2 g^{-1}). Previous studies indicated a higher accuracy and reliability of the DFT method compared with the BJH method (Bardestani et al., 2019). Thus, electrochemical polarization of GAC in the HCD experiments led to a more pronounced increase in the average GAC pore size as determined by the DFT method, lower T- plot micropore area and lower Langmuir surface area in the. Larger GAC pore size after the HCD experiment was also confirmed by the SEM images (**Figure 5.2**). Although there was no visible attrition of GAC during the LCD and HCD experiments it is likely that at the higher applied current led to GAC attrition, even under bipolar polarization. Furthermore, the measured pore widening and a pronounced decrease in Langmuir surface area in the HCD experiments evidence changes in GAC porous structure, likely due to the formation of H_2O_2 and reactive oxygen species at the GAC surface. Larger pores generated under electrochemical polarization of GAC may be beneficial for the removal of organic pollutants. Yet, further studies should be conducted to evaluate whether bipolar polarization of GAC over long-term leads to mass losses due to GAC degradation.

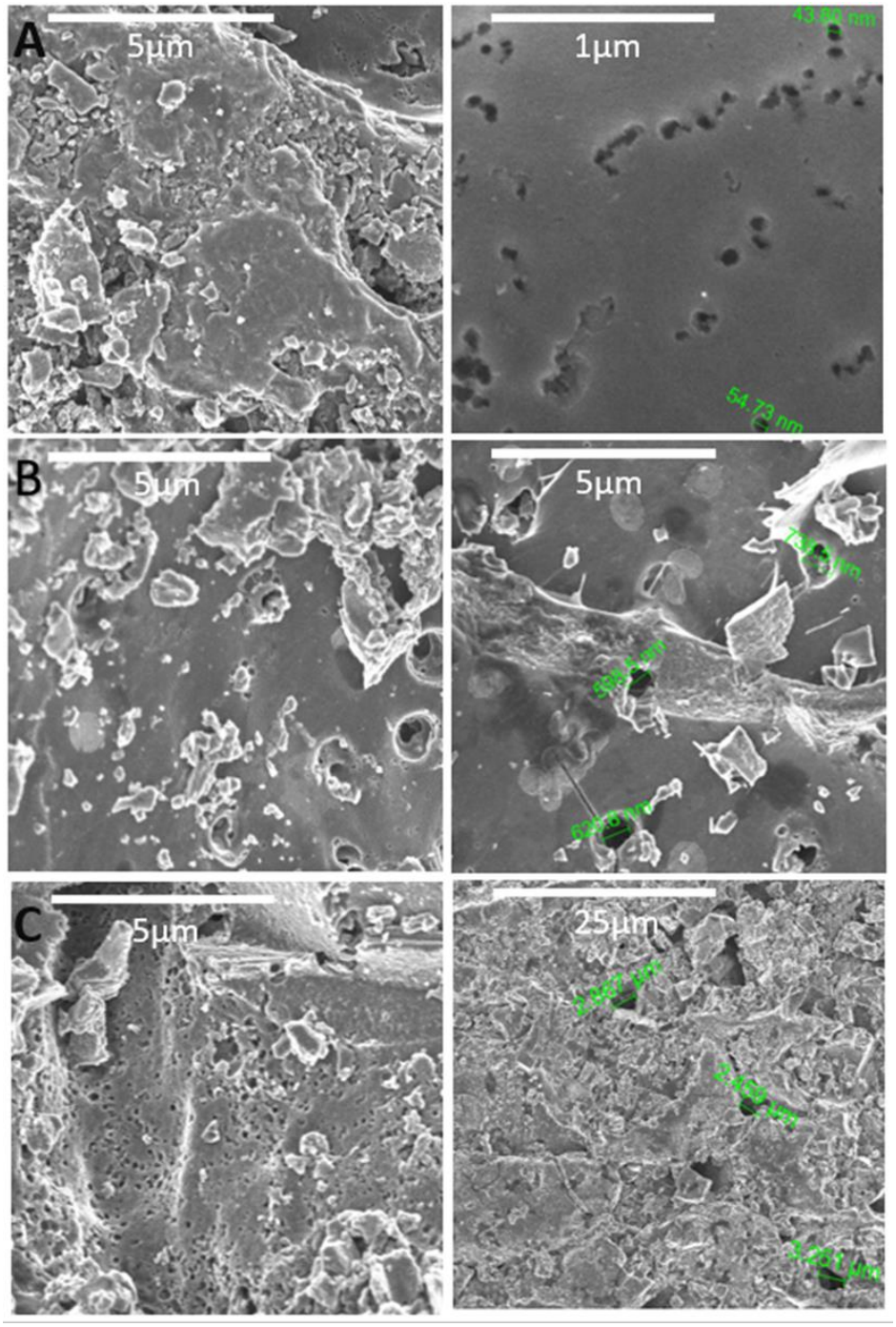

Figure 5.2: SEM images: A) initial, saturated GAC granules before electrochemical polarization, B) GAC granules after the Low Current Density treatment, and C) GAC granules after High Current Density treatment

Table 5.2: Structural properties of the initial (i.e., saturated) GAC and GAC used in 3D ELOX reactor in Low Current Density and High Current Density experiments

	Saturated GAC	LCD GAC	HCD GAC
Langmuir Surface Area (m^2/g):	1129	998	570
The T-Plot Micropore Area (m^2/g)	1108	978	557
DFT Total Area in Pores >22Å (m^2/g)	3	6	11
BJH Adsorption average pore diameter (4V/A) (Å):	36.5	35.8	36.3

5.3.2 Removal of trace organic contaminants in low and high current density experiments

Table 5.3: Apparent first-order removal rate constants (h^{-1}) of the target contaminants at 15 A m^{-2} (LCD experiment) and 100 A m^{-2} (HCD experiment) in 2D ELOX and 3D ELOX system in different runs.

	2D ELOX	ADS	RUN1	RUN 6	RUN 11	R12 ADS	RUN 27	R28 ADS
					IPM			
HCD	0.17±0.02	0.08±0.01	0.32±0.08	0.37±0.054	0.45±0.03	0.10±0.01	0.46±0.12	0.13±0.002
LCD	0.10±0.07		0.20±0.06	0.19±0.03	0.12±0.07	0.029±0.002	0.16±0.05	0.023±0.002
					CPZ			
HCD	0.36±0.10	0.33±0.08	0.81±0.15	0.89±0.01	0.96±0.01	0.41±0.04	1.05±0.02	0.43±0.03
LCD	0.12±0.05		0.70±0.06	0.59±0.03	0.36±0.07	0.17±0.01	0.33±0.05	0.08±0.01
					DTR			
HCD	0.22±0.07	0.02±0.01	0.25±0.04	0.31±0.02	0.32±0.04	0.027±0.014	0.34±0.07	0.032±0.009
LCD	0.12±0.09		0.13±0.02	0.17±0.02	0.12±0.01	0.017±0.004	0.16±0.05	0.014±0.007
					DEET			
HCD	0.17±0.02	0.19±0.07	0.60±0.19	0.68±0.09	0.83±0.10	0.20±0.08	0.84±0.16	0.30±0.03
LCD	0.12±0.07		0.46±0.30	0.51±0.01	0.32±0.05	0.16±0.02	0.33±0.08	0.15±0.03

Table 5.3 summarizes the k_{2D}, k_{3D} and k_{ADS} values for target contaminants in the LCD and HCD experiments. Among the target contaminants, carbamazepine and DEET have the highest octanol-water distribution coefficient (logD), 2.77 and 2.50 (¡Error! No se encuentra el origen de la referencia.) and are thus expected to be adsorbed to the highest degree. The k_{ADS} of DEET was 0.19 h^{-1}, similar to the observed k_{ADS} for carbamazepine (i.e., 0.33 h^{-1}), significantly higher than in the case of iodinated contrast media (ICM) (i.e., 0.08 h^{-1} for iopromide and 0.02 h^{-1} for diatrizoate) (**Table 5.3**). Furthermore, adsorption of larger molecules of iopromide (molecular weight, MW of 791.1 g mol^{-1})

and diatrizoate (613.9 g mol^{-1}) on the micropores of GAC is subject to more pronounced diffusion limitations that in the case of smaller molecules of carbamazepine (236.3 g mol^{-1}) and DEET (191.3 g mol^{-1}) (Li et al., 2018).

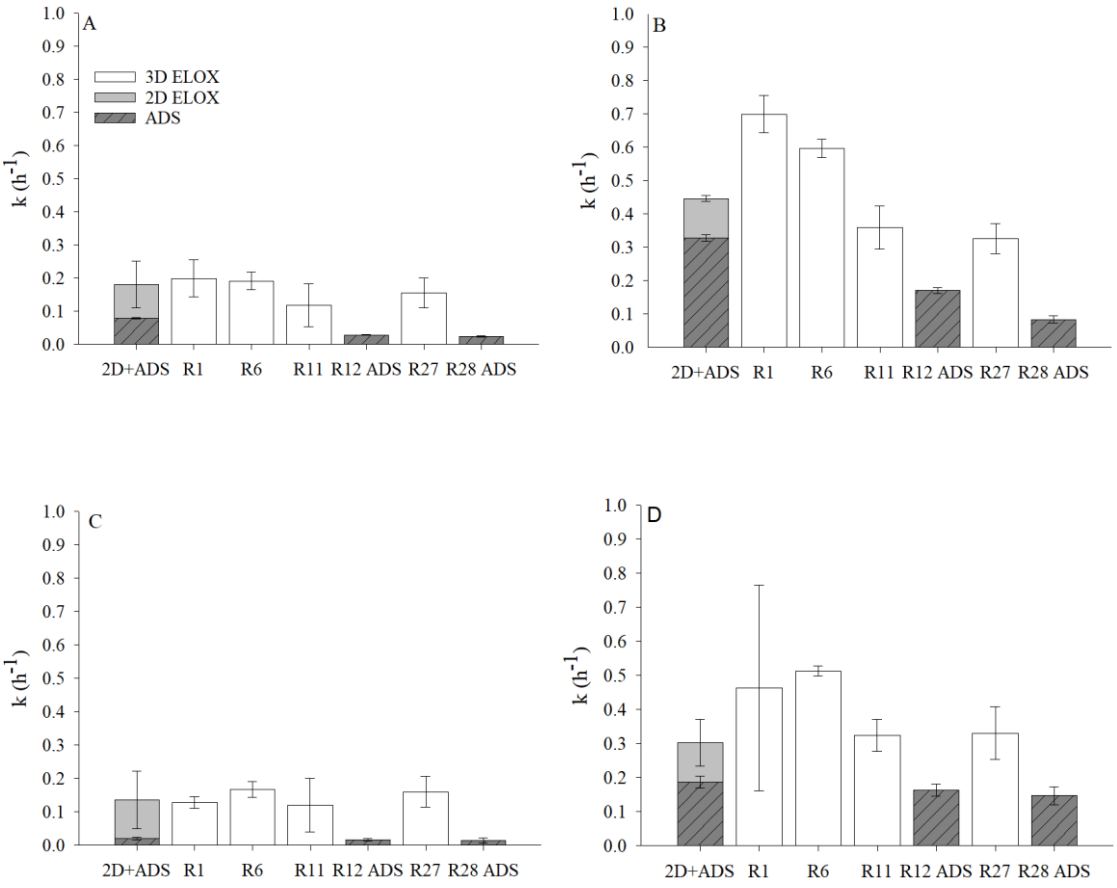

Figure 5.3: Apparent first-order removal rate constants (k, h^{-1}) for: A) IPM, B) CBZ, C) DTR, and D) DEET in the Low Current Density experiments (15 A m^{-2}).

Figure 5.3 shows the removal rate constants observed in the LCD experiments. For carbamazepine and DEET, synergy in the 3D ELOX system was observed in the first runs with saturated GAC (i.e., run 1 and 6), but it was diminished in the subsequent runs, resulting in even negative synergy (**Figure 5.3**). Although higher rate constants were obtained for diatrizoate in runs 6 and 27 compared with the sum of 2D ELOX and ADS removal rate constants (i.e., $k_{2D}+k_{ADS}$=0.12 h^{-1}+0.02h^{-1}), there was no steady trend in k_{3D} that would evidence the synergy between electrochemical oxidation and electrosorption. The removal rates of the other target pollutants in the LCD experiment were significantly decreased in the subsequent application cycles, i.e., from 0.20 h^{-1} (run 1) to 0.16 h^{-1} (run

27) for iopromide, 0.70 h^{-1} (run 1) to 0.33 h^{-1} (run 27) for carbamazepine, and 0.46 h^{-1} (run 1) to 0.33 h^{-1} (run 27) for DEET. The anode potential in these experiments was 2.1 V/SHE, which is lower than the thermodynamic standard potential for $HO^{\bullet}$ formation, i.e., 2.38 V/SHE (Kapałka et al., 2009). Furthermore, the potential difference over the microconductor, $\Delta Umicroconductor$, in the LCD experiment, of 0.9-1.8 V was likely insufficient to induce efficient charge separation in GAC particles. $\Delta Umicroconductor$ depends on the electric field gradient between the terminal electrodes and the length of the conductor. If the applied potential is high enough, the conductive particles in the electric field become polarized, without being in contact with any of the main electrodes. For Faradaic redox reactions to occur at the surface of the microelectrodes, the potential difference over the microconductor needs to be high enough to reach at least the value of the redox potential of the considered redox reaction, e.g., cathodic reduction of oxygen to H_2O_2 (McQuillan et al., 2018; Rahner et al., 2002). The saturation of GAC was also evident from the gradual increase in ohmic resistance in the 3D ELOX system, with total cell potential increasing from 3.6 V in run 1 to 6.9 V in run 27. Given that the conductivity of wastewater was relatively constant in the LCD experiment, this increase in total cell potential could be assigned to a continuous increase in resistance of GAC packed bed.

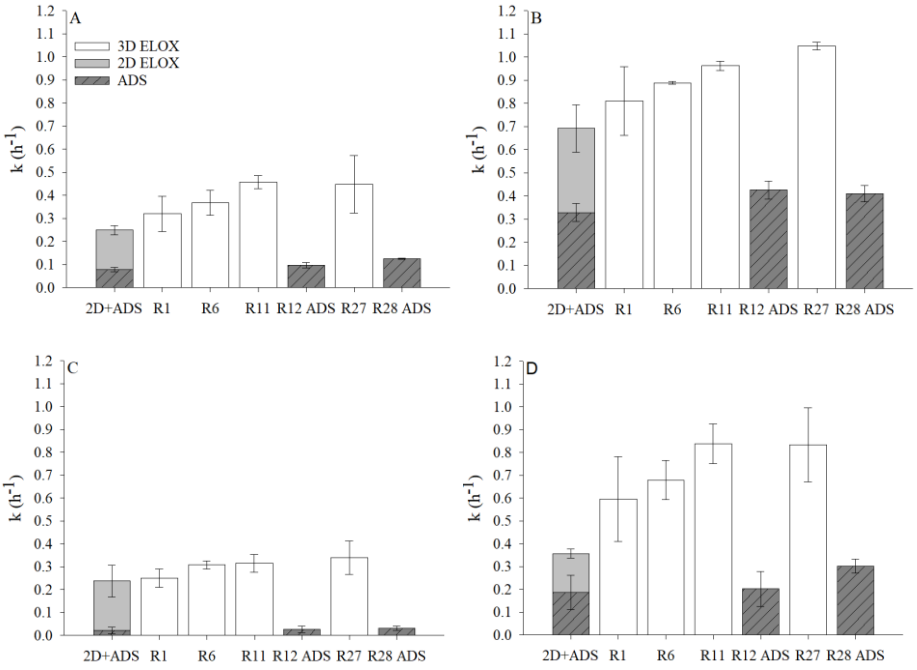

Figure 5.4: Apparent first-order removal rate constants (k, h^{-1}) for: A) IPM, B) CBZ, C) DTR, and D) DEET in the High Current Density experiments (100 A m^{-2}).

In the HCD experiments, synergy between electrochemical oxidation and adsorption/electrosorption was observed for all contaminants, with a gradual increase in their removal rate constants and observed synergy values with the conducted runs (**Figure 5.4**). Synergy of electrosorption and electrooxidation in 3D ELOX system was 22% for iopromide removal in run 1 and was steadily increased to 44-46% (run 11 and run 27). Similar results were obtained for carbamazepine (28-34% synergy), diatrizoate 24-30% synergy) and DEET (57.2-57.4% synergy) in runs 11-27 (**Table 5.4**). In the pH range of the experiment (pH 7.2.- 9.1), iopromide, carbamazepine and DEET are neutral molecules whereas diatrizoate is negatively charged. Electrosorption of uncharged species is still likely to occur due to their polarizability by the external electric field and formation of dipoles (Niu and Conway, 2002; Thamilselvan et al., 2018).

Table 5.4: Synergies (%) between adsorption and electrochemical oxidation for the several runs in the High Current Density experiments

	RUN1	**RUN 6**	**RUN 11**	**RUN 27**
IPM	22,2%	32,3%	44,4%	45,5%
CBZ	14,6%	22,2%	28,1%	34,0%
DTR	4,4%	22,7%	24,4%	29,8%
DEET	40,1%	47,4%	57,2%	57,4%

The highest molecular polarizability is predicted for iopromide (i.e., 56.4 $Å^3$), followed by diatrizoate (39.8 $Å^3$), carbamazepine (28 $Å^3$) and DEET 23.3 $Å^3$ **(**¡Error! No se encuentra el origen de la referencia.). Thus, high synergy values of iopromide may be a consequence of its enhanced electrosorption on the polarized GAC particles. However, the highest increase in k_{3D} values during repeated applications was noted for DEET, for which the removal rate constant was significantly increased already in run 1, from $k_{2D}+k_{ADS}$= 017+0.19 h^{-1} to k_{3D}= 0.60 h^{-1}, resulting in 40% of synergy. This could be explained by efficient adsorption of a relatively hydrophobic (log D=2.50) and small molecule of DEET (191.3 g mol^{-1}) on GAC and its enhanced degradation by the $OH^{\bullet}$, generated in HCD experiment (k_{OH}=5.00x10^9 M^{-1} s^{-1}, **Table 5.5**).

Table 5.5: Bimolecular rate constants (k, M^{-1} s^{-1}) for oxidation of target organic contaminants with homogeneously generated OH•, O_3 and Cl_2.

Contaminant	$k_{OH^{\bullet}}$, M^{-1} s^{-1}	k_{O3}, M^{-1} s^{-1}	k_{Cl2}, M^{-1} s^{-1}
Iopromide	3.30×10^{9}[5]	93.1[6]	0[9]
Carbamazepine	8.80×10^{9}[5]	3×10^{5}[7]	<0.1[10]
Diatrizoate	6.3×10^{8}[5]	48.6[6]	0[9]
DEET	5.00×10^{9}[5]	0.1[8]	1.3×10^{-3} [11]

In the HCD experiment, BDD anode potential was 2.68 V/SHE, thus ensuring the electrogeneration of $OH^{\bullet}$ (Kapałka et al., 2010). Yet, the concentration of anodically formed $OH^{\bullet}$, is expected to decrease exponentially with the distance from the electrode surface and reach zero already at 20 nm distance (Groenen-Serrano et al., 2013; Kapałka et al., 2009). Thus, they are not expected to contribute to the synergy observed in the 3D ELOX and GAC regeneration. The potential difference over the microconductor, $\Delta U_{microconductor}$ in the HCD experiments ranged from 3.6 to 6.9 V, significantly higher than in the LCD experiments, and it ensured electrocatalytic activity of GAC packed bed (Andrés García et al., 2018; Pedersen et al., 2019; Polcaro et al., 2000; Zhu et al., 2011). Intensive generation of oxygen at the BDD anode placed below the GAC packed bed likely enhanced the production of H_2O_2 at the cathodically polarized sides of GAC particles, according to the eq. 2.2:

$$O_2 + 2H^+ + 2e^- \rightarrow H_2O_2,\ E^o=0.67\ V \qquad \text{(eq. 2.2)}$$

Previous studies have demonstrated enhanced electrogeneration of H_2O_2 in the anode-cathode configuration due to the reduction of anodically generated O_2 at the cathode (Zhou et al., 2018). Regardless of the application of current, the formed H_2O_2 can be

decomposed by GAC particles to $OH^{\bullet}$ due to the presence of polyaromatic moieties and functional groups in GAC (Zhang et al., 2013; Zhu et al., 2011). The decomposition of H2O2 to $OH^{\bullet}$ on activated carbon was first reported by Kimura and Miyamoto (Kimura and Miyamoto, 1994), and the postulated mechanism includes the dissociation of the H2O2 to peroxyl radical ($OOH^{\bullet}$) at the carbon surface, which forms superoxide radical ion (eq. 2.3):

$$OOH^{\bullet} \rightleftharpoons H^{+} + O_2^{\bullet -} \qquad \text{(eq. 2.3)}$$

The superoxide radical ion reacts further with H_2O_2 to form $OH^{\bullet}$ (eq. 2.4) (Kimura and Miyamoto, 1994):

$$H_2O_2 + O_2^{\bullet -} \rightarrow OH^{-} + OH^{\bullet} + O_2 \qquad \text{(eq. 2.4)}$$

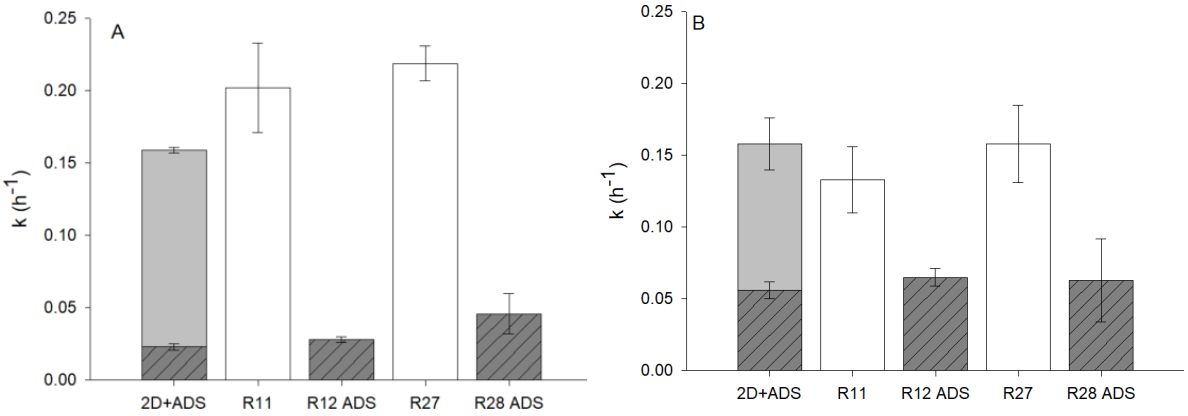

Figure 5.5: Apparent first-order removal rate constants (k, h^{-1}) for: A) COD, and B) TOC removal in the High Current Density experiment.

The generation of H_2O_2 and its activation to $OH^{\bullet}$ are dependent on the carbon porosity, chemical properties of the surface, pH and other factors (Anfruns et al., 2014; Bach and Semiat, 2011). Thus, polarization of GAC can further contribute to the degradation of the adsorbed pollutants and organic matter, and regeneration of GAC in the 3D ELOX system. Higher synergy of electrosorption and electrochemical degradation in the HCD experiment was also evident from the measured COD removal rates (**Figure 5.5A**). On the other hand, TOC removal remained relatively constant and no synergy could be observed in the HCD experiments (**Figure 5.5B**). This could be a consequence of the

formation of halogenated organic byproducts (i.e., AOX) that are more resistant to oxidative degradation (Lan et al., 2017).

In the HCD experiments, only in the case of carbamazepine, a removal higher than 90% was achieved. The electric energy per order (E_{EO}), i.e., energy required to reduce the concentration of a contaminant by one order of magnitude in a unit volume of treated solution) (Andrés García et al., 2018), ranged from 14.3-23.1 kWh m^{-3} for the removal of carbamazepine in 3D ELOX experiments, while it was 42.3 kWh m^{-3} in the 2D ELOX process (**Table 5.6)**. High E_{EO} values determined are a consequence of low electric conductivity of the secondary effluent (1.1 mS cm^{-1}), which resulted in very high total cell potential in both 2D and 3D ELOX systems (15- 25 V). For the rest of the target contaminants, given their high persistency to oxidative degradation, lower removals were achieved and thus E_{Eo} was not calculated. It should be noted here that high values for E_{EO} were a consequence of working with low conductivity wastewater (1.1 mS cm^{-1}), and significant spacing between the GAC packed bed and the anode (1 cm) required to accommodate the Ag/AgCl reference electrode. The ohmic resistance of the system can be significantly reduced by reducing the interelectrode spacing. Furthermore, the electric resistance of the employed GAC can have a significant impact not only on the ohmic drop of the reactor but also on the performance of electrochemical regeneration, as observed previously (Narbaitz and Karimi-Jashni, 2009).

Table 5.6: Electric energy per order (EEO, kWh m^{-3}) during the several runs

E_{EO} (KWH M^{-3})	2D ELOX	RUN 1	RUN 6	RUN 11	RUN 27
IPM	-	-	41.9	46.2	42.8
CBZ	42.3	14.4	17.5	23.1	16.4
DTZ	-	-	-	-	-
DEET	-	20.6	22.4	-	-

In both LCD and HCD experiments, runs 12 and 28 were conducted in the OC, i.e., without the application of current, to investigate the impact of electrochemical polarization of GAC on its adsorption performance. In the LCD treatment, most of the rate constants for the runs were similar or slightly decreased from the initial saturated

GAC to run 12 and run 28 (**Figure 5.3, Table 2.5**). For example, k_{ADS} of iopromide were decreased from 0.08 h^{-1} to 0.03 h^{-1} (run 12) and 0.023 h^{-1} (run 28) when GAC was used in the LCD experiment. On the other hand, in the HCD treatment, kADS was increased from the adsorption on the initial GAC to adsorption on used GAC runs 12 and 28 (**Figure 5.4, Table 2.5**). More notable differences were observed for DEET, for which the k_{ADS} remained constant in the LCD experiment over subsequent runs, whereas in the HCD experiment it was increased from 0.19 h^{-1} to 0.30 h^{-1} in run 28. Also, k_{ADS} of carbamazepine was increased from 0.33 h^{-1} to 0.43 h^{-1} (run 28). Increased amount of mesopores due to the electrochemical polarization of GAC at higher currents would mean better accessibility of the contaminants and easier regeneration compared with the micropores (Xiao and Hill, 2019). Also, pore blockage and competitive adsorption of organic matter with the adsorbed contaminants was reported to be less pronounced in activated carbons with larger pore sizes (Ding et al., 2008; Ebie et al., 2001; F. Li et al., 2003; Li et al., 2018; Q. Li et al., 2003). Considering the above, the wider pores obtained in the HCD experiment should enhance the adsorption of the trace organic contaminant and increase the synergies observed in the 3D ELOX system. Previously, higher adsorption rates of rhodamine-B and ibuprofen were observed for activated carbons with broadened hierarchical pore distribution (Li et al., 2018; Mestre et al., 2009). Furthermore, mesopores are important as transport arteries through which the adsorbate molecules reach the micropores (Moreno-Castilla and Rivera-Utrilla, 2001). The adsorption of the different contaminants depends on their molecular weight in correlation with the pore size distribution of the activated carbon (Li et al., 2018). The micropososity should be large enough to ensure accessibility of big MW compounds (Mestre et al., 2009).

5.3.3 Formation of organic and inorganic chlorinated byproducts

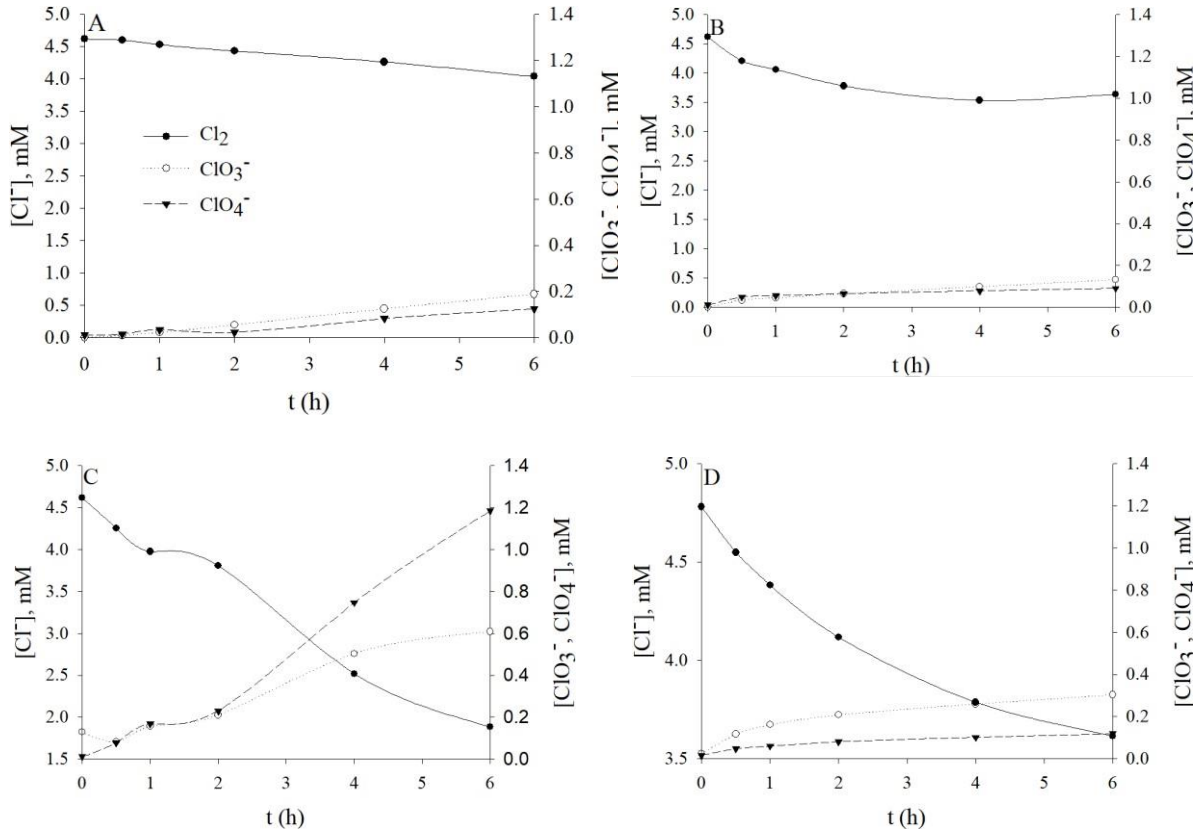

Figure 5.6: Measured concentrations of Cl−, ClO3 −, and ClO4 − in: A) 2D ELOX LCD, B) 3D ELOX LCD, C) 2D ELOX HCD, and D) 3D ELOX HCD experiments

In the presence of chloride, anodic polarization of BDD leads to the formation of free chlorine ($HOCl/OCl^-$), chlorine radicals and in the case of highly saline solutions, gaseous ClO_2 and Cl_2O (Mostafa et al., 2018). Faster decrease in Cl^- was observed in the HCD experiments (0.07 h^{-1}) compared with LCD experiments (0.02 h^{-1}) in the 2D ELOX system in (**Figure 5.6**). The presence of GAC packed bed in 3D ELOX systems did not have a significant impact on the kinetics of chloride oxidation (0.05 h^{-1} and 0.08 h^{-1} in LCD and HCD experiments, respectively). Yet, active chlorine was present only in the 2D ELOX systems, where residual chlorine was measured in concentrations of up to 6.04 and 7.11 mg L^{-1} in LCD and HCD experiments, respectively. In the case of 3D ELOX, residual free chlorine ($Cl2/HOCl/OCl^-$) was measured only in traces (i.e., 0.53-1.07 mg L^{-1}), as it can be seen in **Figure 5.7**. It should be noted here that due to the high reactivity of active chlorine with the organic matter, the measurements of free chlorine using the DPD method represent residual $Cl2/HOCl/OCl^-$, in the system, and not the amount generated.

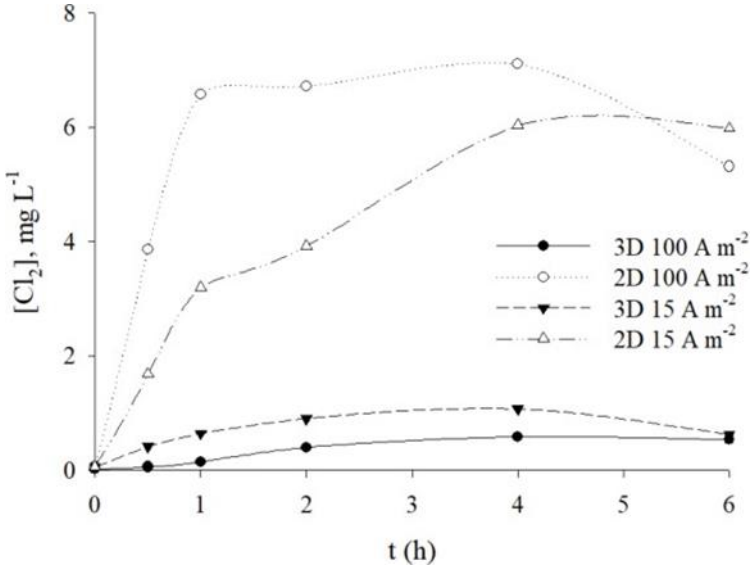

Figure 5.7: Concentrations of residual free chlorine as determined using the DPD method in 2D ELOX and 3D ELOX experiments, in the LCD and HCD experiments.

In the case of high oxidizing power anodes such as BDD, Cl^- is further oxidized to ClO_3^- and ClO_4^- (Lan et al., 2017). In LCD experiments the (anode potential, EAN=2.1 V/SHE), chlorate and perchlorate were measured in concentrations up to 0.19 and 0.13 mM in 2D ELOX, and 0.13 and 0.09 mM in 3D ELOX system, respectively **(Figure 5.6 A, B)**. Thus, addition of GAC packed bed did not have a significant impact on the concentrations of ClO_3^- and ClO_4^-. Both species are formed by further anodic oxidation of chloride (eq. 2.5-2.9) (Bergmann et al., 2009):

$2Cl^- \rightarrow Cl_2 + 2e^-$ (eq. 2.5)

$Cl_2 + H_2O \rightarrow HClO + Cl^- + H^+$ (eq. 2.6)

$HClO \rightleftharpoons ClO^- + H^+$ (eq. 2.7)

$ClO^- + 2H_2O \rightarrow ClO^- + 4H^+ + 4e^-$ (eq. 2.8)

$ClO_3^- + H2O \rightarrow ClO_4^- + 2H^+ + 2e^-$ (eq. 2.9)

Previously, BDD anodic oxidation of secondary sewage effluent at 13 A m^{-2} showed no ClO_4^- formed during 3 h electrolysis, whereas ClO_3^- was formed in concentrations of up to 0.15 mM (Cano et al., 2011). Nevertheless, it is difficult to compare the studies dealing with real wastewater treatment. The formation of perchlorate at low current densities may be inhibited by the presence of organics due to the competition between the organics and ClO_3• for $OH^•$ within a reaction zone (0.02—0.96 μm) adjacent to the BDD anode (eq.

2.10, 2.11) (Donaghue and Chaplin, 2013).

$ClO_3^- \rightarrow ClO^{\bullet} + e^-$ (eq. 2.10)

$ClO_3^{\bullet} + OH^{\bullet} \rightarrow HClO_4$ (eq. 2.11)

Thus, application of low currents in BDD anodic oxidation of wastewater effluent did not avoid the generation of ClO_3^- and ClO_4^-.

As expected, HCD experiments yielded higher chlorate and perchlorate concentrations, in 2D ELOX system, with ClO_3^- reaching a concentration of 0.61 mM and ClO_4^- of 1.18 mM at the end of the experiment (**Figure 5.6C**). In the 3D ELOX system (**Figure 5.6D**) the concentration of both was lower with concentration of ClO_3^- reaching 0.30 mM after 6 h of electrolysis, whereas ClO_4^- was 0.12 mM. Previous studies demonstrated efficient removal of ClO_4^- by capacitive deionization (CDI) on activated carbon felt electrodes, and preferential adsorption of ClO^- over Cl^- (Xing et al., 2019). Enhanced electrosorption of perchlorate versus chlorate in our system can be explained by the higher dipole moment of ClO_4^- and thus its higher polarizability (Howard et al., 1995; Siqueira et al., 2003). Thus, addition of activated carbon to electrochemical systems may be a suitable way to minimize the accumulation of toxic chlorinated byproducts due to their adsorption and electrosorption on GAC.

Table 5.7 summarizes the measured concentrations of AOCl and AOI, whereas AOBr was below the detection limit of the method. The removal of AOI in 2D and 3D ELOX experiments at low applied current was similar, i.e., AOI concentration was decreased from 1,370 µg L^{-1} to 901 and 813 µg L^{-1}, respectively. In the case of HCD, more intense formation of $OH^{\bullet}$ enhanced the degradation of iodinated organics and resulted in decreased concentrations of AOI, i.e., 439 and 307 µg L^{-1} in 2D and 3D ELOX, respectively. Thus, addition of GAC packed bed led to an enhanced AOI removal only in the HCD experiments, likely due to enhanced electrosorption of typically high polarity iodinated organics. In terms of AOCl, the highest concentrations of AOCl measured in HCD experiments were, 576 µg L^{-1} and 462 µg L^{-1} for 2D and 3D ELOX, respectively. This is in accordance with the higher concentrations of residual free chlorine measured at higher current densities, and enhanced chloride oxidation, which thus lead to more intense electrochlorination of the organic matter (Schmalz et al., 2009; Xie et al., 2018; Yusufu Mohammed I., 2012). Nevertheless, addition of GAC packed bed lowered the AOCl

concentration at both low and high current applied, i.e., from 498 µg L^{-1} to 310 µg L^{-1} in the LCD experiments, and from 576 µg L^{-1} to 462 µg L^{-1} in the HCD experiments.

Table 5.7: AOCl and AOI measured for the final sample (6 h) in ADS experiment, 2D ELOX and 3D ELOX experiments after 27 runs, for LCD (15 A m^{-2}) and HCD (100 A m^{-2}) experiments.

	[AOCl], µg L^{-1}	***[AOI], µg L^{-1}***
Secondary effluent	575	1370
ADS	442	743
2D ELOX, LCD	498	901
3D ELOX, LCD	310	813
2D ELOX, HCD	576	439
3D ELOX, HCD	462	308

5.4 Concluding remarks

The performance of the 3D ELOX system with GAC packed bed was investigated at low and high current density (15 and 100 A m^{-2}, respectively). Synergy between electrosorption and electrochemical degradation was demonstrated when high current density applied, where the potential difference of the microconductor was large enough to induce efficient charge separation in GAC particles and electrochemical degradation of the (electro)sorbed contaminants. The highest synergy (up to 57%) was observed for DEET, the smallest molecule among the investigated contaminants and with a relatively high reactivity with $HO^{\bullet}$ (5.00×10^{9}). Surface characterization of GAC showed that at both low and high currents, porous structure of GAC undergoes changes, with an increased mesoporosity after exposing GAC to the electric field. Thus, the strength of the electric field impacts the structural properties of GAC and its ability of charge separation through polarization. Further, in-depth study should be conducted to evaluate the stability of different types of GAC and extent of changes in their porosity and surface area under bipolar polarization. The presence of GAC was demonstrated as beneficial for the

reduction of halogenated organic by-products at both low and high currents applied. At 100 A m^{-2}, addition of GAC packed bed led to a significant decrease in the formed chlorate and perchlorate, from 0.61 to 0.30 mM of ClO_3^- and from 1.18 to 0.12 mM of ClO_4^- in 2D and 3D ELOX systems, respectively, likely due to their electrosorption onto the GAC granules. Thus, addition of relatively small amounts of activated carbon may be a feasible option for minimization of toxic and persistent inorganic chlorinated byproducts in electrochemical oxidation. Furthermore, in this study we intentionally excluded the development of a biofilm to investigate the synergy between electrosorption and electrochemical degradation. Yet, the performance of 3D ELOX system may be further enhanced by allowing the establishment of a biofilm and possibly additional contribution of biodegradation to the removal of organic pollutants,

CHAPTER 6 Chlorine-free electrochemical disinfection using graphene sponge electrodes.

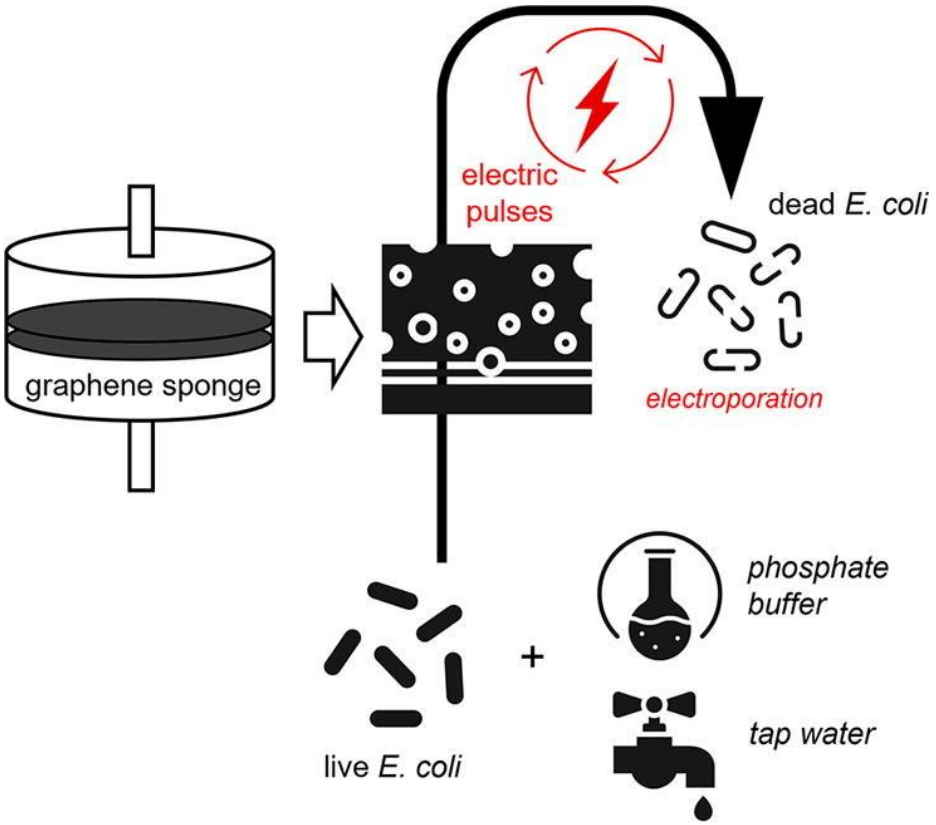

6.1 Framework

The establishment of public water disinfection and treatment is one of the greatest public health achievements of the 20th century. However, billions of people, mostly in rural areas, still lack access to clean drinking water and improved sanitation (Vinet and Zhedanov, 2011). The United nations (UN) 2030 Agenda for Sustainable Development includes a dedicated goal on water and sanitation, with "universal and equitable access to safe and affordable drinking- water for all" as one of the targets to be reached by 2030 (World Health Organization, 2017). To achieve this goal, the often deficient and unreliable centralized drinking water treatment systems in the developing and transition countries will need to be complemented by decentralized units for water treatment and disinfection. The implementation of community or household- managed non-networked water treatment systems requires reliable and robust technologies that will ensure the microbiological quality of the treated water at low cost. In addition to this, small-scale disinfection systems need to satisfy a range of other performance criteria such as ease of use of the system, independence from the energy grid or tap pressure, environmental sustainability, socio-cultural acceptability, and potential for dissemination (e.g., low requirement for skilled personnel and maintenance in general). Among the available physico-chemical technologies that can be used in point of entry and point of use treatment devices (e.g., chemical disinfection, membrane filtration, heat and UV-based disinfection and others), no single small-scale system meets all the performance criteria needed (B. Chen et al., 2021; Peter-Varbanets et al., 2009).

Electrochemical processes offer inherent design advantages that make them very well-suited for decentralized water treatment, and may be the key technologies to ensure access to safe water, even in remote areas (Hand and Cusick, 2021; Radjenovic and Sedlak, 2015). For example, electrochemical systems are modular and have a small footprint, they operate at ambient temperature and pressure, they can be solar-powered, and they do not require any addition of chemicals (Radjenovic and Sedlak, 2015). The production of disinfectants is achieved by water discharge at the anode (i.e., $OH^{\bullet}$, O_3), oxidation/reduction of the dissolved species (i.e., oxidation of chloride to $HOCl/OCl^-$, and oxygen reduction to H_2O_2), and/or anode dissolution (i.e., ferrate). Nevertheless, formation of toxic and persistent chlorinated byproducts in the presence of chloride, present in virtually all natural waters, limits the safe application of electrochemical water

treatment systems (Palmas et al., 2018). Although chlorine is a very efficient disinfectant, it rapidly reacts with the organic matter to form trihalomethanes (THMs), haloacetic acids (HAAs) and other chlorinated organic byproducts(Palmas et al., 2018). At highly oxidizing anodes such as boron-doped diamond (BDD), Ti/SnO_2-based anodes, and Magnéli phase titanium suboxide (Ti_4O_7) electrodes, chloride is oxidized to chlorate and perchlorate, thus further compromising the quality of the treated water (Radjenovic et al., 2020).

In our recent study (Baptista-Pires et al., 2021), we demonstrated excellent electrocatalytic activity of a newly developed graphene-based sponge electrode for the oxidation of persistent organic contaminants, and at the same time, exceptionally low current efficiency for chlorine formation (i.e., only 0.04% of current efficiency in the presence of 20 mM NaCl). Moreover, graphene-based sponge electrodes had excellent electrochemical stability during both anodic and cathodic polarization, likely due to the formation of covalent C- Si and C-O bonds between graphene and SiO_2 (Hintze et al., 2016; Ramezanzadeh et al., 2016; Shemella and Nayak, 2009), a major component of the mineral wool template employed to produce structurally stable sponge. Graphene-based sponges were produced using a simple, bottom-up, low-cost, and easily scalable method which allowed easy incorporation of atomic dopants into the structure of graphene–based coating. In this work, we evaluated the performance of boron-doped reduced graphene oxide (BRGO) and nitrogen-doped reduced graphene oxide (NRGO) coated sponges for electrochemical disinfection of low-conductivity water, including real tap water. Electrochemical inactivation of an indicator microorganism *Escherichia coli* was evaluated in one-pass, flow-through mode at different applied current densities and using different flow directions. The produced electrode materials were characterized using scanning electron microscopy (SEM), X-ray photoelectron spectroscopy (XPS), X-ray diffraction (XRD) and zeta potential analyses. To gain insight into the inactivation mechanism, we evaluated the formation of strong oxidant species (e.g., O_3, H_2O_2, $OH^{\bullet}$) and performed experiments in the presence of a radical scavenger. Complete inactivation of the bacteria was verified by the Live/Dead staining experiments and additional storage experiments with the electrochemically treated samples. In addition, SEM analysis was used to characterize the bacterial morphology before and after the electrochemical treatment. Finally, experiments performed with intermittent current application revealed exceptional disinfection performance of the graphene-based sponges due to their intrinsic

capacitive properties. This study opens a new route towards more energy-efficient, chlorine-free electrochemical disinfection of low-conductivity water.

6.2 Experimental set-up

6.2.1 Electrode material synthesis

Graphene-based sponges were produced using a simplified bottom-up hydrothermal synthesis method reported in our previous study (Baptista-Pires et al., 2021). Briefly, pieces of mineral wool were thoroughly soaked in the specific aqueous solution of GO, namely a mix of GO (2 g L^{-1}) and boric acid (43 g L^{-1}), to produce the BRGO, and a mix of GO (2 g L^{-1}) and urea (300 g L^{-1}), for the production of NRGO, as reported elsewhere (Sun et al., 2012; Wang et al., 2016). The soaked mineral wool was subject to hydrothermal synthesis for 12 h at 180 ºC. The resulting graphene- based sponges were then thoroughly cleaned with the Milli-Q water to remove the unbonded flakes and the remaining impurities.

Characterization methods of the electrode is described in Chapter 3.

6.2.2 Electrochemical disinfection experiments

BRGO and NRGO sponges were connected to a stainless steel current collector and employed as electrodes in a flow-through, cylindrical reactor made of methacrylate (**Figure 6.1)**. All experiments were conducted in one-pass continuous mode, with a flow rate set at 5 mL min^{-1} that corresponds to surface area-normalized permeate flux of 175 L m^{-2} h^{-1} (LMH) and a hydraulic residence time of 3.5 min. The flow rate was controlled using a digital gear pump (Cole-Parmer). Electrochemical disinfection experiments were conducted in the chronopotentiometric mode using a multi-channel potentiostat/galvanostat VMP-300 (BioLogic, U.S.A.) and a leak-free Ag/AgCl reference electrode (Harvard Apparatus, U.S.A.). The applied anodic currents were 50, 100 and 200 mA, resulting in the anodic current densities of 29, 58 and 115 A m^{-2}, respectively, calculated using the projected surface area of the electrode. The employed supporting electrolyte was 10 mM phosphate buffer (Na_2HPO_4/NH_2PO_4, pH 7, electric conductivity of 1.1 mS cm^{-1}). Before each experiment, the reactor was first thoroughly flushed with the clean buffer solution.

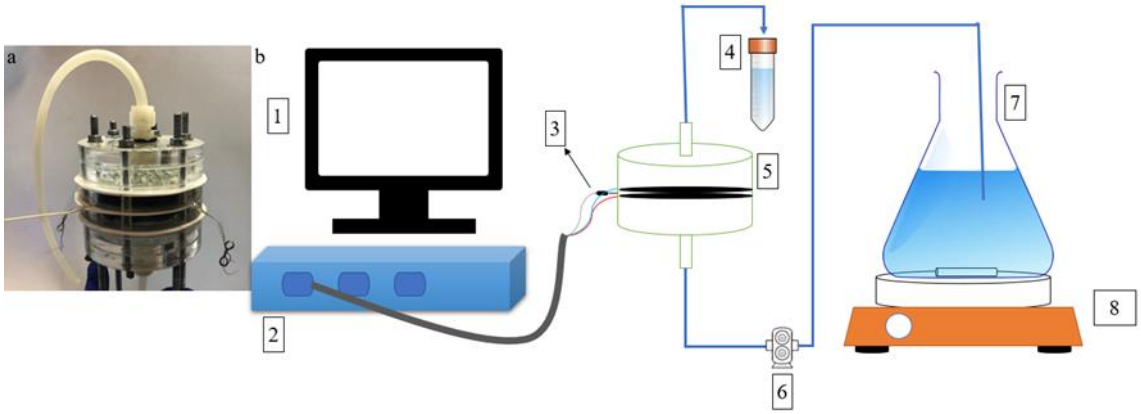

Figure 6.1: ***a)*** *Photo of the flow-through reactor, and* ***b)*** *Scheme of the experimental set-up used (1) computer for the control of current and data acquisition, (2) potentiostat, (3) reference electrode, (4) sample collector, (5) electrochemical reactor, (6) digital gear pump, (7) influent reservoir, and (8) magnetic stirrer.*

To investigate the impact of electrode order on the system performance, the experiments were performed using the anode-cathode (A-C) and cathode-anode (C-A) sequence at all current densities applied. To evaluate the formation of $HO^{\bullet}$, experiments were performed in 10 mM phosphate buffer, pH 7, at 200 mA of anodic current, using terephthalic acid (TA) at 20 mg L^{-1} of initial concentration. TA was previously demonstrated as an ideal probe compound for electrochemically generated $HO^{\bullet}$ (second-order rate constant for the reaction of TA with $HO^{\bullet}$, $k_{TA,OH}=4\times10^{9}$ M^{-1} s^{-1}) (Charbouillot et al., 2011), because it does not react via direct electrolysis (Jing and Chaplin, 2017) and has very low reactivity with ozone (Zang et al., 2009). Experiments with addition of excess methanol (10 mM) were carried out at 200 mA in the NRGO(A) - NRGO(C) configuration, to determine the role of $OH^{\bullet}$ and O_3. The NRGO(A) - NRGO(C) configuration was also used for the following experiments. To investigate the impact of the initial concentration of bacteria, experiments were performed with 10^5–10^6 and 10^6–10^7 CFU mL^{-1} of *Escherichia coli*, at 200 mA of applied anodic current. The initial concentration ranges selected were above the values expected for domestic sewage (i.e., 10^4 CFU mL^{-1}) (Y. Li et al., 2017) to test the system performance under challenging conditions and verify whether all *E. coli* electrosorbed to the graphene sponge electrodes are also further inactivated. To exploit the capacitive properties of graphene, the reactor was operated with intermittent application of the anodic current of 200 mA using three different ON-OFF cycles: *i)* symmetrical cycles with 105 s ON - 105 s OFF equivalent to one hydraulic retention time,

HRT (HRT = 3.5 min = 210 s), *ii)* symmetrical cycles of 52.5 s ON - 52.5 s OFF equivalent to half HRT (105 s), and *iii)* asymmetrical cycles with 75 s ON - 30 s OFF equivalent to half HRT (105 s). To further verify the reactor performance under realistic conditions, experiments with real tap water were performed in both continuous (100 mA) and intermittent current application modes (100 mA and 50 mA), for the cycle of 75 s ON – 30 s OFF. The ohmic drop was calculated from the ohmic internal resistance obtained in the electrochemical impedance spectroscopy (EIS). The EIS experimental data was fitted using the BioLogic EC-lab software.

6.2.3 Chemical Analysis

The production of ozone and free chlorine that are formed at the anode was measured in C-A flow direction at 200 mA of applied anodic current, to avoid their decomposition at the cathode and enable their detection. Likewise, hydrogen peroxide that is formed at the cathode was measured in A-C flow direction, i.e., with cathode being the last electrode of the reactor, at 200 mA of applied anodic current.

Ozone, free chlorine, and hydrogen peroxide were measured immediately after sampling the effluent, to minimize any potential loss of these oxidants. To confirm the destruction of the bacterial cells that leads to the K^+ leakage, the concentration of K^+ ion was also measured using ion chromatography (IC) Dionex ICS- 5000 HPIC system, in samples before and after treatment at 200 mA (Long et al., 2015).

The detailed methods as well as microbiological analysis are described in Chapter 3.

6.3 Results and discussion

6.3.1 Graphene-based sponge characterization

The optoelectronic properties of the graphene-based sponges are presented in **Figure 6.2**, and were similar to the materials produced in our previous study [9]. The XPS analyses revealed a C/O atomic ratio of 1.7, 3.5 and 3.6 for GO, BRGO and NRGO, respectively, demonstrating the efficiency of hydrothermal reduction of GO (**Figure 6.2;Table 6.1**). In the case of NRGO, 7.9% of atomic nitrogen was successfully incorporated into the RGO network (**Table 6.1**).

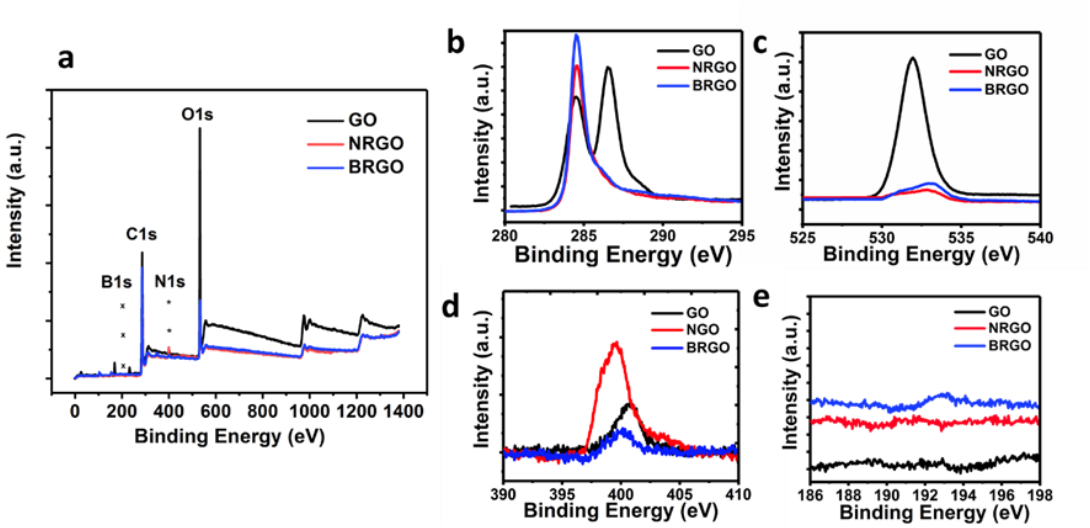

Figure 6.2: X-ray photoelectron spectroscopy (XPS) analysis of the graphene-based sponges with reduced graphene oxide (RGO) coating: ***a)*** *wide region,* ***b)*** *C1s,* ***c)*** *O1s,* ***d)*** *N1s and* ***e)*** *B1s XPS spectra of GO, BRGO and NRGO.*

Table 6.1: The atomic content of the GO precursor solution and synthesized graphene-based sponges, as determined by the XPS analyses.

	GO	**NRGO**	**BRGO**
C (%)	62.6	72.1	75.6
O (%)	36.9	19.9	21.8
N (%)	0.9	7.9	1.2
B (%)	0	0	1.3

The N-active sites were distributed in 0.8% pyrrolic-N (sp3 hybridized and incorporated into a five-membered ring; 399.8 eV), 4.9% pyridinic-N (sp2 hybridized and bonded to two C-atoms; 398.4 eV), 1.4% graphitic-N (401.6 eV) and 0.8% azide groups (402.7 eV) (**Table 6.2**). For BRGO sponge, 1.3% of atomic boron was measured. BRGO and GO contained around 1% of nitrogen originating from the commercial GO solution employed and was not a result of the reduction methodology. Due to the removal of the oxygen functional groups from the basal plane, the interlayer spacing decreased from 8.1 for GO to ≈3.5 for BRGO and NRGO (**Figure 6.3**).

Table 6.2: Percentage of functional groups of C1s, O1s, and N1s in the XPS spectra of the GO precursor solution and synthetized graphene-based sponges, as determined by the deconvolution of peaks in the XPS analyses.

	C1s (%)				O1s (%)			N1s (%)			
	C-C 284.5eV	C-N 285.6eV	C-O 286.9eV	COOH 288.5eV	C-O 531eV	C=O/ C-N-O 533eV	536.3eV	Pyridinic N 398.4eV	Pyrrolic N 399.8eV	Graphitic N 401.6eV	Azide 402.7eV
GO	39.1	4.9	49.7	6.35	96.4	3.6	0	0	100	0	0
NRGO	67.6	18.6	8.61	5.05	23.4	76.6	0	9.6	61.8	18.3	10.2
BRGO	76.4	17.4	4.5	1.7	36.6	63.4	0	21.4	43.1	22.8	12.8

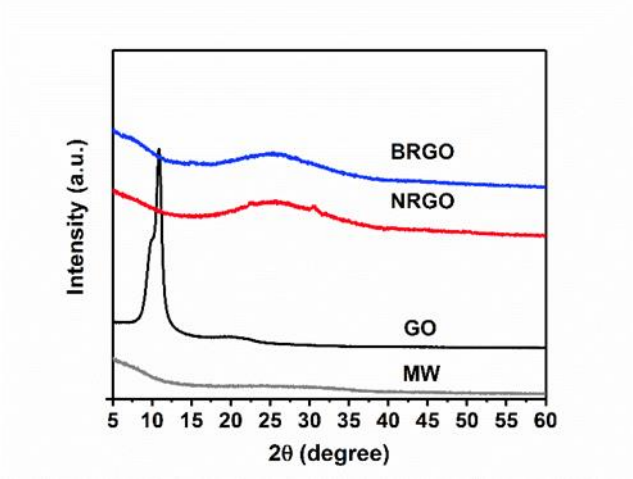

Figure 6.3: Percentage of functional groups of C1s, O1s, and N1s in the XPS spectra of the GO precursor solution and synthetized graphene-based sponges, as determined by the deconvolution of peaks in the XPS analyses.

SEM analysis demonstrated a uniform coating of the mineral wool and the presence of wrinkled graphene-based sheets (**Figure 6.4**).

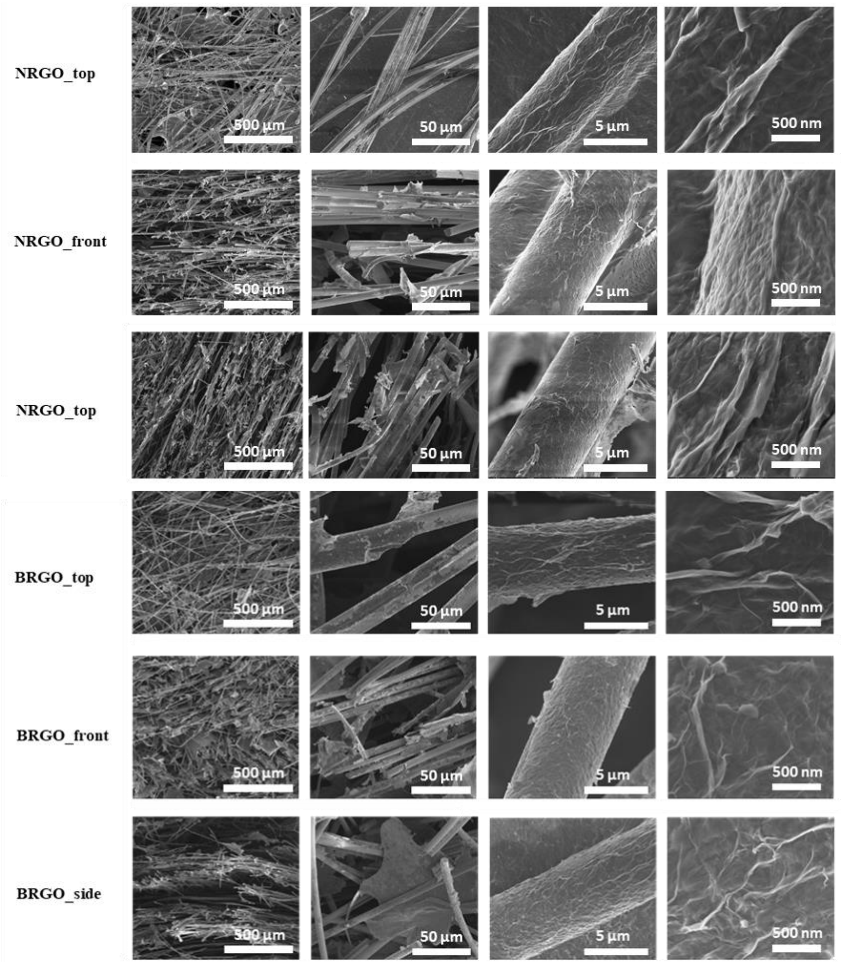

Figure 6.4: SEM images of BRGO and NRGO sponges.

The effect of atomic doping on the surface zeta- potential of graphene-based materials was also investigated at pH 7, as the surface charge can directly affect its interaction with the live bacteria. The zeta potential of the BRGO electrode was –36.2 mV, whereas a less negative value of –13.3 mV was determined for NRGO electrode (**Figure 6.5**), mainly due to the successful incorporation of nitrogen functional groups.

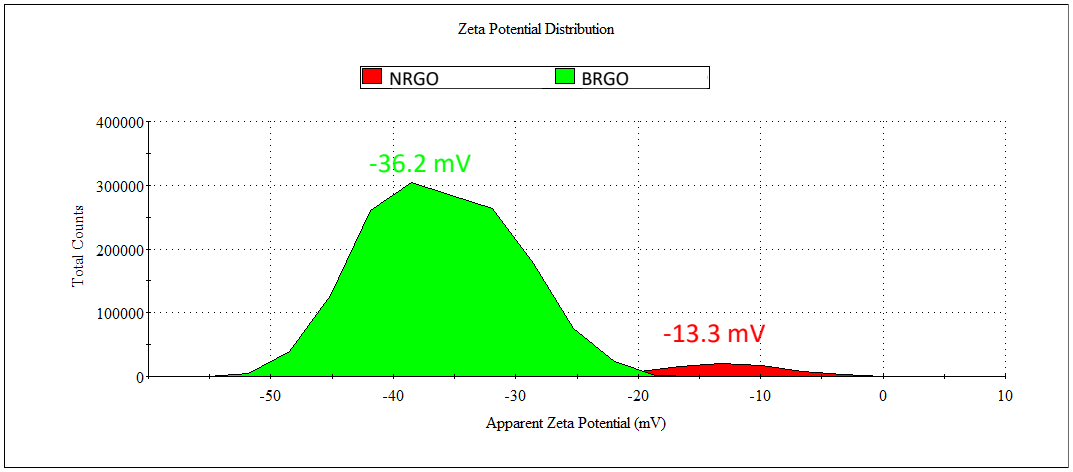

Figure 6.5: Zeta potential distribution of the BRGO and NRGO sponges.

6.3.2 E. coli removal at graphene-based sponge electrodes: impact of atomic doping and current application

The flow direction and anode type did not have any impact on the removal of *E. coli* in the absence of current, and graphene-based sponge electrodes achieved around 0.5–0.8 log removal of *E. coli* in the initial OC run (**Table 6.3**). The surface nanostructure was similar for both BRGO and NRGO sponge, as determined by the SEM analyses (**Figure 6.4).** Previous studies demonstrated antimicrobial activity for GO and RGO in suspension, with 70% and 45% of loss of viability of *E. coli*, respectively (Liu et al., 2011). This activity was mainly assigned to the penetration of the graphene nanosheets into the cell membranes, and extraction of phospholipids (Tu et al., 2013). Yet, "static" graphene-based coatings have a different interaction mechanism with the bacteria compared with graphene in suspension, and rely more on the oxidative stress rather than the membrane stress (Perreault et al., 2015). The exact mechanism behind the antimicrobial properties of graphene-based coatings is still under discussion. Given that both *E. coli* and graphene sponge surface were negatively charged at the experimental pH 7, electrostatic interaction between the bacteria and the electrode in the absence of current was likely minimal. In addition, *E. coli* removal was similar for BRGO-NRGO and NRGO-NRGO systems in the OC experiments, even though the determined surface zeta-potential of the BRGO electrode at pH 7 was more negative compared with the NRGO electrode (**Figure 6.5**). Thus, the 0.5–0.8 log removal of *E. coli* observed in the OC was likely due to the cell deposition, membrane stress caused by the direct contact with sharp nanosheets, and the ensuing reactive oxygen species (ROS)-independent oxidative stress

(Liu et al., 2011). The impact of the anode doping on the *E. coli* removal was evident only with the application of current, as explained further in the text.

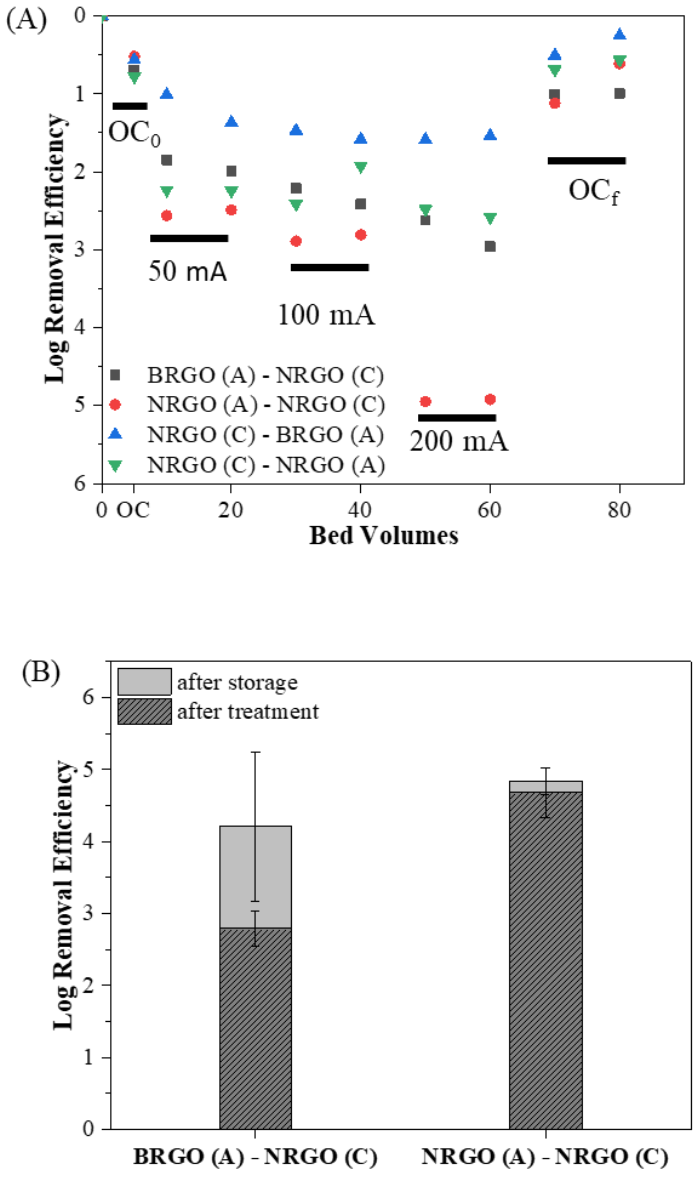

Figure 6.6: Removal of E. coli in phosphate buffer (10 mM, pH 7): A) in anode-cathode (A-C) and cathode-anode (C-A) flow directions using NRGO as cathode, and either BRGO or NRGO as anode, OC0- initial open circuit run, OCf- final open circuit, and B) in NRGO(A)-NRGO(C) system determined immediately after sampling the effluent (i.e., "after treatment"), and after storing the effluent sample at 37 oC for 16 h (i.e., "after storage"); experiment was performed using 10 mM phosphate buffer and 200 mA of anodic current.

Table 6.3: Log removal efficiency (mean ± standard deviation) of E. coli in varying reactor configurations and flow directions, at the samples bed volumes (BV). OC_0-open circuit conducted at the beginning of each experiment. OC_f-final open circuit, conducted at the end of each

experiment (i.e., after the application of current).

Current	BRGO (A) - NRGO (C)	NRGO (A) - NRGO (C)	NRGO (C) - BRGO (A)	NRGO (C) - NRGO (A)
OC_0	0.69±0.43	0.52±0.11	0.56±0.19	0.78±0.02
50 mA, 10 BV	1.85±0.76	2.56±0.61	1.01±0.10	2.23±0.06
50 mA, 20 BV	1.99±0.76	2.49±0.45	1.37±0.53	2.24±0.06
100 mA, 30 BV	2.21±0.51	3.11±0.72	1.47±0.46	2.41±0.07
100 mA, 40 BV	2.42±0.53	2.81±0.55	1.58±0.87	1.93±1.2
200 mA, 50 BV	2.62±0.07	4.54±0.16	1.59±0.52	2.48±1.16
200 mA, 60 BV	2.96±0.73	4.92±0.18	1.54±0.43	2.58±1.38
OC_f, 70 BV	1.00±0.56	1.12±0.65	0.50±0.24	0.69±0.55
OC_f, 80 BV	0.99±0.57	0.61±0.68	0.25±0.12	0.56±0.37

Anodic polarization improves the removal of *E. coli* at both anodes, as can be observed from **Figure 6.6A**. The BRGO-NRGO system resulted in 1.9, 2.3 and 2.6 log removal in A-C flow direction at 50, 100 and 200 mA of applied anodic current, somewhat higher than the *E. coli* removal in the C-A flow direction (i.e., 1.3, 1.5, and 1.6 log removal, respectively) (**Figure 6.6A**). Based on the gradual return of *E. coli* effluent concentrations to the initial value once the current was switched off (i.e., final OC run, OC_f), the removed cells were not only electrosorbed but also inactivated. This was also supported by the storage experiments and Live/Dead analysis, as explained further in the text. Better performance of the A-C configuration using BRGO anode and NRGO cathode was also observed in our previous study focused on the removal of persistent organic contaminants (Baptista-Pires et al., 2021). This was explained by the combination of the following mechanisms: *i)* enhanced activation of O_3 generated at the BRGO anode by the H_2O_2 produced at the NRGO cathode, and *ii)* enhanced production of H_2O_2 via cathodic reduction of O_2 produced at the upstream anode (Staehelln and Hoigne, 1985). The electrogeneration of O_3 and H_2O_2 was confirmed by measuring their formation at 200 mA of applied current, as explained further in the text. Lower *E. coli* removal observed at 50 and 100 mA of applied anodic current is likely a consequence of both lower electrogeneration of oxidants, and worsened interaction of the *E. coli* with the anode surface.

The *E. coli* removal was significantly improved when the dopant of the graphene-based sponge anode was changed from boron to nitrogen (**Figure 6.6A**). For example, at 200

mA of anodic current, *E. coli* removal in the C-A flow direction was improved from 1.6 to 2.6 log removal by substituting the BRGO anode with the NRGO anode. This was even more evident in the better performing A-C configuration, with 2.9 log removal of *E. coli* in BRGO(A)-NRGO(C) system, and up to 5 log *E. coli* removal in NRGO(A)-NRGO(C) system. Thus, the NRGO(A)-NRGO(C) configuration was capable of near complete killing of *E. coli* ($c_0=10^5–10^6$ CFU mL^{-1}) at 200 mA of applied anodic current (i.e., 115 A m^{-2} of projected current density) from a low conductivity supporting electrolyte.

6.3.3 Inactivation mechanism of E. coli cells

To gain further insight into the higher disinfecting ability of the NRGO anode, we determined the formation of major oxidant species at 200 mA of applied anodic current (**Table 6.4**). The amount of ozone formed is presented for the C-A configurations as this configuration avoids its loss at the cathode and enables its detection. The anodes likely had the same electrocatalytic activity towards ozone formation regardless of the flow direction because electrochemical ozone generation is based on water electrolysis ($3H_2O \rightarrow O_3 + 6H^+ + 6e^-$, $E^0=1.51$ V). The NRGO and BRGO anode formed around 0.12 mg L^{-1} and 0.14 mg L^{-1} of ozone, respectively, at 200 mA. Although the amounts of ozone at graphene sponge anodes are well below the typical disinfection doses applied in drinking water treatment (i.e., 1.5 – 3 mg L^{-1}) (Loeb et al., 2012), ozone has high reactivity towards *E. coli* and thus it contributed towards its inactivation (Hunt and Mariñas, 1999, 1997). Similar electrocatalytic activity of the BRGO and NRGO anode towards ozone formation suggests that other mechanisms were determining for the 2-log higher inactivation of *E. coli* using NRGO isntead of the BRGO anode (**Figure 6.6A**). In addition, the inertness of the graphene sponge anodes towards chlorine generation was confirmed by performing electrolysis in the presence of 20 mM NaCl, which revealed very low free chlorine concentration at 200 mA of anodic current (115 A m^{-2}) for both BRGO (0.41 mg L^{-1}) and NRGO anode (0.03 mg L^{-1}). Also, we did not measure any chlorate and perchlorate formation in these conditions, in accordance with our previous study (Baptista-Pires et al., 2021).

Table 6.4: Concentrations of ozone and free chlorine measured using BRGO and NRGO anode in C-A configuration using phosphate buffer (10 mM, pH 7), and in the presence of 20 mM

NaCl, respectively, at 200 mA.

	O_3 (mg L^{-1})	Free Chlorine (mg L^{-1})
NRGO (C) – NRGO (A)	0.12 ± 0.01	0.06 ± 0.003
NRGO (C) – BRGO (A)	0.14 ± 0.006	0.41 ± 0.19

Besides ozone, H_2O_2 was measured in the A-C configurations in which oxygen produced at the upstream anode enhances the cathodic formation of H_2O_2 at the downstream cathode ($O_2 + 2H^+ + 2e^- \rightarrow H_2O_2$, $E^o = -0.67$ V) (Baptista-Pires et al., 2021). In accordance with our previous study (Baptista-Pires et al., 2021), low concentrations of H_2O_2 were measured in both BRGO(A)-NRGO(C) and NRGO(A)-NRGO(C) systems (i.e., 0.88 and 0.66 mg L^{-1} at 200 mA, **Table 6.5**). These amounts likely represented residual and not formed H_2O_2 due to its decomposition to $OH^{\bullet}$ at the N-active sites of the NRGO cathode (Su et al., 2019) , as well as its reaction with the anodically generated ozone ($2O_3 + H_2O_2 \rightarrow 2OH^{\bullet} + 3O_2$). Inactivation of *E. coli* with H_2O_2 is generally inefficient, as significantly higher peroxide concentrations (i.e., 34 mg L^{-1}) did not inactivate *E. coli* (Jeong et al., 2006). On the other hand, $OH^{\bullet}$ are capable of efficient *E. coli* inactivation (Jeong et al., 2006). In the experiments with TA, the estimated steady state concentration of $OH^{\bullet}$ was the same for both BRGO(A)-NRGO(C) and NRGO(A)-NRGO(C) systems (i.e., $1.5\pm0.09\times10^{-13}$ M, *Table 6.5*).

Table 6.5: Concentration of H_2O_2 and quasi steady-state concentration of $OH^{\bullet}$ ($[OH^{\bullet}]SS$) measured using BRGO and NRGO anode in A-C configuration using phosphate buffer (10 mM, pH 7) at 200 mA*

	H_2O_2 (mg/L)	$[OH^{\bullet}]_{SS}$ (M)
NRGO (A) – NRGO (C)	0.66±0.03	$1.54\pm0.09\times10^{-13}$
BRGO (A) - NRGO (C)	0.88±0.22	$1.48\pm0.06\times10^{-13}$

**$[OH^{\bullet}]_{ss} = \frac{k_{TA}}{k_{TA.OH}}$ where $k_{TA,OH}$ (4×10^9 M^{-1} s^{-1}) (Charbouillot et al., 2011) is the second-order rate constant for $OH^{\bullet}$ with terephthalic acid (TA), and k_{TA} (s^{-1}) is the pseudo-first rate constant of TA decay (Moura de Salles Pupo et al., 2020; Nayak and Chaplin, 2018).

The role of $OH^{\bullet}$ in the inactivation of *E. coli* in graphene- based sponge electrodes was

investigated by adding excess methanol. However, the removal of *E. coli* was somewhat higher (i.e., 5.3–6.0 log removal) compared with the removal in the absence of methanol (5.1 log removal) (**Figure 6.7, Table 6.6**). Control experiments showed that the selected concentration of methanol (i.e., 10 mM) was not toxic to *E. coli*, which is in accordance with the literature (Ganske and Bornscheuer, 2006). Nevertheless, the toxicity of methanol to *E. coli* may be increased in the presence of the electric field. Recently, Xie et al. (Xie et al., 2020) reported greater intracellular diffusion of ozone after the application of electric field, which was explained by the formation of pores and disruption of the integrity of the cell membrane in the electric field. Herraiz-Carboné et al. reported recently that the electrogenerated ozone can attack the genetic material inside the bacterial cells, thus inactivating the *Klebsiella pneumoniae* (Herraiz-Carboné et al., 2021a). Once the electric field facilitates the penetration of methanol in the bacterial cell, it can accumulate within the cell and severely affect its function, causing cell death (Dyrda et al., 2019).

This can explain a slightly higher removal of *E. coli* with the addition of a radical scavenger, but at the same time, it makes it difficult to determine the contribution of $OH^{\bullet}$ to *E. coli* inactivation.

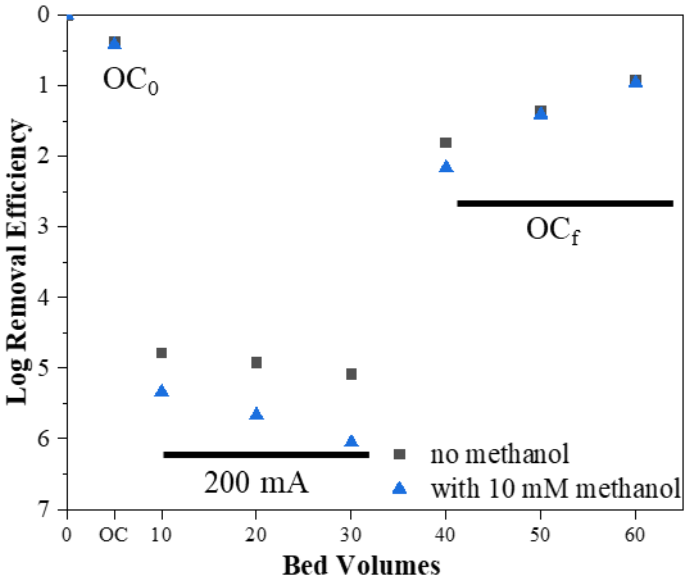

Figure 6.7: Removal of E. coli in 10 mM phosphate buffer (square) and with the addition of 10 mM methanol (triangle), in the initial OC0, 200 mA of applied anodic current, and OC applied at the end of experiment (OCf).

Table 6.6: Log removal efficiency (mean ± standard deviation) of E. coli in the continuous current experiment at 200 mA (10 mM phosphate buffer, pH 7), with and without the addition of 10 mM methanol.

Bed Volumes	No added methanol	With 10 mM methanol
OC_0, 10 BV	0.37±0.11	0.42±0.23
10, X BV	4.79±0.60	5.34±0.91
20, X BV	4.92±0.18	5.66±0.44
30, X BV	5.09±1.23	6.05±0.11
40, X BV	1.81±0.23	2.16±0.13
50 OC_f, X BV	1.35±0.92	1.41±0.02
60 OC_f, X BV	0.92±0.27	0.96±0.06

Given the similar electrocatalytic activity of the BRGO and NRGO anodes towards ozone generation (**Table 6.4**), and similar amounts of H_2O_2 formed at the NRGO in the two investigated configurations (**Table 6.5**), higher removal of *E. coli* when using NRGO anode can be explained by its enhanced electrosorption at the NRGO anode surface, resulting in its more complete inactivation than in the case of the BRGO anode. Electrosorption of the negatively charged bacterial cells at the positively charged anode surface and their subsequent inactivation due to electroporation is an important mechanism of cell inactivation at carbon-based electrodes; electroporation can lead to loss of the structural integrity of the cell membrane and thus cell death (Dandie et al., 2020). Previous study identified oxidative stress as the predominant antibacterial mechanism of N-doped reduced graphene oxide in suspension (Wang et al., 2019). Pyridinic-N and pyrrolic-N identified in the NRGO sponge (4.9% and 0.8%, respectively, section 3.1) are located on the graphene edges and provide a p-type doping, i.e., electron-deficient sites, whereas graphitic-N (1.4%) is an n-type dopant representing an electron-rich site. In the case of BRGO, boron atom is also a p-type dopant, yet the percentage of boron incorporated into graphene is significantly lower (1.3%) compared with the pyridinic-N in NRGO (4.9%). Thus, the NRGO anode attracts more the negatively charged *E. coli* due to more electron-deficient sites (i.e., 5.7% of pyridinic and pyrrolic-N in NRGO anode, versus 1.3% of boron in BRGO anode) and thus higher localized

positive charge accumulated at the NRGO sponge surface during anodic polarization.

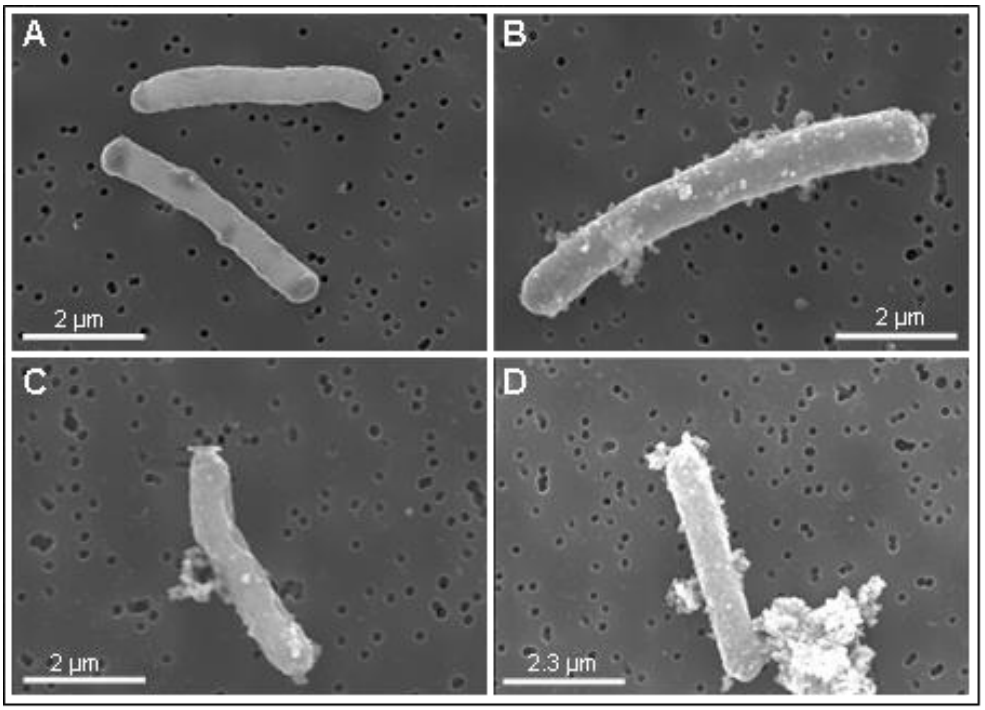

*Figure 6.8: SEM images of E. coli before (**A**) and after (**B-D**) treatment*

FESEM images of the electrochemically treated E. coli cells show the damage induced in the cell membranes via electroporation (**Figure 6.8**). After electrochemical treatment, many cells show protrusions of intracellular content through pores (**Figure 6.8B-D**) and cell walls show sunken surface (**Figure 6.8C**). The formation of pores in the cell membrane is a typical outcome of electroporation that results in bacterial inactivation (C. Liu et al., 2013). Similar low- voltage electroporation was previously reported for carbon nanotube (CNT)-based sponges (Huo et al., 2017). Furthermore, the analyses of potassium showed an increase in K+ concentration, from 0.58 ± 0.02 mg L–1 in the initial solution to 1.18 ± 0.29 mg L–1 after treatment (**Figure 6.9**).

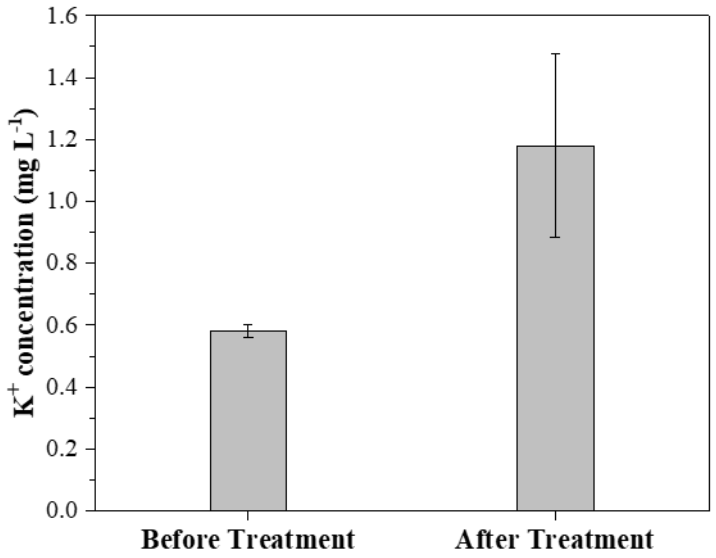

Figure 6.9: K+ concentration in the 10 mM phosphate buffer amended with 107 CFU mL-1 of E. coli before and after electrochemical treatment at 200 mA with the NRGO (A) -NRGO (C) configuration.

The K^+ ion has multiple roles in the *E. coli* cells, serving as an essential osmotic solute, activator of intracellular enzymes, regulator of intracellular pH, and a second messenger to stimulate accumulation of compatible solutes (Radchenko et al., 2006). Leakage of K^+ results from either the change in cell permeability, or complete destruction of the cell, and was previously reported in electrochemical disinfection using BDD anode in sulfate-based solution (Long et al., 2015).

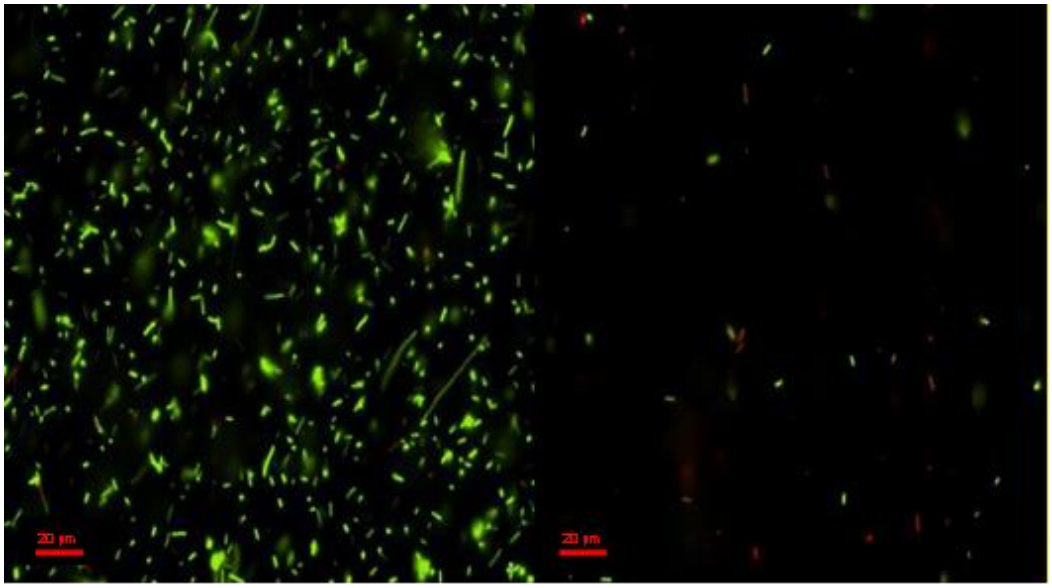

Figure 6.10: Micrograph of E. coli cells before (left) and after (right) treatment using the Live/Dead bacterial viability kit. Green- and red-stained cells correspond to cells with intact and damaged membranes, respectively.

The impairment of membrane integrity of E. coli cells was confirmed with the Live/Dead analyses of the electrochemically treated sample, with a drastic decrease in the number of viable cells (green-stained) and the appearance of damaged ones (red-stained) in the sample treated at 200 mA (**Figure 6.10**). Remarkably, the low number of red-stained cells in the sample corresponding to 5 log E. coli removal are likely due to complete cell lysis for most inactivated cells, making staining with PI unfeasible. Furthermore, samples treated at 200 mA in the BRGO(A)-NRGO(C) and NRGO(A)-NRGO(C) systems showed further decrease in E. coli after storage experiments conducted at optimum growth temperature (37 ºC) for 16 h (**Figure 6.6B**). This decrease was more obvious for the BRGO(A)-NRGO(C) system due to the presence of more E. coli cells that withstand the treatment under this configuration (i.e., ~10^2 CFU mL^{-1}). Further cell death with storage time demonstrates irreparable damage of cell walls after the electrochemical treatment. Near complete removal of *E. coli* in the NRGO(A)-NRGO(C) system made it difficult to see further decrease in *E. coli* concentration. Yet, it confirmed that there was no regrowth of the bacteria during storage.

6.3.4 Impact of the initial E. coli concentration on disinfection performance

When the initial concentration of *E. coli* was increased to 10^6–10^7 CFU mL^{-1}, the resulting removal of *E. coli* increased from 5.1 ± 0.3 log removal to 5.8 ± 1.2 log removal (**Figure 6.11**). Thus, one-pass operation of the graphene sponge-based electrochemical system at 200 mA and with the HRT of 3.5 min was still sufficient to achieve near complete disinfection even at higher initial *E. coli* concentrations, and without any contribution by active chlorine species, which is the common disinfectant employed in electrochemical systems.

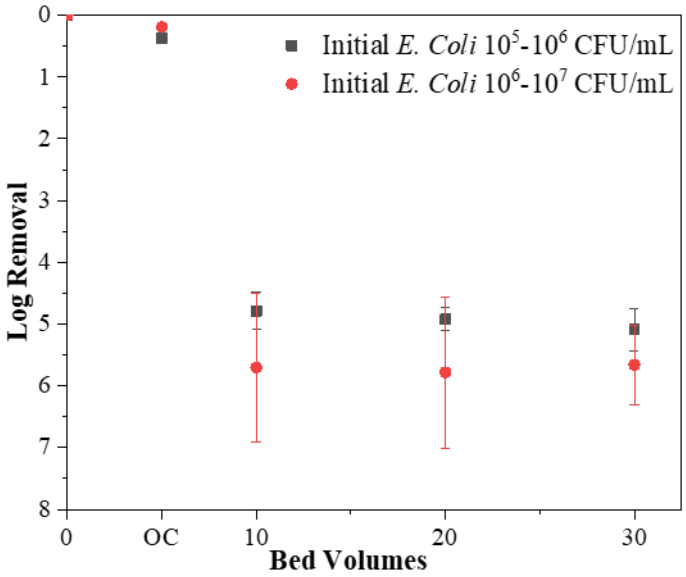

Figure 6.11: Removal of E. coli in phosphate buffer (10 mM, pH 7) at the initial concentration of E. coli of 10^5-10^6 (square) and 10^7 (circle) CFU mL^{-1}.

6.3.5 E. coli removal with intermittent current application

In the scientific literature, one of the main applications of the graphene-based materials has been in the energy storage field, as supercapacitors, due to their pseudocapacitive behavior, high specific surface area, tunable porosity and hierarchical arrangement, in addition to low cost and ease of synthesis (Xu et al., 2011; Zhao et al., 2012) . Given the ability of these materials to perform continuous and fast charge/discharge cycles, we investigated the disinfection capability of the best-performing configuration, NRGO(A)-

NRGO(C), under intermittent current application. As illustrated in **Figure 6.12A**, the obtained removal of *E. coli* was largely dependent on the duration of the ON and OFF cycles. When the current pulse was symmetrical and total cycle time equivalent to one HRT (i.e., ON and OFF cycle duration of half HRT, 105 s each), only up to 3.3 log removal of *E. coli* was achieved, compared with up to 5.1 log removal under continuous current.

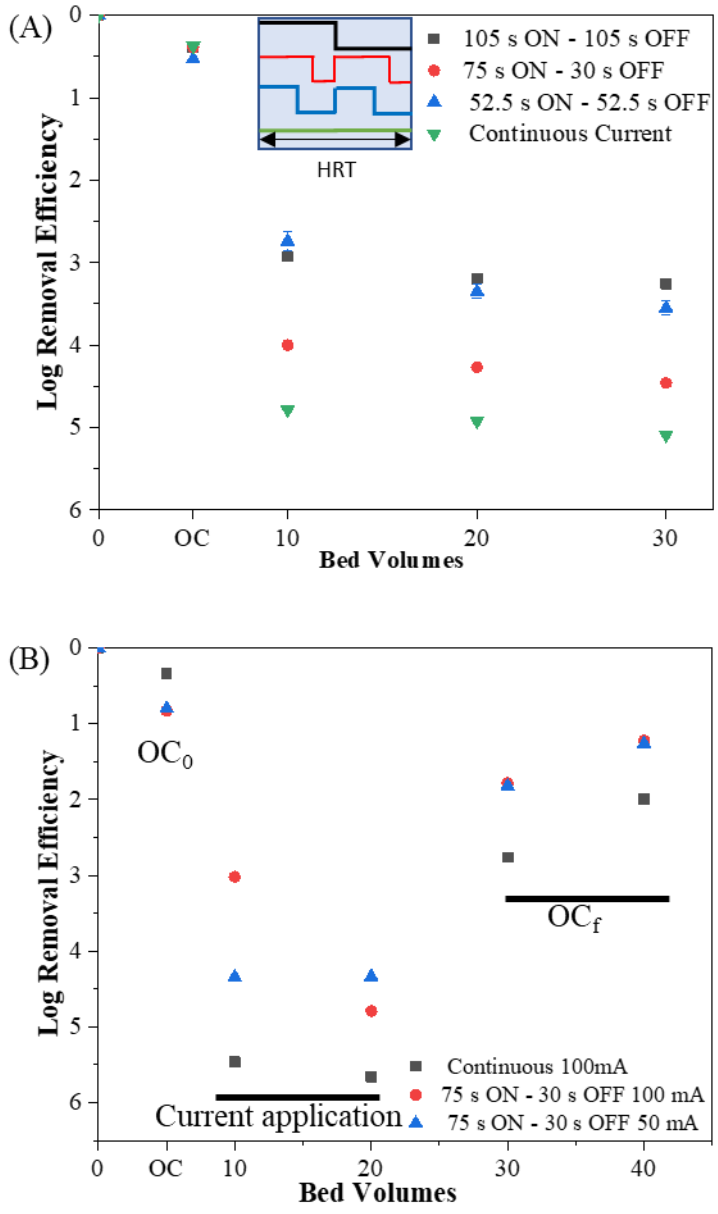

*Figure 6.12: Removal of E. coli in **A)** phosphate buffer (10 mM, pH 7) at continuous current and with intermittent current application, both at 200 mA, with varying durations of ON and OFF cycles, and **B)** tap water at continuous current (100 mA) and with intermittent current application at 50 mA and 100 mA.*

Table 6.7: Log removal efficiency (mean ± standard deviation) of E. coli in the continuous and intermittent current experiments in 10 mM phosphate buffer using the NRGO(A)–NRGO(C) configuration at 200 mA.

Bed Volumes	Continuous	105 s ON 105 s OFF	75 s ON 30 s OFF	52.5 s ON 52.5 s OFF
OC_0	0.37±0.03	0.39±0.03	0.39±0.03	0.53±0.06
10	4.79±0.31	2.93±0.54	4.00±0.04	2.74±0.11
20	4.92±0.18	3.20±0.11	4.27±0.20	3.35±0.08
30	5.09±0.34	3.26±0.39	4.46±0.27	3.55±0.08

Given that graphene-based materials undergo fast charging but also fast discharging (Xu et al., 2011; Zhao et al., 2012) , it is likely that the duration of the OFF cycle was too long for the graphene-based sponges to maintain the sufficient current density and contribute to disinfection during the OFF stage. Very similar results and up to 3.6 log removal of *E. coli* was obtained when the reactor was operated using two symmetrical pulses within one HRT (i.e., ON and OFF cycles of 52.5 s each), and in this case may have been a consequence of too short ON cycles that did not allow sufficient electrosorption of *E. coli* onto the graphene sponge electrodes, thus leading to their lower inactivation (**Figure 6.12A, Table 6.7**).

Thus, we applied asymmetrical pulses with total duration of one HRT, and 75 s of ON cycle/30 s of OFF cycle. This operation resulted in up to 4.5 log removal of *E. coli*. This result is similar to that recorded with continuous current (i.e., up to 5.1 log removal) but the application of intermittent current enabled a significantly lower energy consumption (i.e., 4.82 kWh m^{-3}) compared with the continuous current (i.e., 8.83 kWh m^{-3}) (**Table 6.8**). Thus, pseudocapacitive behavior of graphene-based sponge electrodes may allow saving energy by applying intermittent current and without compromising the disinfection performance.

*Table 6.8: Electric energy consumption** (E, kWh m-3) for the removal of E. coli in the experiments with continuous and intermittent current application in 10 mM phosphate buffer (PB) (anodic current, IAN=200 mA) and tap water (TW) (I_{AN}=50 mA and 100 mA).*

Experiment	Continuous	105 s ON 105 s OFF	75 s ON 30 s OFF	52.5 s ON 52.5 s OFF
PB, I_{AN}=200mA	8.83±0.36 kWh m^{-3}, 4.9±0.2 log removal	3.78±0.07 kWh m^{-3}, 3.1±0.2 log removal	4.82±0.14 kWh m^{-3}, 4.2±0.2 log removal	3.70±0.19 kWh m^{-3}, 3.2±0.4 log removal
TW, I_{AN}=50mA	-	-	1.38±0.14 kWh m^{-3}, 4.3±0.2 log removal	-
TW, I_{AN}=100mA,	5.70±0.24 kWh m^{-3}, 5.6±0.1 log removal	-	4.55±0.01 kWh m^{-3}, 3.9±1.3 log removal	-

**E=(U*I)/q, where U-total cell potential (V), I-applied current (A), q-electrolyte flowrate (L h^{-1})

6.3.6 E. coli removal from real tap water

The performance of the NRGO(A)-NRGO(C) system was investigated with real tap water (characteristics in **Table 6.9)** spiked with *E. coli* (10^6–10^7 CFU mL^{-1}).

Table 6.9: Characteristics of the employed tap water. TAC – total alkalinity, TOC- total organic carbon.

Conductivity (µS cm^{-1})	T_{AC} (mg L^{-1})	Cl^- (mg L^{-1})	SO_4^{2-} (mg L^{-1})	Na^+ (mg L^{-1})	Mg^{2+} (mg L^{-1})	Ca^{2+} (mg L^{-1})	TOC (mg L^{-1})
450	130.1	21.4	13.4	13.8	9.2	51.2	2.1

Electrochemical disinfection of tap water was performed using continuous current application at 100 mA, resulting in the ohmic-drop corrected anode potential of 2.4

V/SHE (recorded anode potential of 5.8 V/SHE), same as in the case of the more conductive 10 mM phosphate buffer at 200 mA (i.e., ohmic-drop corrected potential of 2.4 V/SHE, recorded potential of 5.4 V/SHE) (**Table 6.10**).

Table 6.10: Recorded anode potentials (E_{AN}, V/SHE) and total cell potentials (E_{TOT},V) at different applied anodic currents (I_{AN}, mA), in continuous and intermittent current mode using 10 mM phosphate Buffer (PB) and tap water (TW). Ohmic-drop in TW was calculated 1.7 and 3.4 V for 50 and 100 mA respectively. The present values have not been corrected for the ohmic-drop and represent outputs recorded by the potentiostat.

	PB, I_{AN}=200 mA		**TW, I_{AN}=100 mA**		**TW, I_{AN}=50 mA**	
	E_{AN}, V/SHE	**E_{TOT}, V**	**E_{AN}, V/SHE**	**E_{TOT}, V**	**E_{AN}, V/SHE**	**E_{TOT}, V**
Continuous current	5.4±0.9	15.9±1.8	5.8±1.2	21±1.7	-	-
105 s ON - 105 s OFF	6.3±0.2	14.4±0.2	-	-	-	-
75 s ON - 30 s OFF	5.6±0.1	13.1±0.3	8.9±1.7	22.5±2.8	4.9±0.6	13.2±1.2
52,5 s ON - 52,5 s OFF	6.6±0.4	14.1±0.6	-	-	-	-

The obtained *E. coli* removal was similar for the two experiments, with up to 5.5 log removal obtained for tap water (**Figure 6.12B**). Thus, phosphate anions did not impact negatively the electrosorption and electrochemical inactivation of *E. coli* at the graphene-based sponge electrodes. Application of 100 mA of anodic current in 75 s ON – 30 s OFF mode resulted in up to 4.9 log removal of *E. coli* (**Figure 6.12**). However, although the experiment in tap water using continuous application of 100 mA could be performed without any difficulties, experiment performed in the intermittent mode rapidly led to a large increase in both anode and cathode potentials, resulting in the total cell potential >34 V (limit of the potentiostat unit employed) and frequent process failure in the replicate experiments (**Table 6.10**).

Table 6.11: Recorded anode potentials (EAN, V/SHE) and total cell potentials (ETOT,V) at different applied anodic currents (IAN, mA), in continuous and intermittent current mode using 10 mM phosphate Buffer (PB) and tap water (TW). Ohmic-drop in TW was calculated 1.7 and 3.4 V for 50 and 100 mA respectively. The present values have not been corrected for the ohmic-drop and represent outputs recorded by the potentiostat.

	PB, I_{AN}=200 mA		**TW, I_{AN}=100 mA**		**TW, I_{AN}=50 mA**	
	E_{AN}, V/SHE	**E_{TOT}, V**	**E_{AN}, V/SHE**	**E_{TOT}, V**	**E_{AN}, V/SHE**	**E_{TOT}, V**
Continuous current	5.4±0.9	15.9±1.8	5.8±1.2	21±1.7	-	-
105 s ON - 105 s OFF	6.3±0.2	14.4±0.2	-	-	-	-
75 s ON - 30 s OFF	5.6±0.1	13.1±0.3	8.9±1.7	22.5±2.8	4.9±0.6	13.2±1.2
52,5 s ON - 52,5 s OFF	6.6±0.4	14.1±0.6	-	-	-	-

Limited ion diffusion in the low conductivity tap water, as well as larger ohmic losses will drive the electrode potentials upwards. The capacitance and rate capability of the graphene-based electrodes will be greatly affected by the diffusion of inserted and de-inserted ions, with aqueous electrolytes with lower ionic conductivity and mobility having slower charging and discharging rates (Zhu et al., 2015) . Thus, application of the intermittent current may result in the overall higher total cell potential compared with the continuous current due to the slower discharge during the short 30 s OFF stages of the cycle (Chen et al., 2011; Prakash and Bahadur, 2014). By lowering the current to 50 mA, operation of the reactor in 75 s ON – 30 s OFF cycles was more stable and up to 4.5 log removal of *E. coli* was achieved (**Figure 6.12**). Electrochemical disinfection of real tap water using the intermittent current mode led to significant savings in the energy consumption, which was decreased from 5.70 kWh m^{-3} in continuous current mode (up to 5.5. log removal) at 100 mA, to 4.55 kWh m^{-3} in the intermittent current mode at 100 mA (4.9 log removal), and 1.38 kWh m^{-3} in the intermittent current mode at 50 mA of anodic current (4.5 log removal). These results compare favorably to the energy consumption of electrochemical disinfection systems reported in literature, even including chlorine-mediated disinfection, and yet are achieved in a chloride-free electrolyte. For example, electro-disinfection of the liquid fraction of blackwater required around 4.4 kWh m^{-3}, although the process was chlorine-mediated, and the influent conductivity was significantly higher compared with the tap water used in our study

(Trotochaud et al., 2020) . Electrochemical disinfection of *E. coli* in 30 mM Na_2SO_4 and platinum-based anodes achieved 4 log *E. coli* removal and required 6.3 kWh m^{-3} (Kerwick et al., 2005). BDD anodes can achieve efficient electrochemical disinfection of wastewater at low current densities (e.g., 1-50 A m^{-2}) and thus low energy consumptions (e.g., 0.1-1.1 kWh m^{-3}) (Cano et al., 2016; Herraiz-Carboné et al., 2021b), but the process relies on the generation of chloramines, which in turn may lead to the formation of N-nitrosodimethylamine (NDMA), a highly toxic and carcinogenic DBP (Richardson, 2003). Also, electrochemical disinfection of sewage effluent using an integrated electrodisinfection-electrocoagulation system equipped with a BDD anode and sacrificial iron electrodes required 2.24 kWh m^{-3} for complete inactivation of *E. coli*, whereas the formation of toxic chlorinated byproducts was limited by applying low current densities (<7 A m^{-2}) and electrical charges (<0.07 $kAhm^{-3}$) (Cotillas et al., 2020) . In our study, although the employed tap water contained low concentration of chloride (20 mg L^{-1}, **Table 6.9**), it was not oxidized at the anode to chlorine or other chlorinated species (chlorate, perchlorate), as was previously demonstrated when using graphene sponge anodes and significantly higher chloride concentrations (Baptista-Pires et al., 2021). Given that the graphene sponge electrodes do not oxidize chloride, the formation of disinfection byproducts such as THMs and HAAs typical of chlorine-based disinfection is excluded and makes the electrodes more versatile for use with different water matrices and current densities.

6.4 Concluding remarks

Electrochemical disinfection was investigated in a one-pass flow-through electrochemical system equipped with graphene sponge electrodes, using low conductivity supporting electrolyte and *E. coli* as an indicator microorganism. The main conclusions of the current study are the following:

- The order of the electrodes had a determining impact on the reactor performance, with anode-cathode flow direction yielding on average two-fold higher *E. coli* log removal compared with the cathode-anode configuration.

- Atomic doping of the graphene sponge was crucial to further enhance the disinfection performance. The NRGO sponge anode bearing more positive charge

achieved complete inactivation of *E. coli* (i.e., 5 log removal) in a chloride-free electrolyte, versus 2.6 log removal of *E. coli* using BRGO sponge anode, both at the projected anodic current density of 115 A m^{-2}.

- The main inactivation mechanism of *E. coli* was based on the electrosorption of bacteria to the anode surface and cell lysis due to the disruption of the cell walls by electroporation. The changes in the cell morphology were confirmed by the FESEM analyses and Live/Dead staining experiments. Storage experiments conducted with the electrochemically treated samples also confirmed the damaged cell walls and no regrowth of *E. coli* after treatment. The electrogenerated ozone and hydroxyl radicals were measured, and these species likely contributed to *E. coli* inactivation.

- Electrochemical system equipped with the NRGO anode and cathode was employed for tap water disinfection at 58 A m^{-2}, and achieved up to 5.5 log removal of *E. coli* with an energy consumption of 5.70 kWh m^{-3}. This energy consumption could be further lowered to 1.38 kWh m^{-3} by applying current in an intermittent mode (i.e., in ON/OFF pulses of 29 A m^{-2}), without significant decrease in the inactivation efficiency (i.e., 4.5 log removal), due to the intrinsic capacitive properties of graphene-based materials.

Given the low electrocatalytic activity of the graphene sponge anode towards chloride oxidation (current efficiency <0.1%), and the fact that no chlorine, chlorate, and perchlorate was detected in the system even at high current densities in the presence of high chloride concentration (i.e., 20 mM NaCl), the present study demonstrates great potential of the developed materials for water disinfection without forming disinfection by-products typically observed in chlorine-based disinfection. The estimated cost of graphene-based sponge is only €23 per m^2 of projected surface area, given the lower concentration of the GO dispersion used in the synthesis compared with our previous study (Baptista-Pires et al., 2021). This is extremely competitive compared with the state-of-the-art BDD anodes (~€4,200 per m^2) and dimensionally stable anodes (DSAs) (€3,000 per m^2) (Wenderich et al., 2021). Given that they are produced using a simple and scalable production method, graphene-based sponge electrodes hold great promise for practical applications of electrochemical water treatment systems and their deployment in the developing countries and rural communities. For example, a 1 m^2 solar panel can produce up to 208 kWh/year (i.e., 569 Wh per day) of energy, assuming 16% efficiency (National Renewable Energy Laboratory, 2018). For the treatment of tap water, the system developed

in this study and connected to a 1 m^2 solar panel would produce 118 L per day of disinfected water, which could be further increased to 412 L per day using intermittent current supply. Thus, solar-powered electrochemical disinfection using low- cost graphene sponge electrodes may provide clean water for impoverished communities not connected to the energy grid.

CHAPTER 7 General discussion & future perspectives

Despite the progress of electrochemical technologies in wastewater treatment, certain limitations hinder their widespread industrial use, including the short lifespan of electrode materials and low current efficiency. Additional restrictions are the mass transfer limitations, small space-time yields and low area-volume ratios in traditional electrochemical reactors, especially when dealing with low-conductivity wastewater. In this thesis, ways of overcoming these challenges were explored, by utilizing 3D reactors for the treatment of persistent organic contaminants and disinfection. During the two first chapters the introduction of a bed electrode between the two main electrodes was examined, while in the last chapter of the thesis, 3D electrodes were used as anodes and cathodes. Overall, in both cases, the 3D system performed better than the 2D system.

RGO-coated graphite granules as particle electrodes in 3D electrochemical reactor

In the fourth chapter of this thesis, graphite granules were used as particle electrodes in a three-dimensional flow-through reactor treating persistent contaminants, spiked in synthetic electrolyte (Na_2SO_4), in a low initial concentration (2 μM). The low concentration of the contaminants was used to simulate actual wastewater conditions, where the contaminants concentration is lower than that of dissolved salts and organic matter. The results showed that graphite granules can be effective as particle electrodes in 3D reactors and that coating them with RGO and doping with nitrogen and/or manganese oxide can enhance their performance. Apart from BDD (which is a widely recognized anode material for wastewater treatment), Ti/RuO_2-IrO_2 has demonstrated good performance in the 3D system. Ti/RuO_2-IrO_2 is also more cost-effective compared to BDD, making it an attractive alternative option (Zhang et al., 2013). For both anode materials, the 3D system presented higher removal rates and lower energy consumption compared with the 2D system, due the contribution of the particle electrodes. The improvement of the efficiency is based on the synergy between electrochemical oxidation and adsorption/electrosorption of pollutants on the granules. Each granule functions as an electrode, where direct oxidation of the contaminants that are in contact occurs via electron transfer, as well as indirect oxidation by the produced oxidant species. Also, adsorption on the granules and electrosorption because of their charge under the electric field occur. Therefore, the total electroactive area of the system is increased. When comparing the performance of BDD and Ti/RuO_2-IrO_2 anodes, it was observed that the removal rates of contaminants were higher with the BDD anode. However, the system

with the Ti/IrRuO$_2$ anode exhibited a higher synergy. This difference in synergy can be attributed to the relatively lower degradation performance of contaminants by Ti/RuO$_2$-IrO$_2$ compared to BDD in the 2D system. Therefore, the impact of the particle electrode addition is more noticeable. Another difference between BDD and Ti/RuO$_2$-IrO$_2$ is the overpotential of oxygen evolution. BDD has higher overpotential for oxygen evolution and thus the oxidation of the contaminants on its surface is more efficient. What is more, the decomposition process of Ti/RuO$_2$-IrO$_2$ anodes is highly based on chlorine evolution, whereas BDD can produce more $OH^{\bullet}$ (Okur et al., 2022). Thus, in the Na_2SO_4 electrolyte that was used in the experiments, Ti/RuO$_2$-IrO$_2$ performance is more limited. Besides, in this electrolyte persulfate ($S_2O_8^{2-}$) , which also contributes to the contaminants oxidation, is also formed on the BDD anode (Sopaj et al., 2015). In matrices with Cl^- present, the organo-chlorinated by-products formation with Ti/RuO$_2$-IrO$_2$ is expected to be higher than with BDD. On the other hand, formation of chlorate and perchlorate is expected to be higher with BDD (Gonzaga et al., 2021).

Graphite granules were selected because of their high conductivity and low porosity, which can enhance their regeneration. Correia-Sá compared biochars with different adsorption capacities as particle electrodes for the removal of carbamazepine and concluded that the polarizability of the particle electrodes is more important than their adsorption capacity in 3D reactors (Correia-sá et al., 2021). Non-porous materials seem to have better capacity for applications that combine adsorption and electrochemical treatment (McQuillan et al., 2018), as in such materials the regeneration can be faster, due to the fact that the adsorbed contaminants are more accessible to reactive oxygen species that degrade them (Asghar et al., 2019; Sharif et al., 2017). Graphite is a material that has not been used extensively as a particle electrode and it could be a representative example of other non-porous materials as well. Granular graphite particles (Shen et al., 2017), graphite intercalation compounds (Nyex) and natural large flake graphite (NFLG) are among the graphite-based materials that have been used as particle electrodes in 3D processes (Asghar et al., 2019).

RGO coating of granules increased the contaminants removal rate and reduced the energy consumption of the system compared to the non-coated granules, as it enhances the conductivity, specific surface area and adsorption capacity of the granules (Gao et al., 2011). Introduction of manganese oxide in the RGO coating further enhanced the contaminants adsorption and their removal rate, due to the ability of manganese oxide to

increase the specific surface area (Li et al., 2013), boost $OH^{\bullet}$ production and charge transfer on the surface of the granules (Massa et al., 2017). Li et al synthesized a hybrid material of manganese oxide (Mn_2O_3) coated graphene oxide which had higher specific area from the GO without Mn_2O_3, 108 $m^2\ g^{-1}$ and 32 $m^2\ g^{-1}$ respectively. Furthermore, the adsorption capacity of the Mn_2O_3-GO was found 8 times higher than that of GO without Mn_2O_3 (Li et al., 2013).

The main challenge faced during the experiments was the corrosion of the graphite granules, when high current densities were applied. Shen et al. also observed that application of high current densities causes the release of graphite powder to the bulk solution, due to the destruction of the graphite granules surface (Shen et al., 2017). Different coating methods and coating materials were applied, but a uniform coating that was stable and could protect the granules from corrosion could not be achieved. SEM analysis confirmed the presence of the coated material, but it also revealed the lack of homogeneity of the coating. RGO coating managed to reduce the corrosion of the graphite granules, but not prevent it completely. We hypothesize that a uniform RGO coating could protect the granules from corrosion, as well as improve the system´s efficiency further. Besides, RGO has been reported to show anticorrosive properties (Bordbar-Khiabani et al., 2019; Kiran et al., 2017) and in combination with polymer materials it was also reported to increase anti-corrosion properties and conductivity. For example, Cai et al. improved the anti-corrosion ability of steel by coating it with polyaniline/graphene (PANI/RGO), with waterborne polyurethane (WPU) as matrix. Except for its anticorrosive properties, RGO was selected as a coating of because its high conductivity, high surface area and it´s oxygen functionalities capable of acting as active sites for ROS electrogeneration, that can enhance removal of contaminants. Besides, combining RGO with polymers can further increase the conductivity, removal efficiency and stability of the granules (Zhang et al., 2018).

The main objective of proving that 3D systems based on particle electrodes are more efficient than 2D systems was achieved. The introduction of a cheap material as a particle electrode managed to increase the removal rate of the various persistent contaminants (e.g. up to three times for IPM) while decreasing the E_{Eo} (up to 60% for IPM). Furthermore, coating with RGO and doping with nitrogen and/or manganese oxide proved to enhance the performance of the granules, as it managed to further increase the removal rate of the contaminants (e.g., 12% more for IPM) and decrease the energy

demand (e.g., 23% lower for IPM).

Regarding future research, one of the main aims would be to optimize the coating method and coating material of the granules. A uniform and stable coating, that increases the conductivity and surface area of the granules and protects them from corrosion would be ideal. Once the coating optimization is achieved, the regeneration capacity of the granules could be studied, like it is described in the second chapter of this thesis. Stability and long-term performance are very important for particle electrodes, as the system cost and sustainability depend on them. The same coating could be applied on both the GAC and graphite granules followed by a comparison of their performance towards the degradation of the persistent contaminants and the minimization of toxic by-products, such as chlorinated and halogenated by-products. In the current chapter, these species were not measured and thus the effect of the presence of graphite granules on their concentration was not evaluated. Experiments using NaCl as an electrolyte, in the 2D and 3D system, should also be conducted in the future to examine this factor as well. Once the previous mentioned steps are taken, the reactor could be tested for its inactivation capacity against bacteria and viruses and eventually also tested for the treatment of real wastewater.

Contaminants removal and simultaneous GAC regeneration using a hybrid 3D electrochemical system

In the fifth chapter, the same concept was examined, but with another particle electrode, GAC, which is a material that has been extensively studied and used as a particle electrode (J. Ma et al., 2021). The change of the particle electrode was made because of the corrosion of the graphite granules during experiments that were presented in the first chapter of this thesis. GAC has important properties such as high porosity and high specific surface area, making it very suitable for adsorption applications. In order to focus more on the electrochemical capacity of GAC as particle electrode, but also to study the possibility of its regeneration, GAC was previously saturated with wastewater. The system was used for the degradation of the same persistent contaminants that were studied in the first chapter, but this time spiked in real secondary treated municipal wastewater effluent. To minimize the impact of the possible biofilm formation on the contaminants´ degradation, the secondary effluent was autoclaved before its use.

The objective of this work was to study the simultaneous degradation of persistent organic

contaminants and the in-situ regeneration of the GAC during consecutive runs. The first experiments were conducted using a low current density of 15 A m^{-2}. A synergy between adsorption/electrosorption and electrochemical oxidation was observed in the 3D process during the first runs. Nevertheless, after several runs, the efficiency of the system declined while the adsorption capacity of GAC was decreasing as well, leading to the conclusion that GAC was not being regenerated. The total number of runs performed was 27. To overcome the problem of the system´s performance deterioration over consecutive runs, the current density was increased to 100 A m^{-2}. After the current density increase, the removal rate of the contaminants and synergy was increasing through the runs. In the case of IPM for example, synergy increased from 22% during run 1 to 32%, 44% and 46% during runs 6, 11 and 27 consecutively. Besides, the increase of the contaminants´ adsorption on GAC after several runs proved that part of GAC´s adsorption ability was regenerated. In the case of IPM, this increase was from 0.08 h^{-1}, during run 1, to 0.13 h^{-1} during run 28. Except for the studied contaminants, the increase in synergy and adsorption on GAC was observed for COD removal as well. The difference in the system performance when a low current and a high current density were applied reveals an important factor concerning this kind of electrochemical systems, which is the intensity of the electric field applied. It must be sufficient to induce a charge separation on the particle electrode surface, in order to achieve their polarization and thus their capacity of functioning as particle electrodes. Therefore, when designing such systems, the magnitude of the applied current density should be calculated theoretically, but also tested experimentally, in order to maximize the system efficiency and minimize the energy consumption. The electric field can also impact the structural properties of GAC and its regeneration ability, proving to be a key factor in 3D processes (McQuillan et al., 2018). Except for improving the performance of the reactor, the addition of GAC also reduced the toxicity of the effluent, since chlorate, perchlorate as well as halogenated organic byproducts produced in the system were electro-sorbed at the surface of GAC. This can be very beneficial for such treatments since chloride is present in most wastewater sources and the production of these toxic byproducts cannot always be avoided in electrochemical processes (Muddemann et al., 2018). An alternative way to reduce the generation of such by-products is to apply lower current densities, but as mentioned above, the current density needs to be sufficient to ensure the contaminants degradation and particle electrode polarization(Radjenovic and Sedlak, 2015). Changing the anode can also be a

solution, as it is known that active DSA anodes (such as RuO_2 and IrO_2) have higher active chlorine generation efficiency and lower formation of chlorate and perchlorate (Martínez-Huitle et al., 2015). Perchlorate is generated by the reaction of the electrochemically generated $OH^{\bullet}$ with chlorate. Though, when organics are also present, $OH^{\bullet}$ react with them faster and ClO_4^- generation is limited (Donaghue and Chaplin, 2013). Isidro et al. managed to limit chlorate and perchlorate production, during an electrochemical disinfection process, by limiting the contact time of hydroxyl radicals with hypochlorite, due to the configuration of their electrode cell, which functioned in one pass mode with low HRT. The contact time between the treated water and the electrode was short, thus preventing the hydroxyl radicals which are mainly in the proximity of the electrode (Isidro et al., 2020). Wang et al. prevented the formation of chlorate and perchlorate by adding H_2O_2 in the reaction solutions, as it functions as scavengers for it (Wang et al., 2022).

The particle electrode used in 3D systems plays a crucial role in the process, in terms of the contaminants degradation and energy consumption, and should fulfill some criteria to ensure its suitability for such processes. The ideal particle electrode can be considered the one which is stable, has good electrocatalytic activity, adsorption capacity and it can be regenerated rapidly using low current densities. It should also have some characteristics that promote electrosorption of contaminants on its surface. Among the influencing parameters of electrosorption are the morphology, the specific surface area, porosity, roughness, conductivity, surface functions and surface wettability (Lissaneddine et al., 2022). The above characteristics can assure that the particle electrode can effectively participate in the removal of the contaminants, either by adsorption/electrosorption or direct and indirect electrochemical degradation and thus achieve synergy between the 2D and the OC processes. The ability to get regenerated is also key as far as the particle electrode reuse is concerned. Reusing the particle electrode can make the process more sustainable and increase the energy efficiency of the system. Efficient regeneration has been reported for both porous and non-porous materials. On porous materials it may be slower, due to the slower desorption of contaminants in the pores. The porosity of particle electrodes may also change after many regenerations cycle, thus affecting their long-term performance. On the other hand, due to their increased adsorption and bigger surface area, they can contribute more to the contaminants removal. The physicochemical changes on the particle electrode surface should be studied thoroughly before their use. In this study,

the average pore diameter increased with regeneration cycles, that lead to the increase of granules adsorption capacity.

Treating real secondary effluent in this study gave promising results for the further application on wastewater. Evaluating the simultaneous degradation of more than one contaminant was also a step towards real-world conditions, since wastewaters are complex, heterogenous mixtures of solutes, which may compete for delivered electrons or electrogenerated oxidants. Future research should turn its attention towards the treatment of more realistic water matrices, both considering composition and concentration of the contaminants, since most of the current studies use concentration ranges orders of magnitude higher than real-world scenarios (Garcia-Segura et al., 2020a). Transformation products, toxicity and mineralization studies should be conducted as well, to ensure the improvement of the water quality after treatment. The above can be considered as preliminary steps for the further advancement towards the scaling up of the system and its real application. Once the system is scaled up, various working parameters, such as the flowrate, the current density, the quantity of particle electrodes etc. could be studied and optimized.

An ideal electrochemical water treatment system would be an integrated system, where the particle electrode would contribute to the contaminants removal and would be regenerated at the same time. Evidently, there would be a limit on the number of times that the particle electrodes could be reused, because the regeneration process can have an impact on the surface morphology and characteristics of the particle electrode and thus reduce its efficiency long term (Mohammad et al., 2020). Usually, these changes depend on the mechanism of the electrochemical regeneration method that is selected and their prior identification is crucial for the designing of the treatment systems (Zhou et al., 2021). Considering that electrochemical systems are very suitable for decentralized applications, particle electrode could be selected depending on the matrix of the water treated in every application. To increase the sustainability of the system, it would also be important for the particle electrode to get produced from environmentally friendly materials using sustainable methods. For example, GAC can be produced from biomass wastes, with great potential for water treatment and regeneration (Jjagwe et al., 2021). To further improve the performance of the particle electrode, a coating can be applied on them. The selection of the coating can also be specific, depending on the matrix of water treated. Overall, ideal electrochemical reactors of the future should be versatile and allow

the easy and simple replacement of the particle electrode bed when it is exhausted or when the treated water matrix is changed.

A parameter that should always be considered as well is the financial cost of the process. An estimated cost of industrial BDD anodes is around 4200 € per m^2 and for DSA 3000€ per m^2 (Wenderich et al., 2021), while the cost of GAC is estimated at 1.34 € per kg (Matsena et al., 2021). Considering these prices above, the dimensions of the electrodes used in the reactor and the quantity of GAC used, it can be calculated that the additional cost of the granules´ addition corresponds to briefly 0.25% and 0.35% of the cost of BDD and DSA anode respectively. The increase in cost is very low compared to the increase in removal efficiency and energy demand decrease of the system. For instance, in the case of CPZ, the removal rate of the 3D process was three times higher than the 2D, while the E_{Eo} decreased by 60%. If the GAC was to be coated with RGO, considering the price of GO approximately 1350€ per kg (Baptista-Pires et al., 2021) as well as the concentration and quantity of GO used for the coating of the graphite granules in the previous chapter, the cost would increase an additional 0.18% and 0.25% of the cost of the BDD and DSA respectively, which can be considered again very competitive. Besides, it is expected that ongoing technological development will lead in the reduction of the cost of electrodes and graphene oxide in the future, reducing the capital cost of such applications.

3D graphene sponge electrodes for chlorine-free electrochemical disinfection

In the sixth chapter of this thesis, electrochemical disinfection was studied. The electrodes used in the experiments were synthesized using a low-cost, simple and self-assembly method, which can be easily scaled up. The size of the electrodes can be adapted to the application, their production cost, including the material cost and the capital cost of the necessary equipment for their production, is very competitive compared to commercial electrodes and allows their production for decentralized applications, which could be powered by renewable energy sources (Kumar and Pan, 2020). It was also proven that the energy consumption of the system can be reduced when intermittent current is used, due to the intrinsic capacitive properties of graphene.

In this study, the produced electrodes showed low electrocatalytic activity towards chloride oxidation, as there was no chlorine, chlorate and perchlorate production. Similarly, when these electrodes were employed in real tap water, no traces of chlorine,

chlorate, or perchlorate were detected, whereas a significant bacteria removal was achieved. This is a great advantage in comparison with other conventional electrodes, as chlorine byproducts can compromise the quality of the treated water. In other studies, it has been reported that the avoidance of chlorine species can be achieved by reducing the applied cell potential. For example, Liu. Et al. used a flow through system with carbon fiber felt electrodes and avoided the free chlorine production by applying low total cell potential (3V) and achieved 6.5 *E. coli* log removal (Liu et al., 2019). Similar results were achieved with 3D macroscopic carbon nanotube (CNT) sponge electrodes and copper oxide nanowire (CuONW)-modified 3D copper foam electrode , with total bacteria removal using low applied total cell potential (<2 V) and thus avoiding free chlorine production (Huo et al., 2017, 2016).

Compared to the studies above, the advantage of our study is that chlorine formation was very low even when applying high voltages and current densities, whereas a high log removal of *E. coli* was achieved. Higher current densities may be required for the complete inactivation of the different bacteria species and viruses and eventually if the process is used for the degradation of organic contaminants as well. Besides, gram-positive bacteria strains, for example, have thicker layer of peptidoglycan than gram-negative strains and can be more resistant to disinfection. Even within the same species of bacteria, certain strains may be more resistant compared to others. For example, the strain we used in our studies has an altered external membrane structure, potentially making it more susceptible to damage via electroporation compared to other *E. coli* strains (Segues Codina et al., 2023). The water quality and the concentration of natural organic matter in them may also affect the disinfection process, due to the oxidant species scavenging effect by the organic matter in the case of indirect oxidation and the competitive adsorption onto the electrodes surface in the case of direct oxidation (Huo et al., 2020). For example, Ding et al. had to increase the applied electric charge to 0.072 A h L^{-1} in order to achieve the complete inactivation of *E. coli* in real wastewater effluent, while complete disinfection could be achieved at 0.061 A h L^{-1} in synthetic wastewater. The difference in the charge requirement was attributed to the competitive consumption of oxidants by ammonia and other organic pollutants in the real wastewater (Ding et al., 2017). Moreover, Wang et al. achieved the simultaneous removal of *Salmonela enterica*, antibiotics and antibacterial resistance genes (ARGs) using a Magnéli phase Ti_4O_7 anode in a batch reactor. Significant (4 log), but not complete, removal of bacteria in wastewater

was achieved. The incomplete inactivation was attributed to the diversity of microbial communities and the physicochemical properties of wastewater, such as the presence of dissolved organic matter (Wang et al., 2021).

In a previous study, it was proven that the same electrodes could be used for the degradation of persistent contaminants. It was shown that introduction of different dopants into the graphene-based electrodes can be used for the functionalization of their surface and tailoring of electrocatalytic activity and properties, and thus specialized for the inactivation of specific groups of contaminants (Baptista-Pires et al., 2021). The degradation of the contaminants was achieved by direct electron transfer on the electrodes as well as the in-situ produced oxidants like $OH^{\bullet}$, H_2O_2 and O_3. The same sponges were also employed successfully for the electrochemical degradation of per- and polyfluoroalkyl substances (PFAS) (Duinslaeger and Radjenovic, 2022) and antibiotics (Ormeno-Cano and Radjenovic, 2022), showing the potential of their application for integrated water treatment. They can also be functionalized with 2D materials which enhance their electrocatalytic activity and tailor them for the degradation of specific contaminants (Cuervo Lumbaque et al., 2022). The subsequent challenge would involve conducting tests on the reactor to assess its efficacy in inactivating phages and viruses. The final step would entail utilizing the reactor for the treatment of real wastewater, simultaneously addressing all the aforementioned aspects. The possibility of stacking two or more reactors in parallel or in series is an option as well. The reactors can be equipped with differently tailored electrodes, in order to enhance the treatment of a variety of contaminants. The use of high surface area electrodes in flow-through mode increases the reaction rates, compared to flow-by operation that traditional electrochemical cells utilize (Chaplin, 2019).

One of the main questions concerning the produced electrodes is their lifetime. Further experimental testing considering their stability and long-term performance have to be conducted, as well as a thorough life-cycle and technoeconomic analysis. Furthermore, a standardized production method of the electrodes has to be established, since currently their production is done manually and slight changes between the different 3D electrodes may exist. For its financial sustainability, the cost of their production and replacement over several years of function should not exceed the cost of a commercial electrode, like for instance BDD which can have a service life time ten years but costs 4200€ (Stirling et al., 2020). Another challenge that needs to be faced is the further reduction of energy

consumption of the system. This can be achieved by increasing the conductivity of the electrodes, e.g. by changing the percentage content of RGO in the electrode, enhancing the coating or combining it with a conductive polymer (Mohan et al., 2018). An alternative approach could involve enhancing the electric field near the electrode and inducing electroporation by incorporating nanowires into the graphene oxide sponges. (Huo et al., 2020). Manganese oxide can be a good candidate for combination with RGO, as it can enhance the catalytic activity of the electrode and also its capacitance (Hamade et al., 2021; Radich and Kamat, 2012). Combination of carbon based materials with transition metals enable electrochemical properties that cannot be achieved by each component alone (Hamade et al., 2021).

It was observed during our experiments, that applying intermittent current resulted in a similar log removal observed with continuous current (4.5 and 5.1 log removal respectively, in phosphate buffer), while energy consumption was reduced significantly (from 8.8 to 4.8 kWh m^{-3}). This is attributed to the fact that the electrode could maintain part of its charge after the current was switched off, due to the capacitance of RGO. The charge is stored for brief durations and dissipates more during extended OFF periods. This capacitive behavior derives from the electrostatic double-layer capacitance and pseudocapacitive behavior resulting from redox reactions. This unique combination is facilitated by the presence of hydrophilic, oxygen functional groups separated by hydrophobic regions. These characteristics ensure that the active surface of the electrodes remains accessible to the electrolyte (Neto and Fileti, 2018). During the charging phase, electric charges and counter ions become concentrated on the surface of the electrode. This accumulation directly determines the output capacitance or energy/power density. The extent of counter ions adsorption is influenced by factors such as surface binding energy, surface heterogeneity, pore size, pore volume, and specific surface area. Furthermore, the electrochemical activity is enhanced by the dynamics and phenomena of charge/electron transfer, as well as the interfacial area between the electrolyte and electrode (Gadipelli et al., 2023). The production of oxidant species can be affected by the ON-OFF cycles, and it is essential to adjust these cycles to avoid a reduction in their generation which would consequently lower the degradation efficiency of contaminants. In a recent study with graphene sponge electrodes, short OFF cycles were proven to be more effective in producing oxidizing species and removing of organic contaminants (Lumbaque and Radjenovic, 2023). On the other hand, excessively short OFF cycles may

not provide enough time for effective electrosorption of contaminants at the electrode surface, resulting in reduced removal efficiency. Thus, optimization of the ON/OFF cycles should ensure the decrease of the energy demand, without a deficit in the contaminant's degradation. Ni et al. also managed to decrease the energy consumption of the disinfection process they used from 37.7 Wh m^{-3} with direct current, to 11.4 Wh m^{-3}, using alternating current pulses. In their study they utilized a flow-through reactor equipped with two 3D graphitized carbon fiber felts, serving as the anode and cathode, achieving 6 log removal of *E. coli* (Ni et al., 2021).

Another challenge that was faced during the experiments was the bubble generation. Bubbles can decrease the electroactive area of the electrode and inhibit the diffusion of the bacteria or organic contaminants to the electrode surface, thus decreasing the electrode´s efficiency. Besides, the bubbles can also get detached and move on the bulk solution resulting to a decrease in the electrical conductivity and an increase in the ohmic drop, which can consequently lead to an increase in the energy consumption and hydrodynamic resistance (Mareev et al., 2021). A possible solution to reduce the bubble generation would be reducing the applied current density. Alternatively, a change in the geometry and hydrodynamics of the reactor could facilitate the mass transfer and thus reduce the negative impact of the bubbles (Mareev et al., 2021; Taqieddin et al., 2017).

.

Future Perspectives

3D reactors possess significant potential in the future of electrochemical systems. They are poised to play a crucial role in decentralized electrochemical systems, and their application can have an immediate impact. The transformation of a 2D system into a 3D one can be relatively simple, affordable and can indeed increase the efficiency and lower the energy consumption of the system. Particle electrodes play a key role in the 3D processes, as they can contribute to the contaminants´ degradation via direct and indirect oxidation, as well as adsorption and electrosorption. Low cost materials that have been already used in water treatment processes, such as GAC, could be used in integrated electrochemical processes, even after they get saturated and require regeneration. Already spent GAC, used in treatment plants, could be used for the process, thus reducing the cost and environmental impact. In order to enhance the sustainability of the system, it is crucial to ensure that the particle electrode is manufactured using environmentally friendly materials and sustainable methods. For example, GAC can be produced from biomass

wastes, with great potential for water treatment and regeneration (Jjagwe et al., 2021). Evidently, there would be a limit on the number of times that the particle electrodes could be reused, because the regeneration process can have an impact on the surface morphology and characteristics of the particle electrode and thus reduce its efficiency long term (Mohammad et al., 2020). The particle electrode can be replaced, when it is exhausted or when the treated water matrix is changed. The physiochemical changes on their surface and their influence on the particle electrode regeneration should be studied in more detail, during an extended number of consecutive runs. Further studies should be also conducted comparing the performance of porous and non-porous particle electrodes, both short-term and long-term. What is more, studies on the coating of already spent particle electrodes would be of great interest since they can unlock the possibility of their re-functionalization and reuse. Different coatings can be combined and modify the physicochemical characteristics of the granules, according to the application. Moreover, a combination of particle electrodes with different coatings can be used in a single reactor, according to the matrix of the wastewater effluent that is treated. RGO proved to be a material with great potential for application in 3D water treatment as coating of the particle electrodes. What is more, new green synthesis methods have also been reported for GO and GO-based nanomaterials, which can reduce the environmental and financial cost of its use (Fathy et al., 2019; Park et al., 2017; Pei et al., 2018; Tewari et al., 2022).
Some of the main challenges for electrochemical technologies, such as the high capital costs, formation of toxic by-products and high energy consumption have been tackled in the thesis. The 3D electrodes used in this study were produced in a facile and affordable way and are easy to scale up, whereas they have low electrocatalytic activity towards chloride oxidation. The application of intermittent current has been found to be a solution for energy saving as well. Combining the results of the three chapters, the graphene-based electrodes could be used as main electrodes in a reactor with a packed bed of RGO coated granules as a particle electrode. Theoretically, this combines the benefits of both systems and could be used both for disinfection and degradation of organic contaminants. Besides, it has been shown before that porous electrodes, used in 3D electrochemical systems equipped with particle electrodes, can be more efficient for the degradation of contaminants compared to planar electrodes, due to the bigger surface area and increased active sites (Rahmani et al., 2021). Such a system could be used for example as a solar-powered water disinfection treatment in impoverished communities that are not

connected to the energy grid. Besides, this technology could also be applied in small scale, with small devices used for the disinfection of drinking water in areas with limited access to safe water. Another possible application would be for the decentralized treatment of wastewater in urban areas, in big blocks (such as hospitals, shopping centers, airports) or even industries, where the contaminants and microbial burden is high and needs to be lowered before the further treatment of the wastewater in a centralized treatment plant. According to the wastewater matrix and the investment capacity, either the 3D particle system or the 3D structure electrode system (or a combination of both) can be used. In the scenario of application in centralized wastewater treatment plants, 3D electrochemical systems can potentially be combined with other processes during pre-treatment or post-treatment. In pre-treatment, it can be the step before anaerobic-aerobic biological treatment for example with the purpose to improve the biodegradability of wastewaters with high biological toxicity, such as antibiotics and pesticides. Considering post-treatment of wastewater, it can serve for the degradation of persistent organic and inorganic contaminants that cannot be degraded by conventional methods. It can follow, for instance, processes such as membrane bioreactors.

3D systems are more complex than 2D systems, with many parameters that need to be studied and optimized. Even minor changes can have a significant impact on the system´s efficiency. Considering the 3D structured electrodes, future research should focus its attention on the energy consumption, mass transport phenomena in the system, aging and fouling of the newly fabricated electrodes as well as the generation of toxic halogenated by-products. Detailed knowledge of the 3D electrode architecture can give more insight on the mass transfer within the porous electrodes and the current distribution. Mathematical modelling and computational fluid dynamics could be used to predict these parameters and 3D printing could be used to design the electrode accordingly, in order to minimize mass transfer limitations and achieve an even current distribution. Uneven current distribution may result in different reaction zones and different potential distribution, that can lead to reduced electrocatalytic efficiency and thus increased energy consumption. Fouling and aging can affect the stability long-term performance of the electrode, because of the deactivation of its surface and thus diminishing of its electrocatalytic activity. Whereas fouling can be reversible, aging can lead to permanent changes in the electrode structure morphology. Hence, more research should focus on these two phenomena and possible ways to prevent them. Standard anti-fouling, aging

and lifetime analysis methods must be developed to evaluate the practical applicability of 3D electrodes in bigger scale. The generation of toxic halogenated by-products should also be studied more extensively, therefore developed bench-scaled systems should be tested with real wastewater as well. Newly developed electrodes should not produce chlorine species and they should be selective towards the oxidation and complete mineralization of organic contaminants (Garcia-Segura et al., 2020b; Li et al., 2023). For the particle electrodes systems, future studies should focus more on the study of reactor design, in order to optimize the mass transfer and the current distribution on the particle electrodes.

Concluding PhD thoughts

I would like to finish writing this thesis with some personal thoughts. Considering technological development and investment, I believe that it is very important to change the perception of "cost" and transfer it from pure financial cost to the real cost of the developed technologies´ impact on the environment and human life. This should be the principal criteria when selecting the water treatment technologies that will be developed and applied in the future. Living in a planet with limited resources, we should start investing in technologies that are based on sustainable resources and reuse. Researchers should put this issue on the table when discussing with the stakeholders and policy makers and try to convince them about the concept.

Considering the doctorate, PhD students could be described as a hybrid between a student and a worker. They are gaining and producing scientific knowledge at the same time. During my PhD, I had to take some courses from the University of Girona. One of them was about writing papers in science and I have to admit that it was really useful and provided me with tools to improve my writing and facilitate the publishing of the articles. Another subject was about Open Science, which highlighted the importance of Open Access and free sharing of knowledge. I believe that the scientific community should aim towards publishing in open access and pressure the journals to decrease or even eliminate the costs of publishing in open access, so that everyone has equal chances to reach knowledge. It is a common secret among scientists that Sci-Hub has been the most used website during their research. Furthermore, the culture of publishing negative results could be embraced, as it can benefit the scientific community interpret better even positive results and increase the chances of success by avoiding repeating mistakes that have been

made (Weintraub, 2016). Also, the scientific community could provide feedback to the research groups and thus help then advance in their investigation. Another benefit could be that less papers with manipulated data would be published, since the pressure for positive data could decrease. Currently, there are still some journals for publishing negative results, although they could also be submitted to journals containing the publications that the negative results contradict (Nimpf and Keays, 2020). The success in PhD thesis and science in general is not for granted. Failure is also an option, and we should learn to embrace it as well, prioritizing more the quality of work and collaboration between scientists and not only the publishable results.

The last course I followed was about Ethics applied in Science and I would highly recommend a similar course to all PhD students and researchers in general. It can help scientists to reconsider their motivations and base their research on important values, such as respect and honesty. Prioritizing the wellbeing of their colleagues and society in general. Ethics in Science is more important than ever. Besides, the diploma obtained could reflect better the title of Doctor of Philosophy, which etymologically derives from the greek words "philo" and "sophia", that translates as "love" and "wisdom", respectively, meaning the love for wisdom, for asking questions and searching for answers. It is about questioning even our decisions, the way we are applying science and eventually what the purpose of science is. Philosophy is not about finding certain answers but asking the correct questions that can help us in the process of collective improvement. Being members of a greater chain of people, scientists should be able to recognize the direct and indirect impact of their work to their community and society in general, short term and long term. To overcome what Hannah Arendt called "banality of evil", realizing the collective responsibility and consequences of what "I am just doing my job" means and based on them decide the best way of doing research. I believe that the objective of the PhD students should be more holistic and both try to perform quality research and also contribute in the improvement of the community they belong, being this the University or a research center. I think that by realizing our responsibility for the commons, we can have a more prosperous and fair society for everyone, which for me should be one of the main objectives of science. A change in the mentality, turning from arrivisme to altruism could be a key for this transition.

Finally, I would like to mention that along with other PhD colleagues we were also

awarded with funding for a project we applied in the frame of University Development Cooperation program of the University of Girona. The project was about studying the efficiency of different local plants for their function in wetlands for water purification. The project was supposed to be implemented in Belen de Andaquies, a rural area of Colombia. Its objective was to provide knowledge for the design of a wetland, a natural based solution, for the improvement of water quality of the area, promoting the horizontal collaboration between all parts included and encouraging the participation of the local community in every step of the project implementation. To ensure the above, we cooperated with local NGO´s and collectives and were in communication with the local community via videocalls. Unfortunately, due to the pandemic situation, the implementation of the project was not possible. Nevertheless, the whole experience introduced us in the concept of project management, which is a necessary tool in the career of a researcher. It also gave us experience on interdisciplinary collaboration and taught us the necessity of communication with the local society before, during and after the project implementation.

CHAPTER 8 Conclusions

RGO-coated graphite granules as particle electrodes in 3D electrochemical reactor.

- Converting the 2D electrochemical reactor into a 3D, by using graphite granules as particle electrodes, can increase the removal efficiency of organic contaminants and decrease the energy demand of the system. This improvement is attributed to the synergy between adsorption/electrosorption and electrochemical oxidation in the 3D process.
- Coating the granules with RGO further increases the removal rates of the persistent organic contaminants and decreases the energy demand of the system in terms of E_{EO}. For example, in the case of IPM, the E_{EO} of the system with the RGO granules was 19% and 10% lower, for the Ti/RuO_2-IrO_2 and BDD systems respectively, compared to the systems with non-coated granules.
- Functionalizing RGO with other materials, such as atomic nitrogen and manganese oxide, can improve the adsorption of the contaminants on the granules as well as the 3D ELOX system performance.

Contaminants removal and simultaneous GAC regeneration using a hybrid 3D electrochemical system

- GAC, previously saturated with secondary treated municipal wastewater effluent, was effectively utilized as a particle electrode in a 3D electrochemical reactor and enhanced the removal efficiency of persistent organic contaminants, spiked in real secondary effluent.
- The adsorption ability of GAC was partially regenerated in situ for 27 consecutive runs. In the case of IPM, the adsorption rate increased from 0.08 to 0.13 h^{-1}. The removal rate of the contaminants increased from run 1 to run 27 (e.g. from 0.17 to 0.46 h^{-1} for IPM), proving the simultaneous degradation of contaminants and regeneration of GAC.
- A synergy (up to 57%) between adsorption/electrosorption on the granules and electrochemical degradation was demonstrated when the current density was sufficient to induce efficient charge separation in the GAC particles, without being in contact with any of the main electrodes.
- The presence of GAC was proved as beneficial for the reduction of halogenated organic by-products and the minimization of toxic and persistent inorganic chlorinated byproducts. AOCl decreased from 576 μg L^{-1} to 462 μg L^{-1}, while AOI decreased from 439 μg L^{-1} to 308 μg L^{-1}. Similarly, the concentration of ClO_3^- was limited from 0.61 mM to 0.30 mM, whereas ClO_4^- decreased from 1.18 mM to 0.12 mM.

3D graphene sponge electrodes for chlorine-free electrochemical disinfection

- Almost complete removal (up to 5 log removal with 10^5–10^6 CFU mL^{-1} initial bacteria concentration) of *E. coli* was achieved by employing a one-pass flow-through electrochemical system equipped with graphene sponge electrodes, that were produced in the laboratory, in both phosphate buffer electrolyte and real tap water.
- The electrocatalytic activity of the graphene sponge towards chloride is low, resulting in minimal production of chlorine species even at high current densities (115 A m^{-2}) and in the presence of high chloride concentration (20 mM NaCl).
- Atomic doping of the graphene sponges can enhance their disinfection capability, with nitrogen doping proving to be more effective than boron doping, due to its more positive charge.
- The order of the electrodes has an impact on the system performance, with the anode-cathode configuration being more effective.
- The main inactivation mechanism is electroporation which lead to cell lysis and thus bacteria deactivation, ass confirmed by FESEM and Live/Dead staining experiments. Electrogenerated ozone and hydroxyl radicals also contributed to the inactivation. Contribution of chlorine species to the disinfection was negligible.
- No regrowth of the bacteria was observed in the storage samples examined, after the treatment.
- The energy consumption of the system was able to be reduced by using intermittent current (pulses of ON/OFF), due to the intrinsic capacitive properties of the graphene-based sponge.
- The simple, scalable, and low-cost production method of the graphene sponges, this system is a good candidate for practical applications in electrochemical decentralized water treatment.

References

Akhavan, O., Ghaderi, E., 2010. Toxicity of graphene and graphene oxide nanowalls against bacteria. ACS Nano 4, 5731–5736. https://doi.org/10.1021/NN101390X/ASSET/IMAGES/LARGE/NN-2010-01390X_0005.JPEG

Ali, I., Basheer, A.A., Mbianda, X.Y., Burakov, A., Galunin, E., Burakova, I., Mkrtchyan, E., Tkachev, A., Grachev, V., 2019. Graphene based adsorbents for remediation of noxious pollutants from wastewater. Environ. Int. 127, 160–180. https://doi.org/10.1016/j.envint.2019.03.029

Andrés García, E., Agulló-Barceló, M., Bond, P., Keller, J., Gernjak, W., Radjenovic, J., 2018. Hybrid electrochemical-granular activated carbon system for the treatment of greywater. Chem. Eng. J. 352, 405–411. https://doi.org/10.1016/j.cej.2018.07.042

Anfruns, A., García-Suárez, E.J., Montes-Morán, M.A., Gonzalez-Olmos, R., Martin, M.J., 2014. New insights into the influence of activated carbon surface oxygen groups on H2O2 decomposition and oxidation of pre-adsorbed volatile organic compounds. Carbon N. Y. 77, 89–98. https://doi.org/10.1016/j.carbon.2014.05.009

Anglada, Angela, Urtiaga, A., Ortiz, I., 2009. Contributions of electrochemical oxidation to waste-water treatment: fundamentals and review of applications. J. Chem. Technol. Biotechnol. 84, 1747–1755. https://doi.org/10.1002/jctb.2214

Aradhana, R., Mohanty, S., Nayak, S.K., 2018. Comparison of mechanical, electrical and thermal properties in graphene oxide and reduced graphene oxide filled epoxy nanocomposite adhesives. Polymer (Guildf). 141, 109–123. https://doi.org/10.1016/j.polymer.2018.03.005

Asghar, H.M.A., Hussain, S.N., Brown, N.W., Roberts, E.P.L., 2019. Comparative adsorption–regeneration performance for newly developed carbonaceous adsorbent. J. Ind. Eng. Chem. 69, 90–98. https://doi.org/10.1016/j.jiec.2018.09.012

Asim, S., Zhu, Y., Batool, A., Hailili, R., Luo, J., Wang, Y., Wang, C., 2017. Electrochemical treatment of 2, 4–dichlorophenol using a nanostructured 3D–porous Ti/Sb–SnO2–Gr anode: Reaction kinetics, mechanism, and continuous operation. Chemosphere 185, 11–19. https://doi.org/10.1016/j.chemosphere.2017.06.125

Bach, A., Semiat, R., 2011. The role of activated carbon as a catalyst in GAC/iron oxide/H2O2 oxidation process. Desalination 273, 57–63. https://doi.org/10.1016/j.desal.2010.04.020

Bagastyo, A.Y., Radjenovic, J., Mu, Y., Rozendal, R.A., Batstone, D.J., Rabaey, K., 2011. Electrochemical oxidation of reverse osmosis concentrate on mixed metal oxide (MMO) titanium coated electrodes. Water Res. 45, 4951–4959. https://doi.org/10.1016/j.watres.2011.06.039

Bañuelos, J.A., El-Ghenymy, A., Rodríguez, F.J., Manríquez, J., Bustos, E., Rodríguez, A., Brillas, E., Godínez, L.A., 2014. Study of an air diffusion activated carbon packed electrode for an electro-fenton wastewater treatment. Electrochim. Acta 140, 412–418. https://doi.org/10.1016/j.electacta.2014.05.078

Baptista-Pires, L., Norra, G.F., Radjenovic, J., 2021. Graphene-based sponges for electrochemical degradation of persistent organic contaminants. Water Res. 203. https://doi.org/10.1016/j.watres.2021.117492

Bardestani, R., Patience, G.S., Kaliaguine, S., 2019. Experimental methods in chemical engineering: specific surface area and pore size distribution measurements—BET, BJH, and DFT. Can. J. Chem. Eng. https://doi.org/10.1002/cjce.23632

Bejan, D., Guinea, E., Bunce, N.J., 2012. On the nature of the hydroxyl radicals produced at boron-doped diamond and Ebonex® anodes. Electrochim. Acta 69, 275–281. https://doi.org/10.1016/j.electacta.2012.02.097

Bergmann, M.E.H., Rollin, J., Iourtchouk, T., 2009. The occurrence of perchlorate during drinking water electrolysis using BDD anodes. Electrochim. Acta 54, 2102–2107. https://doi.org/10.1016/j.electacta.2008.09.040

Bernal, D., Restrepo, I., Grueso-Casquete, S., 2021. Key criteria for considering decentralization in municipal wastewater management. Heliyon 7, e06375.

https://doi.org/10.1016/j.heliyon.2021.e06375
Bordbar-Khiabani, A., Ebrahimi, S., Yarmand, B., 2019. Highly corrosion protection properties of plasma electrolytic oxidized titanium using rGO nanosheets. Appl. Surf. Sci. 486, 153–165. https://doi.org/10.1016/j.apsusc.2019.05.026
Brillas, E., Martínez-Huitle, C.A., 2015. Decontamination of wastewaters containing synthetic organic dyes by electrochemical methods. An updated review. Appl. Catal. B Environ. 166–167, 603–643. https://doi.org/10.1016/j.apcatb.2014.11.016
Bruguera-Casamada, C., Sirés, I., Brillas, E., Araujo, R.M., 2017. Effect of electrogenerated hydroxyl radicals, active chlorine and organic matter on the electrochemical inactivation of Pseudomonas aeruginosa using BDD and dimensionally stable anodes. Sep. Purif. Technol. 178, 224–231. https://doi.org/10.1016/j.seppur.2017.01.042
Butkovskyi, A., Jeremiasse, A.W., Hernandez Leal, L., Van Der Zande, T., Rijnaarts, H., Zeeman, G., 2014. Electrochemical conversion of micropollutants in gray water. Environ. Sci. Technol. 48, 1893–1901. https://doi.org/10.1021/es404411p
Cañizares, P., Lobato, J., García-Gómez, J., Rodrigo, M.A., 2004. Combined adsorption and electrochemical processes for the treatment of acidic aqueous phenol wastes. J. Appl. Electrochem. 34, 111–117. https://doi.org/10.1023/B:JACH.0000005607.37738.71
Cano, A., Barrera, C., Cotillas, S., Llanos, J., Cañizares, P., Rodrigo, M.A., 2016. Use of DiaCell modules for the electro-disinfection of secondary-treated wastewater with diamond anodes. Chem. Eng. J. 306, 433–440. https://doi.org/10.1016/j.cej.2016.07.090
Cano, A., Cañizares, P., Barrera, C., Sáez, C., Rodrigo, M.A., 2011. Use of low current densities in electrolyses with conductive-diamond electrochemical - Oxidation to disinfect treated wastewaters for reuse. Electrochem. commun. 13, 1268–1270. https://doi.org/10.1016/j.elecom.2011.08.027
Chaplin, B.P., 2019. The Prospect of Electrochemical Technologies Advancing Worldwide Water Treatment. Acc. Chem. Res. 52, 596–604. https://doi.org/10.1021/acs.accounts.8b00611
Chaplin, B.P., 2018. Advantages, disadvantages, and future challenges of the use of electrochemical technologies for water and wastewater treatment. Electrochem. Water Wastewater Treat. 451–494. https://doi.org/10.1016/B978-0-12-813160-2.00017-1
Chaplin, B.P., 2014. Critical review of electrochemical advanced oxidation processes for water treatment applications. Environ. Sci. Process. Impacts 16, 1182–1203. https://doi.org/10.1039/c3em00679d
Charbouillot, T., Brigante, M., Mailhot, G., Maddigapu, P.R., Minero, C., Vione, D., 2011. Performance and selectivity of the terephthalic acid probe for •oH as a function of temperature, pH and composition of atmospherically relevant aqueous media. J. Photochem. Photobiol. A Chem. 222, 70–76. https://doi.org/10.1016/j.jphotochem.2011.05.003
Chen, B., Jiang, J., Yang, X., Zhang, X., Westerhoff, P., 2021. Roles and Knowledge Gaps of Point-of-Use Technologies for Mitigating Health Risks from Disinfection Byproducts in Tap Water: A Critical Review. Water Res. 200, 117265. https://doi.org/10.1016/j.watres.2021.117265
Chen, W., Yang, X., Huang, J., Zhu, Y., Zhou, Y., Yao, Y., Li, C., 2016. Iron oxide containing graphene/carbon nanotube based carbon aerogel as an efficient E-Fenton cathode for the degradation of methyl blue. Electrochim. Acta 200, 75–83. https://doi.org/10.1016/j.electacta.2016.03.044
Chen, Y., Duan, X., Zhou, X., Wang, R., Wang, S., Ren, N., Ho, S.-H., 2021. Advanced oxidation processes for water disinfection: Features, mechanisms and prospects. Chem. Eng. J. 409, 128207. https://doi.org/10.1016/j.cej.2020.128207
Chen, Y., Zhang, X., Zhang, D., Yu, P., Ma, Y., 2011. High performance supercapacitors based on reduced graphene oxide in aqueous and ionic liquid electrolytes. Carbon N. Y. 49, 573–580. https://doi.org/10.1016/j.carbon.2010.09.060
Chen, Z., Zhang, Y., Zhou, L., Zhu, H., Wan, F., Wang, Y., Zhang, D., 2017. Performance of nitrogen-doped graphene aerogel particle electrodes for electro-catalytic oxidation of

simulated Bisphenol A wastewaters. J. Hazard. Mater. 332, 70–78. https://doi.org/10.1016/j.jhazmat.2017.02.048

Chi, Z., Wang, Z., Liu, Y., Yang, G., 2018. Preparation of organosolv lignin-stabilized nano zero-valent iron and its application as granular electrode in the tertiary treatment of pulp and paper wastewater. Chem. Eng. J. 331, 317–325. https://doi.org/10.1016/j.cej.2017.08.121

Cho, K., Qu, Y., Kwon, D., Zhang, H., Cid, C.A., Aryanfar, A., Hoffmann, M.R., 2014. Effects of anodic potential and chloride ion on overall reactivity in electrochemical reactors designed for solar-powered wastewater treatment. Environ. Sci. Technol. 48, 2377–2384. https://doi.org/10.1021/es404137u

Choudhary, P., Das, S.K., 2019. Bio-Reduced Graphene Oxide as a Nanoscale Antimicrobial Coating for Medical Devices. ACS Omega 4, 387–397. https://doi.org/10.1021/acsomega.8b02787

Comninellis, C., 1994. Electrocatalysis in the electrochemical conversion/combustion of organic pollutants for waste water treatment. Electrochim. Acta 39, 1857–1862. https://doi.org/10.1016/0013-4686(94)85175-1

Correia-sá, L., Soares, C., Freitas, O.M., Moreira, M.M., Nouws, H.P.A., Correia, M., Paíga, P., Rodrigues, A.J., Oliveira, C.M., Figueiredo, S.A., Delerue-matos, C., 2021. A three-dimensional electrochemical process for the removal of carbamazepine. Appl. Sci. 11, 6432. https://doi.org/10.3390/app11146432

Cotillas, S., Llanos, J., Moraleda, I., Cañizares, P., Rodrigo, M.A., 2020. Scaling-up an integrated electrodisinfection-electrocoagulation process for wastewater reclamation. Chem. Eng. J. 380, 122415. https://doi.org/10.1016/j.cej.2019.122415

Cuervo Lumbaque, E., Baptista-Pires, L., Radjenovic, J., 2022. Functionalization of graphene sponge electrodes with two-dimensional materials for tailored electrocatalytic activity towards specific contaminants of emerging concern. Chem. Eng. J. 446, 137057. https://doi.org/10.1016/j.cej.2022.137057

Cui, S., Chen, S., Wang, H., Dong, L., Wang, S., 2021. N-Doped Carbon-Coated Cu7S4Nanowires on Cu Foam Supports for Water Disinfection. ACS Appl. Nano Mater. 4, 6124–6134. https://doi.org/10.1021/acsanm.1c00930

Cuthbertson, A.A., Kimura, S.Y., Liberatore, H.K., Summers, R.S., Knappe, D.R.U., Stanford, B.D., Maness, J.C., Mulhern, R.E., Selbes, M., Richardson, S.D., 2019. Does Granular Activated Carbon with Chlorination Produce Safer Drinking Water? from Disinfection Byproducts and Total Organic Halogen to Calculated Toxicity. Environ. Sci. Technol. 53, 5987–5999. https://doi.org/10.1021/acs.est.9b00023

Dandie, C.E., Ogunniyi, A.D., Ferro, S., Hall, B., Drigo, B., Chow, C.W.K., Venter, H., Myers, B., Deo, P., Donner, E., Lombi, E., 2020. Disinfection options for irrigation water: Reducing the risk of fresh produce contamination with human pathogens. Crit. Rev. Environ. Sci. Technol. 50, 2144–2174. https://doi.org/10.1080/10643389.2019.1704172

Dickenson, E.R.V., Drewes, J.E., Sedlak, D.L., Wert, E.C., Snyder, S.A., 2009. Applying surrogates and indicators to assess removal efficiency of trace organic chemicals during chemical oxidation of wastewaters. Environ. Sci. Technol. 43, 6242–6247. https://doi.org/10.1021/es803696y

Díez-Pascual, A.M., 2020. Antibacterial action of nanoparticle loaded nanocomposites based on graphene and its derivatives: A mini-review. Int. J. Mol. Sci. 21, 3563. https://doi.org/10.3390/ijms21103563

Ding, L., Snoeyink, V.L., Mariñas, B.J., Yue, Z., Economy, J., 2008. Effects of powdered activated carbon pore size distribution on the competitive adsorption of aqueous atrazine and natural organic matter. Environ. Sci. Technol. 42, 1227–1231. https://doi.org/10.1021/es0710555

Donaghue, A., Chaplin, B.P., 2013. Effect of select organic compounds on perchlorate formation at boron-doped diamond film anodes. Environ. Sci. Technol. 47, 12391–12399. https://doi.org/10.1021/es4031672

Doyle, M.P., Schoeni, J.L., 1984. Survival and growth characteristics of Escherichia coli

associated with hemorrhagic colitis. Appl. Environ. Microbiol. 48, 855–856. https://doi.org/10.1128/aem.48.4.855-856.1984

Drennan, D.M., Koshy, R.E., Gent, D.B., Schaefer, C.E., 2019. Electrochemical treatment for greywater reuse: Effects of cell configuration on COD reduction and disinfection byproduct formation and removal. Water Sci. Technol. Water Supply 19, 891–898. https://doi.org/10.2166/ws.2018.138

Du, X., Oturan, M.A., Zhou, M., Belkessa, N., Su, P., Cai, J., Trellu, C., Mousset, E., 2021. Nanostructured electrodes for electrocatalytic advanced oxidation processes: From materials preparation to mechanisms understanding and wastewater treatment applications. Appl. Catal. B Environ. 296, 120332. https://doi.org/10.1016/j.apcatb.2021.120332

Duinslaeger, N., Radjenovic, J., 2022. Electrochemical degradation of per- and polyfluoroalkyl substances (PFAS) using low-cost graphene sponge electrodes. Water Res. 213, 118148. https://doi.org/10.1016/j.watres.2022.118148

Đuričić, T., Prosen, H., Kravos, A., Mićin, S., Kalčíková, G., Malinović, B.N., 2023. Electrooxidation of Phenol on Boron-doped Diamond and Mixed-metal Oxide Anodes: Process Evaluation, Transformation By-products, and Ecotoxicity. J. Electrochem. Soc. 170, 023503. https://doi.org/10.1149/1945-7111/acb84b

Dyrda, G., Boniewska-Bernacka, E., Man, D., Barchiewicz, K., Słota, R., 2019. The effect of organic solvents on selected microorganisms and model liposome membrane. Mol. Biol. Rep. 46, 3225–3232. https://doi.org/10.1007/s11033-019-04782-y

Ebba, M., Asaithambi, P., Alemayehu, E., 2022. Development of electrocoagulation process for wastewater treatment: optimization by response surface methodology. Heliyon 8, e09383. https://doi.org/10.1016/j.heliyon.2022.e09383

Ebie, K., Li, F., Azuma, Y., Yuasa, A., Hagishita, T., 2001. Pore distribution effect of activated carbon in adsorbing organic micropollutants from natural water. Water Res. 35, 167–179. https://doi.org/10.1016/S0043-1354(00)00257-8

El-Deen, A.G., Boom, R.M., Kim, H.Y., Duan, H., Chan-Park, M.B., Choi, J.H., 2016. Flexible 3D Nanoporous Graphene for Desalination and Bio-decontamination of Brackish Water via Asymmetric Capacitive Deionization. ACS Appl. Mater. Interfaces 8, 25313–25325. https://doi.org/10.1021/acsami.6b08658

Ersan, G., Cerrón-Calle, G.A., Ersan, M.S., Garcia-Segura, S., 2023. Opportunities for in situ electro-regeneration of organic contaminant-laden carbonaceous adsorbents. Water Res. 232, 119718. https://doi.org/10.1016/j.watres.2023.119718

Fan, H.J., Anderson, P.R., 2005. Copper and cadmium removal by Mn oxide-coated granular activated carbon. Sep. Purif. Technol. 45, 61–67. https://doi.org/10.1016/j.seppur.2005.02.009

Farhat, A., Keller, J., Tait, S., Radjenovic, J., 2015. Removal of Persistent Organic Contaminants by Electrochemically Activated Sulfate. Environ. Sci. Technol. 49, 14326–14333. https://doi.org/10.1021/acs.est.5b02705

Feng, X., Wang, J., Cai, P., Yang, Z., Shen, J., Zhang, Y., Zhang, X., 2021. Graphene/protamine assembled hybrid paper with antibacterial activity. Colloids Surfaces A Physicochem. Eng. Asp. 625, 126977. https://doi.org/10.1016/j.colsurfa.2021.126977

Fortuny, A., Font, J., Fabregat, A., 1998. Wet air oxidation of phenol using active carbon as catalyst. Appl. Catal. B Environ. 19, 165–173. https://doi.org/10.1016/S0926-3373(98)00072-1

Gadipelli, S., Guo, J., Li, Z., Howard, C.A., Liang, Y., Zhang, H., Shearing, P.R., Brett, D.J.L., 2023. Understanding and Optimizing Capacitance Performance in Reduced Graphene-Oxide Based Supercapacitors. Small Methods 7, 2201557. https://doi.org/10.1002/smtd.202201557

Ganiyu, S.O., de Araújo, M.J.G., de Araújo Costa, E.C.T., Santos, J.E.L., dos Santos, E.V., Martínez-Huitle, C.A., Pergher, S.B.C., 2021. Design of highly efficient porous carbon foam cathode for electro-Fenton degradation of antimicrobial sulfanilamide. Appl. Catal. B Environ. 283, 119652. https://doi.org/10.1016/j.apcatb.2020.119652

Ganske, F., Bornscheuer, U.T., 2006. Growth of Escherichia coli, Pichia pastoris and Bacillus

cereus in the presence of the ionic liquids [BMIM][BF4] and [BMIM][PF6] and organic solvents. Biotechnol. Lett. 28, 465–469. https://doi.org/10.1007/s10529-006-0006-7

Gao, W., Majumder, M., Alemany, L.B., Narayanan, T.N., Ibarra, M.A., Pradhan, B.K., Ajayan, P.M., 2011. Engineered graphite oxide materials for application in water purification. ACS Appl. Mater. Interfaces 3, 1821–1826. https://doi.org/10.1021/am200300u

Garcia-Rodriguez, O., Mousset, E., Olvera-Vargas, H., Lefebvre, O., 2022. Electrochemical treatment of highly concentrated wastewater: A review of experimental and modeling approaches from lab- to full-scale. Crit. Rev. Environ. Sci. Technol. 52, 240–309. https://doi.org/10.1080/10643389.2020.1820428

Garcia-Segura, S., Keller, J., Brillas, E., Radjenovic, J., 2015. Removal of organic contaminants from secondary effluent by anodic oxidation with a boron-doped diamond anode as tertiary treatment. J. Hazard. Mater. 283, 551–557. https://doi.org/10.1016/j.jhazmat.2014.10.003

Garcia-Segura, S., Nienhauser, A.B., Fajardo, A.S., Bansal, R., Conrad, C.L., Fortner, J.D., Marcos-Hernández, M., Rogers, T., Villagran, D., Wong, M.S., Westerhoff, P., 2020a. Disparities between experimental and environmental conditions: Research steps toward making electrochemical water treatment a reality. Curr. Opin. Electrochem. 22, 9–16. https://doi.org/10.1016/j.coelec.2020.03.001

Garcia-Segura, S., Ocon, J.D., Chong, M.N., 2018. Electrochemical oxidation remediation of real wastewater effluents — A review. Process Saf. Environ. Prot. 113, 48–67. https://doi.org/10.1016/j.psep.2017.09.014

Garcia-Segura, S., Qu, X., Alvarez, P.J.J., Chaplin, B.P., Chen, W., Crittenden, J.C., Feng, Y., Gao, G., He, Z., Hou, C.H., Hu, X., Jiang, G., Kim, J.H., Li, J., Li, Q., Ma, J.J., Ma, J.J., Nienhauser, A.B., Niu, J., Pan, B., Quan, X., Ronzani, F., Villagran, D., Waite, T.D., Walker, W.S., Wang, C., Wong, M.S., Westerhoff, P., 2020b. Opportunities for nanotechnology to enhance electrochemical treatment of pollutants in potable water and industrial wastewater-a perspective. Environ. Sci. Nano 7, 2178–2194. https://doi.org/10.1039/d0en00194e

Garg, R., Elmas, S., Nann, T., Andersson, M.R., 2017. Deposition Methods of Graphene as Electrode Material for Organic Solar Cells. Adv. Energy Mater. 7. https://doi.org/10.1002/aenm.201601393

Gedam, N., Neti, N.R., 2014. Carbon attrition during continuous electrolysis in carbon bed based three-phase three-dimensional electrode reactor: Treatment of recalcitrant chemical industry wastewater. J. Environ. Chem. Eng. 2, 1527–1532. https://doi.org/10.1016/j.jece.2014.06.025

Ghernaout, D., Ghernaout, B., 2010. From chemical disinfection to electrodisinfection: The obligatory itinerary? Desalin. Water Treat. 16, 156–175. https://doi.org/10.5004/dwt.2010.1085

Golberg, A., Rubinsky, B., 2013. Mass Transfer Phenomena in Electroporation, in: Transport in Biological Media. Elsevier, pp. 455–492. https://doi.org/10.1016/B978-0-12-415824-5.00012-6

Golovko, O., Anton, L. de B., Cascone, C., Ahrens, L., Lavonen, E., Köhler, S.J., 2020. Sorption characteristics and removal efficiency of organic micropollutants in drinking water using Granular Activated Carbon (GAC) in pilot-scale and full-scale tests. Water (Switzerland) 12. https://doi.org/10.3390/w12072053

Gonzaga, I.M.D., Moratalla, A., Eguiluz, K.I.B., Salazar-Banda, G.R., Cañizares, P., Rodrigo, M.A., Saez, C., 2021. Novel Ti/RuO2IrO2 anode to reduce the dangerousness of antibiotic polluted urines by Fenton-based processes. Chemosphere 270, 129344. https://doi.org/10.1016/j.chemosphere.2020.129344

Gorito, A.M., Pesqueira, J.F.J.R., Moreira, N.F.F., Ribeiro, A.R., Pereira, M.F.R., Nunes, O.C., Almeida, C.M.R., Silva, A.M.T., 2021. Ozone-based water treatment (O3, O3/UV, O3/H2O2) for removal of organic micropollutants, bacteria inactivation and regrowth prevention. J. Environ. Chem. Eng. 9, 105315. https://doi.org/10.1016/j.jece.2021.105315

GracePavithra, K., Senthil Kumar, P., Jaikumar, V., SundarRajan, P.S., 2020. A review on three-dimensional eletrochemical systems: analysis of influencing parameters and cleaner

approach mechanism for wastewater. Rev. Environ. Sci. Biotechnol. 19, 873–896. https://doi.org/10.1007/s11157-020-09550-0

Groenen-Serrano, K., Weiss-Hortala, E., Savall, A., Spiteri, P., 2013. Role of Hydroxyl Radicals During the Competitive Electrooxidation of Organic Compounds on a Boron-Doped Diamond Anode. Electrocatalysis 4, 346–352. https://doi.org/10.1007/s12678-013-0150-5

Groenen Serrano, K., 2018. Indirect Electrochemical Oxidation Using Hydroxyl Radical, Active Chlorine, and Peroxodisulfate, in: Electrochemical Water and Wastewater Treatment. Elsevier, pp. 133–164. https://doi.org/10.1016/B978-0-12-813160-2.00006-7

Guo, C., Liu, H., Wang, C., Zhao, J., Zhao, W., Lu, N., Qu, J., Yuan, X., Zhang, Y., 2020. Electrochemical removal of levofloxacin using conductive graphene/polyurethane particle electrodes in a three-dimensional reactor. Environ. Pollut. 260, 114101. https://doi.org/10.1016/j.envpol.2020.114101

Haaken, D., Dittmar, T., Schmalz, V., Worch, E., 2014. Disinfection of biologically treated wastewater and prevention of biofouling by UV/electrolysis hybrid technology: Influence factors and limits for domestic wastewater reuse. Water Res. 52, 20–28. https://doi.org/10.1016/j.watres.2013.12.029

Haas, C.N., Aturaliye, D., 1999. Semi-quantitative characterization of electroporation-assisted disinfection processes for inactivation of Giardia and Cryptosporidium. J. Appl. Microbiol. 86, 899–905. https://doi.org/10.1046/j.1365-2672.1999.00725.x

Hamade, F., Radich, E., Davis, V.A., 2021. Microstructure and electrochemical properties of high performance graphene/manganese oxide hybrid electrodes. RSC Adv. 11, 31608–31620. https://doi.org/10.1039/d1ra05323j

Han, R., Zou, W., Li, H., Li, Y., Shi, J., 2006a. Copper(II) and lead(II) removal from aqueous solution in fixed-bed columns by manganese oxide coated zeolite. J. Hazard. Mater. 137, 934–942. https://doi.org/10.1016/j.jhazmat.2006.03.016

Han, R., Zou, W., Zhang, Z., Shi, J., Yang, J., 2006b. Removal of copper(II) and lead(II) from aqueous solution by manganese oxide coated sand. I. Characterization and kinetic study. J. Hazard. Mater. 137, 384–395. https://doi.org/10.1016/j.jhazmat.2006.02.021

Hand, S., Cusick, R.D., 2021. Electrochemical Disinfection in Water and Wastewater Treatment: Identifying Impacts of Water Quality and Operating Conditions on Performance. Environ. Sci. Technol. 55, 3470–3482. https://doi.org/10.1021/acs.est.0c06254

Herraiz-Carboné, M., Cotillas, S., Lacasa, E., Cañizares, P., Rodrigo, M.A., Sáez, C., 2021a. Disinfection of urines using an electro-ozonizer. Electrochim. Acta 382, 138343. https://doi.org/10.1016/j.electacta.2021.138343

Herraiz-Carboné, M., Lacasa, E., Cotillas, S., Vasileva, M., Cañizares, P., Rodrigo, M.A., Sáez, C., 2021b. The role of chloramines on the electrodisinfection of Klebsiella pneumoniae in hospital urines. Chem. Eng. J. 409, 128253. https://doi.org/10.1016/j.cej.2020.128253

Hintze, C., Morita, K., Riedel, R., Ionescu, E., Mera, G., 2016. Facile sol-gel synthesis of reduced graphene oxide/silica nanocomposites. J. Eur. Ceram. Soc. 36, 2923–2930. https://doi.org/10.1016/j.jeurceramsoc.2015.11.033

Howard, S.T., Attard, G.A., Lieberman, H.F., 1995. The polarizabilities of perchlorate, bisulphate and dihydrogen phosphate anions. Chem. Phys. Lett. 238, 180–186. https://doi.org/10.1016/0009-2614(95)00335-5

Hu, W., Peng, C., Luo, W., Lv, M., Li, X., Li, D., Huang, Q., Fan, C., 2010. Graphene-based antibacterial paper. ACS Nano 4, 4317–4323. https://doi.org/10.1021/nn101097v

Hu, Z., Cai, J., Song, G., Tian, Y., Zhou, M., 2021. Anodic oxidation of organic pollutants: Anode fabrication, process hybrid and environmental applications. Curr. Opin. Electrochem. 26, 100659. https://doi.org/10.1016/j.coelec.2020.100659

Huang, T., Zhang, S., Liu, L., Xu, J., 2018. Graphite particle electrodes that enhance the detoxification of municipal solid waste incineration fly ashes in a three-dimensional electrokinetic platform and its mechanisms. Environ. Pollut. 243, 929–939. https://doi.org/10.1016/j.envpol.2018.08.101

Huang, X., Qu, Y., Cid, C.A., Finke, C., Hoffmann, M.R., Lim, K., Jiang, S.C., 2016. Electrochemical disinfection of toilet wastewater using wastewater electrolysis cell. Water Res. 92, 164–172. https://doi.org/10.1016/j.watres.2016.01.040

Hunt, N.K., Mariñas, B.J., 1999. Inactivation of Escherichia coli with ozone: Chemical and inactivation kinetics. Water Res. 33, 2633–2641. https://doi.org/10.1016/S0043-1354(99)00115-3

Hunt, N.K., Mariñas, B.J., 1997. Kinetics of Escherichia coli inactivation with ozone. Water Res. 31, 1355–1362. https://doi.org/10.1016/S0043-1354(96)00394-6

Huo, Z.-Y., Li, G.-Q., Yu, T., Feng, C., Lu, Y., Wu, Y.-H., Yu, C., Xie, X., Hu, H.-Y., 2018. Cell Transport Prompts the Performance of Low-Voltage Electroporation for Cell Inactivation. Sci. Rep. 8, 15832. https://doi.org/10.1038/s41598-018-34027-0

Huo, Z.Y., Du, Y., Chen, Z., Wu, Y.H., Hu, H.Y., 2020. Evaluation and prospects of nanomaterial-enabled innovative processes and devices for water disinfection: A state-of-the-art review. Water Res. 173, 115581. https://doi.org/10.1016/j.watres.2020.115581

Huo, Z.Y., Liu, H., Wang, W.L., Wang, Y.H., Wu, Y.H., Xie, X., Hu, H.Y., 2019. Low-voltage alternating current powered polydopamine-protected copper phosphide nanowire for electroporation-disinfection in water. J. Mater. Chem. A 7, 7347–7354. https://doi.org/10.1039/C8TA10942G

Huo, Z.Y., Luo, Y., Xie, X., Feng, C., Jiang, K., Wang, J., Hu, H.Y., 2017. Carbon-nanotube sponges enabling highly efficient and reliable cell inactivation by low-voltage electroporation. Environ. Sci. Nano 4, 2010–2017. https://doi.org/10.1039/c7en00558j

Huo, Z.Y., Xie, X., Yu, T., Lu, Y., Feng, C., Hu, H.Y., 2016. Nanowire-Modified Three-Dimensional Electrode Enabling Low-Voltage Electroporation for Water Disinfection. Environ. Sci. Technol. 50, 7641–7649. https://doi.org/10.1021/acs.est.6b01050

Hussain, S.N., Roberts, E.P.L., Asghar, H.M.A., Campen, A.K., Brown, N.W., 2013. Oxidation of phenol and the adsorption of breakdown products using a graphite adsorbent with electrochemical regeneration. Electrochim. Acta 92, 20–30. https://doi.org/10.1016/j.electacta.2013.01.020

Ikematsu, M., Kaneda, K., Iseki, M., Yasuda, M., 2007. Electrochemical treatment of human urine for its storage and reuse as flush water. Sci. Total Environ. 382, 159–164. https://doi.org/10.1016/j.scitotenv.2007.03.028

Isidro, J., Brackemeyer, D., Sáez, C., Llanos, J., Lobato, J., Cañizares, P., Matthée, T., Rodrigo, M.A., 2020. How to avoid the formation of hazardous chlorates and perchlorates during electro-disinfection with diamond anodes? J. Environ. Manage. 265, 110566. https://doi.org/10.1016/j.jenvman.2020.110566

Jana, P., Yadav, M., Kumar, T., Kanvah, S., 2020. Benzimidazole-acrylonitriles as chemosensors for picric acid detection. J. Environ. Chem. Eng. 8, 104424. https://doi.org/10.1016/j.jece.2020.104424

Jeong, J., Kim, J.Y., Yoon, J., 2006. The role of reactive oxygen species in the electrochemical inactivation of microorganisms. Environ. Sci. Technol. 40, 6117–6122. https://doi.org/10.1021/es0604313

Jiang, J., Zhang, X., Zhu, X., Li, Y., 2017. Removal of Intermediate Aromatic Halogenated DBPs by Activated Carbon Adsorption: A New Approach to Controlling Halogenated DBPs in Chlorinated Drinking Water. Environ. Sci. Technol. 51, 3435–3444. https://doi.org/10.1021/acs.est.6b06161

Jiang, Y., Zhao, H., Liang, J., Yue, L., Li, T., Luo, Y., Liu, Q., Lu, S., Asiri, A.M., Gong, Z., Sun, X., 2021. Anodic oxidation for the degradation of organic pollutants: Anode materials, operating conditions and mechanisms. A mini review. Electrochem. commun. 123, 106912. https://doi.org/10.1016/j.elecom.2020.106912

Jiao, Y., Ma, L., Tian, Y., Zhou, M., 2020. A flow-through electro-Fenton process using modified activated carbon fiber cathode for orange II removal. Chemosphere 252, 126483. https://doi.org/10.1016/j.chemosphere.2020.126483

Jimenez-Cervantes, E., López-Barroso, J., Martínez-Hernández, A.L., Velasco-Santos, C., 2016. Graphene-Based Materials Functionalization with Natural Polymeric Biomolecules.

Recent Adv. Graphene Res. https://doi.org/10.5772/64001
Jing, Y., Chaplin, B.P., 2017. Mechanistic Study of the Validity of Using Hydroxyl Radical Probes to Characterize Electrochemical Advanced Oxidation Processes. Environ. Sci. Technol. 51, 2355–2365. https://doi.org/10.1021/acs.est.6b05513
Jjagwe, J., Olupot, P.W., Menya, E., Kalibbala, H.M., 2021. Synthesis and Application of Granular Activated Carbon from Biomass Waste Materials for Water Treatment: A Review. J. Bioresour. Bioprod. 6, 292–322. https://doi.org/10.1016/j.jobab.2021.03.003
Joannes, C., Sipaut, C.S., Dayou, J., Yasir, S.M., Mansa, R.F., 2015. Review paper on cell membrane electroporation of microalgae using electric field treatment method for microalgae lipid extraction. IOP Conf. Ser. Mater. Sci. Eng. 78, 012034. https://doi.org/10.1088/1757-899X/78/1/012034
Kapałka, A., Fóti, G., Comninellis, C., 2010. Basic principles of the electrochemical mineralization of organic pollutants for wastewater treatment, in: Electrochemistry for the Environment. pp. 1–23. https://doi.org/10.1007/978-0-387-68318-8_1
Kapałka, A., Fóti, G., Comninellis, C., 2009. The importance of electrode material in environmental electrochemistry. Formation and reactivity of free hydroxyl radicals on boron-doped diamond electrodes. Electrochim. Acta 54, 2018–2023. https://doi.org/10.1016/j.electacta.2008.06.045
Kapałka, A., Fóti, G., Comninellis, C., 2008. Kinetic modelling of the electrochemical mineralization of organic pollutants for wastewater treatment. J. Appl. Electrochem. 38, 7–16. https://doi.org/10.1007/s10800-007-9365-6
Kerwick, M.I., Reddy, S.M., Chamberlain, A.H.L., Holt, D.M., 2005. Electrochemical disinfection, an environmentally acceptable method of drinking water disinfection?, in: Electrochimica Acta. Pergamon, pp. 5270–5277. https://doi.org/10.1016/j.electacta.2005.02.074
Khalid, U., Orozco Garcia, C., 2019. Integrated Decentralised Wastewater Treatment for Rural Areas with a Focus on Resource Recovery. RUVIVAL Publ. Ser., RUVIVAL publication series 4, 39–64.
Kim, H.W., Ross, M.B., Kornienko, N., Zhang, L., Guo, J., Yang, P., McCloskey, B.D., 2018. Efficient hydrogen peroxide generation using reduced graphene oxide-based oxygen reduction electrocatalysts. Nat. Catal. 1, 282–290. https://doi.org/10.1038/s41929-018-0044-2
Kimura, M., Miyamoto, I., 1994. Discovery of the Activated-Carbon Radical AC + and the Novel Oxidation-Reactions Comprising the AC/AC + Cycle as a Catalyst in an Aqueous Solution . Bull. Chem. Soc. Jpn. 67, 2357–2360. https://doi.org/10.1246/bcsj.67.2357
Kiran, N.U., Dey, S., Singh, B.P., Besra, L., 2017. Graphene coating on copper by electrophoretic deposition for corrosion prevention. Coatings 7, 214. https://doi.org/10.3390/coatings7120214
Kılıç, M.Y., Kestioglu, K., Yonar, T., 2007. Landfill leachate treatment by the combination of physicochemical methods with adsorption process. J. Biol. Environ. Sci 1, 37–43.
Kraft, A., 2008. Electrochemical Water Disinfection: A Short Review. Platin. Met. Rev. 52, 177–185. https://doi.org/10.1595/147106708X329273
Kumar, A., Pan, S.-Y., 2020. Opportunities and challenges of electrochemical water treatment integrated with renewable energy at the water-energy nexus. Water-Energy Nexus 3, 110–116. https://doi.org/10.1016/j.wen.2020.03.006
Kumar, S., Ghosh, S., Munichandraiah, N., Vasan, H.N., 2013. 1.5 v battery driven reduced graphene oxide-silver nanostructure coated carbon foam (rGO-Ag-CF) for the purification of drinking water. Nanotechnology 24, 235101. https://doi.org/10.1088/0957-4484/24/23/235101
Lan, Y., Coetsier, C., Causserand, C., Groenen Serrano, K., 2017. On the role of salts for the treatment of wastewaters containing pharmaceuticals by electrochemical oxidation using a boron doped diamond anode. Electrochim. Acta 231, 309–318. https://doi.org/10.1016/j.electacta.2017.01.160
Le, T.X.H., Bechelany, M., Lacour, S., Oturan, N., Oturan, M.A., Cretin, M., 2015. High

removal efficiency of dye pollutants by electron-Fenton process using a graphene based cathode. Carbon N. Y. 94, 1003–1011. https://doi.org/10.1016/j.carbon.2015.07.086

Li, F., Yuasa, A., Ebie, K., Azuma, Y., 2003. Microcolumn test and model analysis of activated carbon adsorption of dissolved organic matter after precoagulation: Effects of pH and pore size distribution. J. Colloid Interface Sci. 262, 331–341. https://doi.org/10.1016/S0021-9797(03)00116-4

Li, H., Yang, H., Cheng, J., Hu, C., Yang, Z., Wu, C., 2021. Three-dimensional particle electrode system treatment of organic wastewater: A general review based on patents. J. Clean. Prod. 308, 127324. https://doi.org/10.1016/j.jclepro.2021.127324

Li, H., Zhu, X., Ni, J., 2010. Inactivation of Escherichia coli in Na2SO4 electrolyte using boron-doped diamond anode. Electrochim. Acta 56, 448–453. https://doi.org/10.1016/j.electacta.2010.08.055

Li, L., Sun, F., Gao, J., Wang, L., Pi, X., Zhao, G., 2018. Broadening the pore size of coal-based activated carbon: Via a washing-free chem-physical activation method for high-capacity dye adsorption. RSC Adv. 8, 14488–14499. https://doi.org/10.1039/c8ra02127a

Li, L., Tang, C., Zheng, Y., Xia, B., Zhou, X., Xu, H., Qiao, S.Z., 2020. Tailoring Selectivity of Electrochemical Hydrogen Peroxide Generation by Tunable Pyrrolic-Nitrogen-Carbon. Adv. Energy Mater. 10, 2000789. https://doi.org/10.1002/aenm.202000789

Li, Q., Snoeyink, V.L., Mariñas, B.J., Campos, C., 2003. Pore blockage effect of NOM on atrazine adsorption kinetics of PAC: The roles of PAC pore size distribution and NOM molecular weight. Water Res. 37, 4863–4872. https://doi.org/10.1016/j.watres.2003.08.018

Li, R., Mansukhani, N.D., Guiney, L.M., Ji, Z., Zhao, Y., Chang, C.H., French, C.T., Miller, J.F., Hersam, M.C., Nel, A.E., Xia, T., 2016. Identification and Optimization of Carbon Radicals on Hydrated Graphene Oxide for Ubiquitous Antibacterial Coatings. ACS Nano 10, 10966–10980. https://doi.org/10.1021/acsnano.6b05692

Li, X., Lu, S., Zhang, G., 2023. Three-dimensional structured electrode for electrocatalytic organic wastewater purification: Design, mechanism and role. J. Hazard. Mater. 445, 130524. https://doi.org/10.1016/j.jhazmat.2022.130524

Li, X.F., Mitch, W.A., 2018. Drinking Water Disinfection Byproducts (DBPs) and Human Health Effects: Multidisciplinary Challenges and Opportunities. Environ. Sci. Technol. 52, 1681–1689. https://doi.org/10.1021/acs.est.7b05440

Li, Y., Du, Q., Wang, J., Liu, T., Sun, J., Wang, Y., Wang, Z., Xia, Y., Xia, L., 2013. Defluoridation from aqueous solution by manganese oxide coated graphene oxide. J. Fluor. Chem. 148, 67–73. https://doi.org/10.1016/j.jfluchem.2013.01.028

Li, Y., Yang, M., Zhang, X., Jiang, J., Liu, J., Yau, C.F., Graham, N.J.D., Li, X., 2017. Two-step chlorination: A new approach to disinfection of a primary sewage effluent. Water Res. 108, 339–347. https://doi.org/10.1016/j.watres.2016.11.019

Li, Z., Liu, H., Ruan, H., Hu, R., Su, Y., Hu, Z., Huang, J., 2017. In situ synthesis rodlike MnO2/reduced graphene oxide composite as anode materials for Li-ion batteries. J. Mater. Sci. Mater. Electron. 28, 18099–18105. https://doi.org/10.1007/s10854-017-7754-0

Liang, S., Lin, H., Habteselassie, M., Huang, Q., 2018. Electrochemical inactivation of bacteria with a titanium sub-oxide reactive membrane. Water Res. 145, 172–180. https://doi.org/10.1016/j.watres.2018.08.010

Lissaneddine, A., Pons, M.N., Aziz, F., Ouazzani, N., Mandi, L., Mousset, E., 2022. A critical review on the electrosorption of organic compounds in aqueous effluent – Influencing factors and engineering considerations. Environ. Res. 204, 112128. https://doi.org/10.1016/j.envres.2021.112128

Liu, C., Xie, X., Zhao, W., Liu, N., Maraccini, P.A., Sassoubre, L.M., Boehm, A.B., Cui, Y., 2013. Conducting nanosponge electroporation for affordable and high-efficiency disinfection of bacteria and viruses in water. Nano Lett. 13, 4288–4293. https://doi.org/10.1021/nl402053z

Liu, H., Ni, X.Y., Huo, Z.Y., Peng, L., Li, G.Q., Wang, C., Wu, Y.H., Hu, H.Y., 2019. Carbon Fiber-Based Flow-Through Electrode System (FES) for Water Disinfection via Direct

Oxidation Mechanism with a Sequential Reduction-Oxidation Process. Environ. Sci. Technol. 53, 3238–3249. https://doi.org/10.1021/acs.est.8b07297

Liu, H., Wu, Y.H., Ni, X.Y., Chen, Z., Peng, L., Huo, Z.Y., Wang, Q., Hu, H.Y., 2020. Construction and optimization mechanisms of carbon fiber-based flow-through electrode system (FES) with stackable multi-cathode units for water disinfection. J. Hazard. Mater. 399, 123065. https://doi.org/10.1016/j.jhazmat.2020.123065

Liu, Q., Yang, H., Jing, B., Chen, Wenjuan, Chen, Wu, Yin, X., 2017. Study on the Degradation of Oilfield Wastewater Treatment by Three-Dimensional Electrode. Open J. Yangtze Oil Gas 02, 67–81. https://doi.org/10.4236/ojogas.2017.22005

Liu, S., Zeng, T.H., Hofmann, M., Burcombe, E., Wei, J., Jiang, R., Kong, J., Chen, Y., 2011. Antibacterial activity of graphite, graphite oxide, graphene oxide, and reduced graphene oxide: Membrane and oxidative stress. ACS Nano 5, 6971–6980. https://doi.org/10.1021/nn202451x

Liu, W., Ai, Z., Zhang, L., 2012. Design of a neutral three-dimensional electro-Fenton system with foam nickel as particle electrodes for wastewater treatment. J. Hazard. Mater. 243, 257–264. https://doi.org/10.1016/J.JHAZMAT.2012.10.024

Liu, Y., He, L.F., Deng, Y.Y., Zhang, Q., Jiang, G.M., Liu, H., 2022. Recent progress on the recovery of valuable resources from source-separated urine on-site using electrochemical technologies: A review. Chem. Eng. J. 442, 136200. https://doi.org/10.1016/j.cej.2022.136200

Liu, Y., Ma, J., Wu, T., Wang, X., Huang, G., Liu, Yu, Qiu, H., Li, Y., Wang, W., Gao, J., 2013. Cost-effective reduced graphene oxide-coated polyurethane sponge as a highly efficient and reusable oil-absorbent. ACS Appl. Mater. Interfaces 5, 10018–10026. https://doi.org/10.1021/am4024252

Loeb, B.L., Thompson, C.M., Drago, J., Takahara, H., Baig, S., 2012. Worldwide Ozone Capacity for Treatment of Drinking Water and Wastewater: A Review. Ozone Sci. Eng. 34, 64–77. https://doi.org/10.1080/01919512.2012.640251

Long, Y., Ni, J., Wang, Z., 2015. Subcellular mechanism of Escherichia coli inactivation during electrochemical disinfection with boron-doped diamond anode: A comparative study of three electrolytes. Water Res. 84, 198–206. https://doi.org/10.1016/j.watres.2015.07.035

Lumbaque, E.C., Radjenovic, J., 2023. Electro-oxidation of persistent organic contaminants at graphene sponge electrodes using intermittent current. Chem. Eng. J. 476, 146910. https://doi.org/10.1016/j.cej.2023.146910

Ma, D., Yi, H., Lai, C., Liu, X., Huo, X., An, Z., Li, L., Fu, Y., Li, B., Zhang, M., Qin, L., Liu, S., Yang, L., 2021. Critical review of advanced oxidation processes in organic wastewater treatment. Chemosphere 275, 130104. https://doi.org/10.1016/j.chemosphere.2021.130104

Ma, J., Gao, M., Shi, H., Ni, J., Xu, Y., Wang, Q., 2021. Progress in research and development of particle electrodes for three-dimensional electrochemical treatment of wastewater: a review. Environ. Sci. Pollut. Res. 28, 47800–47824. https://doi.org/10.1007/s11356-021-13785-x

Ma, J., Zhang, J., Xiong, Z., Yong, Y., Zhao, X.S., 2011. Preparation, characterization and antibacterial properties of silver-modified graphene oxide. J. Mater. Chem. 21, 3350–3352. https://doi.org/10.1039/c0jm02806a

Ma, P., Ma, H., Sabatino, S., Galia, A., Scialdone, O., 2018. Electrochemical treatment of real wastewater. Part 1: Effluents with low conductivity. Chem. Eng. J. 336, 133–140. https://doi.org/10.1016/j.cej.2017.11.046

Mao, R., Zhao, X., Lan, H., Liu, H., Qu, J., 2014. Efficient electrochemical reduction of bromate by a Pd/rGO/CFP electrode with low applied potentials. Appl. Catal. B Environ. 160–161, 179–187. https://doi.org/10.1016/j.apcatb.2014.04.040

Mareev, S., Skolotneva, E., Cretin, M., Nikonenko, V., 2021. Modeling the formation of gas bubbles inside the pores of reactive electrochemical membranes in the process of the anodic oxidation of organic compounds. Int. J. Mol. Sci. 22, 5477. https://doi.org/10.3390/ijms22115477

Martínez-Huitle, C.A., Brillas, E., 2021. A critical review over the electrochemical disinfection

of bacteria in synthetic and real wastewaters using a boron-doped diamond anode. Curr. Opin. Solid State Mater. Sci. 25, 100926. https://doi.org/10.1016/j.cossms.2021.100926
Martínez-Huitle, C.A., Brillas, E., 2008. Electrochemical alternatives for drinking water disinfection. Angew. Chemie - Int. Ed. 47, 1998–2005. https://doi.org/10.1002/anie.200703621
Martínez-Huitle, C.A., dos Santos, E.V., de Araújo, D.M., Panizza, M., 2012. Applicability of diamond electrode/anode to the electrochemical treatment of a real textile effluent. J. Electroanal. Chem. 674, 103–107. https://doi.org/10.1016/j.jelechem.2012.02.005
Martínez-Huitle, C.A., Rodrigo, M.A., Sirés, I., Scialdone, O., 2015. Single and Coupled Electrochemical Processes and Reactors for the Abatement of Organic Water Pollutants: A Critical Review. Chem. Rev. 115, 13362–13407. https://doi.org/10.1021/acs.chemrev.5b00361
Massa, A., Hernández, S., Lamberti, A., Galletti, C., Russo, N., Fino, D., 2017. Electro-oxidation of phenol over electrodeposited MnOx nanostructures and the role of a TiO2 nanotubes interlayer. Appl. Catal. B Environ. 203, 270–281. https://doi.org/10.1016/j.apcatb.2016.10.025
Matsena, M.T., Mabuse, M., Tichapondwa, S.M., Chirwa, E.M.N., 2021. Improved performance and cost efficiency by surface area optimization of granular activated carbon in air-cathode microbial fuel cell. Chemosphere 281, 130941. https://doi.org/10.1016/j.chemosphere.2021.130941
McQuillan, R. V., Stevens, G.W., Mumford, K.A., 2018. The electrochemical regeneration of granular activated carbons: A review. J. Hazard. Mater. https://doi.org/10.1016/j.jhazmat.2018.04.079
Mei, R., Wei, Q., Zhu, C., Ye, W., Zhou, B., Ma, L., Yu, Z., Zhou, K., 2019. 3D macroporous boron-doped diamond electrode with interconnected liquid flow channels: A high-efficiency electrochemical degradation of RB-19 dye wastewater under low current. Appl. Catal. B Environ. 245, 420–427. https://doi.org/10.1016/j.apcatb.2018.12.074
Mestre, A.S., Pires, J., Nogueira, J.M.F., Parra, J.B., Carvalho, A.P., Ania, C.O., 2009. Waste-derived activated carbons for removal of ibuprofen from solution: Role of surface chemistry and pore structure. Bioresour. Technol. 100, 1720–1726. https://doi.org/10.1016/j.biortech.2008.09.039
Miao, D., Li, Z., Chen, Y., Liu, G., Deng, Z., Yu, Y., Li, S., Zhou, K., Ma, L., Wei, Q., 2022. Preparation of macro-porous 3D boron-doped diamond electrode with surface micro structure regulation to enhance electrochemical degradation performance. Chem. Eng. J. 429, 132366. https://doi.org/10.1016/j.cej.2021.132366
Michaud, P.A., Panizza, M., Ouattara, L., Diaco, T., Foti, G., Comninellis, C., 2003. Electrochemical oxidation of water on synthetic boron-doped diamond thin film anodes. J. Appl. Electrochem. 33, 151–154. https://doi.org/10.1023/A:1024084924058
Miklos, D.B., Remy, C., Jekel, M., Linden, K.G., Drewes, J.E., Hübner, U., 2018. Evaluation of advanced oxidation processes for water and wastewater treatment – A critical review. Water Res. 139, 118–131. https://doi.org/10.1016/j.watres.2018.03.042
Mohammad, H., Martin, A.D., Hill, P.I., Hodson, N., Brown, N., Roberts, E.P.L., 2020. Effect of electrochemical regeneration on the surface of a graphite adsorbent loaded with an organic contaminant. Int. J. Environ. Sci. Technol. 17, 3131–3142. https://doi.org/10.1007/s13762-020-02624-0
Mohammed, F.M., Roberts, E.P.L., Hill, A., Campen, A.K., Brown, N.W., 2011. Continuous water treatment by adsorption and electrochemical regeneration. Water Res. 45, 3065–3074. https://doi.org/10.1016/j.watres.2011.03.023
Mohammed, H., Kumar, A., Bekyarova, E., Al-Hadeethi, Y., Zhang, X., Chen, M., Ansari, M.S., Cochis, A., Rimondini, L., 2020. Antimicrobial Mechanisms and Effectiveness of Graphene and Graphene-Functionalized Biomaterials. A Scope Review. Front. Bioeng. Biotechnol. 8, 465. https://doi.org/10.3389/fbioe.2020.00465
Mohan, V.B., Lau, K. tak, Hui, D., Bhattacharyya, D., 2018. Graphene-based materials and their composites: A review on production, applications and product limitations. Compos. Part B

Eng. 142, 200–220. https://doi.org/10.1016/j.compositesb.2018.01.013
Moreno-Castilla, C., Rivera-Utrilla, J., 2001. Carbon materials as adsorbents for the removal of pollutants from the aqueous phase. MRS Bull. 26, 890–894. https://doi.org/10.1557/mrs2001.230
Morimoto, N., Kubo, T., Nishina, Y., 2016. Tailoring the oxygen content of graphite and reduced graphene oxide for specific applications. Sci. Rep. 6, 21715. https://doi.org/10.1038/srep21715
Mostafa, E., Reinsberg, P., Garcia-Segura, S., Baltruschat, H., 2018. Chlorine species evolution during electrochlorination on boron-doped diamond anodes: In-situ electrogeneration of Cl2, Cl2O and ClO2. Electrochim. Acta 281, 831–840. https://doi.org/10.1016/j.electacta.2018.05.099
Moura de Salles Pupo, M., Albahaca Oliva, J.M., Barrios Eguiluz, K.I., Salazar-Banda, G.R., Radjenovic, J., 2020. Characterization and comparison of Ti/TiO2-NT/SnO2–SbBi, Ti/SnO2–SbBi and BDD anode for the removal of persistent iodinated contrast media (ICM). Chemosphere 253, 126701. https://doi.org/10.1016/j.chemosphere.2020.126701
Mousset, E., Ko, Z.T., Syafiq, M., Wang, Z., Lefebvre, O., 2016. Electrocatalytic activity enhancement of a graphene ink-coated carbon cloth cathode for oxidative treatment. Electrochim. Acta 222, 1628–1641. https://doi.org/10.1016/j.electacta.2016.11.151
Muddemann, T., Bulan, A., Sievers, M., Kunz, U., 2018. Avoidance of Chlorine Formation during Electrolysis at Boron-Doped Diamond Anodes in Highly Sodium Chloride Containing and Organic-Polluted Wastewater. J. Electrochem. Soc. 165, J3281–J3287. https://doi.org/10.1149/2.0371815jes
Muddemann, T., Haupt, D., Sievers, M., Kunz, U., 2019. Electrochemical Reactors for Wastewater Treatment. ChemBioEng Rev. 6, 142–156. https://doi.org/10.1002/cben.201900021
Muzioreva, H., Gumbo, T., Kavishe, N., Moyo, T., Musonda, I., 2022. Decentralized wastewater system practices in developing countries: A systematic review. Util. Policy 79, 101442. https://doi.org/10.1016/j.jup.2022.101442
Nageswara Rao, N., Rohit, M., Nitin, G., Parameswaran, P.N., Astik, J.K., 2009. Kinetics of electrooxidation of landfill leachate in a three-dimensional carbon bed electrochemical reactor. Chemosphere 76, 1206–1212. https://doi.org/10.1016/j.chemosphere.2009.06.009
Narayanan, K.B., Park, G.T., Han, S.S., 2021. Antibacterial properties of starch-reduced graphene oxide–polyiodide nanocomposite. Food Chem. 342, 128385. https://doi.org/10.1016/j.foodchem.2020.128385
Narbaitz, R.M., Karimi-Jashni, A., 2009. Electrochemical regeneration of granular activated carbons loaded with phenol and natural organic matter. Environ. Technol. 30, 27–36. https://doi.org/10.1080/09593330802422803
National Renewable Energy Laboratory, 2018. PVWatts Calculator - Version 5 [WWW Document]. Lab. Natl. Renew. Energy. URL http://pvwatts.nrel.gov/version_5.php
Nayak, S., Chaplin, B.P., 2018. Fabrication and characterization of porous, conductive, monolithic Ti4O7 electrodes. Electrochim. Acta 263, 299–310. https://doi.org/10.1016/j.electacta.2018.01.034
Neto, A.J.P., Fileti, E.E., 2018. Differential Capacitance and Energetics of the Electrical Double Layer of Graphene Oxide Supercapacitors: Impact of the Oxidation Degree. J. Phys. Chem. C 122, 21824–21832. https://doi.org/10.1021/acs.jpcc.8b07349
Ni, X.-Y., Liu, H., Wang, C., Wang, W.-L., Xu, Z.-B., Chen, Z., Wu, Y.-H., Hu, H.-Y., 2020. Comparison of carbonized and graphitized carbon fiber electrodes under flow-through electrode system (FES) for high-efficiency bacterial inactivation. Water Res. 168, 115150. https://doi.org/10.1016/j.watres.2019.115150
Ni, X.Y., Liu, H., Xin, L., Xu, Z. Bin, Wang, Y.H., Peng, L., Chen, Z., Wu, Y.H., Hu, H.Y., 2020. Disinfection performance and mechanism of the carbon fiber-based flow-through electrode system (FES) towards Gram-negative and Gram-positive bacteria. Electrochim. Acta 341, 135993. https://doi.org/10.1016/j.electacta.2020.135993
Ni, X.Y., Wu, Y.H., Liu, H., Zhang, X.J., Xu, Z. Bin, Peng, L., Wang, W.L., Wang, H. Bin,

Chen, Z., Hu, H.Y., 2021. Enhancing disinfection performance of the carbon fiber-based flow-through electrode system (FES) by alternating pulse current (APC) with low-frequency square wave. Chem. Eng. J. 410, 128399. https://doi.org/10.1016/j.cej.2020.128399

Nidheesh, P.V., Ganiyu, S.O., Martínez-Huitle, C.A., Mousset, E., Olvera-Vargas, H., Trellu, C., Zhou, M., Oturan, M.A., 2023. Recent advances in electro-Fenton process and its emerging applications. Crit. Rev. Environ. Sci. Technol. 53, 887–913. https://doi.org/10.1080/10643389.2022.2093074

Niu, J., Conway, B.E., 2002. Adsorptive and electrosorptive removal of aniline and bipyridyls from waste-waters. J. Electroanal. Chem. 536, 83–92. https://doi.org/10.1016/S0022-0728(02)01206-8

Noor, R., Islam, Z., Munshi, S.K., Rahman, F., 2013. Influence of temperature on Escherichia coli growth in different culture media. J. Pure Appl. Microbiol. 7, 899–904.

Norra, G.F., Radjenovic, J., 2021. Removal of persistent organic contaminants from wastewater using a hybrid electrochemical-granular activated carbon (GAC) system. J. Hazard. Mater. 415, 125557. https://doi.org/10.1016/j.jhazmat.2021.125557

Novoselov, K.S., Geim, A.K., Morozov, S. V., Jiang, D., Zhang, Y., Dubonos, S. V., Grigorieva, I. V., Firsov, A.A., 2004. Electric field in atomically thin carbon films. Science (80-.). 306, 666–669. https://doi.org/10.1126/science.1102896

Okur, M.C., Akyol, A., Nayir, T.Y., Kara, S., Ozturk, D., Civas, A., 2022. Performance of Ti/RuO2-IrO2 electrodes and comparison with BDD electrodes in the treatment of textile wastewater by electro-oxidation process. Chem. Eng. Res. Des. 183, 398–410. https://doi.org/10.1016/j.cherd.2022.05.016

Ormeno-Cano, N., Radjenovic, J., 2022. Electrochemical degradation of antibiotics using flow-through graphene sponge electrodes. J. Hazard. Mater. 431, 128462. https://doi.org/10.1016/j.jhazmat.2022.128462

Palmas, S., Mascia, M., Vacca, A., Mais, L., Corgiolu, S., Petrucci, E., 2018. Practical aspects on electrochemical disinfection of urban and domestic wastewater, in: Electrochemical Water and Wastewater Treatment. Elsevier, pp. 421–427. https://doi.org/10.1016/B978-0-12-813160-2.00016-X

Pan, M., Shan, C., Zhang, X., Zhang, Y., Zhu, C., Gao, G., Pan, B., 2018. Environmentally Friendly in Situ Regeneration of Graphene Aerogel as a Model Conductive Adsorbent. Environ. Sci. Technol. 52, 739–746. https://doi.org/10.1021/acs.est.7b02795

Panizza, M., Cerisola, G., 2005. Application of diamond electrodes to electrochemical processes. Electrochim. Acta 51, 191–199. https://doi.org/10.1016/j.electacta.2005.04.023

Pedersen, N.L., Nikbakht Fini, M., Molnar, P.K., Muff, J., 2019. Synergy of combined adsorption and electrochemical degradation of aqueous organics by granular activated carbon particulate electrodes. Sep. Purif. Technol. 208, 51–58. https://doi.org/10.1016/j.seppur.2018.05.023

Pérez, G., Fernández-Alba, A.R., Urtiaga, A.M., Ortiz, I., 2010. Electro-oxidation of reverse osmosis concentrates generated in tertiary water treatment. Water Res. 44, 2763–2772. https://doi.org/10.1016/j.watres.2010.02.017

Perreault, F., De Faria, A.F., Nejati, S., Elimelech, M., 2015. Antimicrobial Properties of Graphene Oxide Nanosheets: Why Size Matters. ACS Nano 9, 7226–7236. https://doi.org/10.1021/acsnano.5b02067

Peter-Varbanets, M., Zurbrügg, C., Swartz, C., Pronk, W., 2009. Decentralized systems for potable water and the potential of membrane technology. Water Res. https://doi.org/10.1016/j.watres.2008.10.030

Pi, S.Y., Sun, M.Y., Zhao, Y.F., Chong, Y.X., Chen, D., Liu, H., 2022. Electroporation-coupled electrochemical oxidation for rapid and efficient water disinfection with Co3O4 nanowire arrays-modified graphite felt electrodes. Chem. Eng. J. 435, 134967. https://doi.org/10.1016/j.cej.2022.134967

Pointer Malpass, G.R., de Jesus Motheo, A., 2021. Recent advances on the use of active anodes in environmental electrochemistry. Curr. Opin. Electrochem. 27, 100689.

https://doi.org/10.1016/j.coelec.2021.100689
Polcaro, A.M., Palmas, S., Renoldi, F., Mascia, M., 2000. Three-dimensional electrodes for the electrochemical combustion of organic pollutants. Electrochim. Acta 46, 389–394. https://doi.org/10.1016/S0013-4686(00)00596-X
Pourzamani, H., Mengelizadeh, N., Hajizadeh, Y., Mohammadi, H., 2018. Electrochemical degradation of diclofenac using three-dimensional electrode reactor with multi-walled carbon nanotubes. Environ. Sci. Pollut. Res. 25, 24746–24763. https://doi.org/10.1007/s11356-018-2527-8
Prakash, A., Bahadur, D., 2014. The role of ionic electrolytes on capacitive performance of ZnO-reduced graphene oxide nanohybrids with thermally tunable morphologies. ACS Appl. Mater. Interfaces 6, 1394–1405. https://doi.org/10.1021/am405031y
Qi, X., Wang, T., Long, Y., Ni, J., 2015. Synergetic antibacterial activity of reduced graphene oxide and boron doped diamond anode in three dimensional electrochemical oxidation system. Sci. Rep. 5, 1–10. https://doi.org/10.1038/srep10388
Qiao, J., Xiong, Y., 2021. Electrochemical oxidation technology: A review of its application in high-efficiency treatment of wastewater containing persistent organic pollutants. J. Water Process Eng. 44, 102308. https://doi.org/10.1016/j.jwpe.2021.102308
Radchenko, M. V., Tanaka, K., Waditee, R., Oshimi, S., Matsuzaki, Y., Fukuhara, M., Kobayashi, H., Takabe, T., Nakamura, T., 2006. Potassium/proton antiport system of Escherichia coli. J. Biol. Chem. 281, 19822–19829. https://doi.org/10.1074/jbc.M600333200
Radha, K. V., Sirisha, K., 2018. Electrochemical Oxidation Processes. Adv. Oxid. Process. Wastewater Treat. Emerg. Green Chem. Technol. 359–373. https://doi.org/10.1016/B978-0-12-810499-6.00011-5
Radich, J.G., Kamat, P. V., 2012. Origin of reduced graphene oxide enhancements in electrochemical energy storage. ACS Catal. 2, 807–816. https://doi.org/10.1021/cs3001286
Radjenovic, J., Bagastyo, A., Rozendal, R.A., Mu, Y., Keller, J., Rabaey, K., 2011. Electrochemical oxidation of trace organic contaminants in reverse osmosis concentrate using RuO2/IrO2-coated titanium anodes. Water Res. 45, 1579–1586. https://doi.org/10.1016/j.watres.2010.11.035
Radjenovic, J., Duinslaeger, N., Avval, S.S., Chaplin, B.P., 2020. Facing the Challenge of Poly- And Perfluoroalkyl Substances in Water: Is Electrochemical Oxidation the Answer? Environ. Sci. Technol. https://doi.org/10.1021/acs.est.0c06212
Radjenovic, J., Sedlak, D.L., 2015. Challenges and Opportunities for Electrochemical Processes as Next-Generation Technologies for the Treatment of Contaminated Water. Environ. Sci. Technol. 49, 11292–11302. https://doi.org/10.1021/acs.est.5b02414
Rahmani, A., Leili, M., Seid-mohammadi, A., Shabanloo, A., Ansari, A., Nematollahi, D., Alizadeh, S., 2021. Improved degradation of diuron herbicide and pesticide wastewater treatment in a three-dimensional electrochemical reactor equipped with PbO2 anodes and granular activated carbon particle electrodes. J. Clean. Prod. 322, 129094. https://doi.org/10.1016/j.jclepro.2021.129094
Rahner, D., Ludwig, G., Röhrs, J., 2002. Electrochemically induced reactions in soils - A new approach to the in-situ remediation of contaminated soils? Part 1: The microconductor principle. Electrochim. Acta 47, 1395–1403. https://doi.org/10.1016/S0013-4686(01)00854-4
Rajkumar, D., Palanivelu, K., Balasubramanian, N., 2005. Combined electrochemical degradation and activated carbon adsorption treatments for wastewater containing mixed phenolic compounds. J. Environ. Eng. Sci. 4, 1–9. https://doi.org/10.1139/s04-037
Ramezanzadeh, B., Haeri, Z., Ramezanzadeh, M., 2016. A facile route of making silica nanoparticles-covered graphene oxide nanohybrids (SiO2-GO); fabrication of SiO2-GO/epoxy composite coating with superior barrier and corrosion protection performance. Chem. Eng. J. 303, 511–528. https://doi.org/10.1016/j.cej.2016.06.028
Ren, G., Zhou, M., Zhang, Q., Xu, X., Li, Y., Su, P., 2020. A novel stacked flow-through

electro-Fenton reactor as decentralized system for the simultaneous removal of pollutants (COD, NH3-N and TP) and disinfection from domestic sewage containing chloride ions. Chem. Eng. J. 387, 124037. https://doi.org/10.1016/j.cej.2020.124037

Richardson, S.D., 2003. Disinfection by-products and other emerging contaminants in drinking water. TrAC - Trends Anal. Chem. 22, 666–684. https://doi.org/10.1016/S0165-9936(03)01003-3

Rizzo, L., Malato, S., Antakyali, D., Beretsou, V.G., Đolić, M.B., Gernjak, W., Heath, E., Ivancev-Tumbas, I., Karaolia, P., Lado Ribeiro, A.R., Mascolo, G., McArdell, C.S., Schaar, H., Silva, A.M.T., Fatta-Kassinos, D., 2019. Consolidated vs new advanced treatment methods for the removal of contaminants of emerging concern from urban wastewater. Sci. Total Environ. 655, 986–1008. https://doi.org/10.1016/j.scitotenv.2018.11.265

Rogers, T.W., Rogers, T.S., Stoner, M.H., Sellgren, K.L., Lynch, B.J., Forbis-Stokes, A.A., Stoner, B.R., Hawkins, B.T., 2018. A granular activated carbon/electrochemical hybrid system for onsite treatment and reuse of blackwater. Water Res. 144, 553–560. https://doi.org/10.1016/j.watres.2018.07.070

Salazar-Banda, G.R., Santos, G. de O.S., Duarte Gonzaga, I.M., Dória, A.R., Barrios Eguiluz, K.I., 2021. Developments in electrode materials for wastewater treatment. Curr. Opin. Electrochem. 26, 100663. https://doi.org/10.1016/j.coelec.2020.100663

Schmalz, V., Dittmar, T., Haaken, D., Worch, E., 2009. Electrochemical disinfection of biologically treated wastewater from small treatment systems by using boron-doped diamond (BDD) electrodes – Contribution for direct reuse of domestic wastewater. Water Res. 43, 5260–5266. https://doi.org/10.1016/j.watres.2009.08.036

Segues Codina, A., Sergienko, N., Borrego, C.M., Radjenovic, J., 2023. Manganese oxide-functionalized graphene sponge electrodes for electrochemical chlorine-free disinfection of tap water. Chem. Eng. J. 472, 145082. https://doi.org/10.1016/j.cej.2023.145082

Sergienko, N., Lumbaque, E.C., Duinslaeger, N., Radjenovic, J., 2023. Electrocatalytic removal of persistent organic contaminants at molybdenum doped manganese oxide coated TiO2 nanotube-based anode. Appl. Catal. B Environ. 334, 122831. https://doi.org/10.1016/j.apcatb.2023.122831

Sergienko, N., Radjenovic, J., 2020. Manganese oxide-based porous electrodes for rapid and selective (electro)catalytic removal and recovery of sulfide from wastewater. Appl. Catal. B Environ. 267, 118608. https://doi.org/10.1016/j.apcatb.2020.118608

Shan, D., Deng, S., Jiang, C., Chen, Y., Wang, B., Wang, Y., Huang, J., Yu, G., Wiesner, M.R., 2018. Hydrophilic and strengthened 3D reduced graphene oxide/nano-Fe3O4 hybrid hydrogel for enhanced adsorption and catalytic oxidation of typical pharmaceuticals. Environ. Sci. Nano 5, 1650–1660. https://doi.org/10.1039/c8en00422f

Sharif, F., Gagnon, L.R., Mulmi, S., Roberts, E.P.L., 2017. Electrochemical regeneration of a reduced graphene oxide/magnetite composite adsorbent loaded with methylene blue. Water Res. 114, 237–245. https://doi.org/10.1016/j.watres.2017.02.042

Shemella, P., Nayak, S.K., 2009. Electronic structure and band-gap modulation of graphene via substrate surface chemistry. Appl. Phys. Lett. 94, 32101. https://doi.org/10.1063/1.3070238

Shen, B., Wen, X. hua, Huang, X., 2017. Enhanced removal performance of estriol by a three-dimensional electrode reactor. Chem. Eng. J. 327, 597–607. https://doi.org/10.1016/j.cej.2017.06.121

Shi, H., Wang, Q., Ni, J., Xu, Y., Song, N., Gao, M., 2020. Highly efficient removal of amoxicillin from water by three-dimensional electrode system within granular activated carbon as particle electrode. J. Water Process Eng. 38, 101656. https://doi.org/10.1016/j.jwpe.2020.101656

Singh, S.P., Rathinam, K., Gupta, T., Agarwal, A.K., 2021. Nanomaterials and Nanocomposites for Environmental Remediation. Energy, Environ. Sustain., Energy, Environment, and Sustainability 1–4. https://doi.org/10.1007/978-981-16-3256-3_1

Siqueira, L.J.A., Urahata, S.M., Ribeiro, M.C.C., 2003. Molecular dynamics simulation of

molten sodium chlorate. J. Chem. Phys. 119, 8002–8012. https://doi.org/10.1063/1.1609983

Sopaj, F., Rodrigo, M.A., Oturan, N., Podvorica, F.I., Pinson, J., Oturan, M.A., 2015. Influence of the anode materials on the electrochemical oxidation efficiency. Application to oxidative degradation of the pharmaceutical amoxicillin. Chem. Eng. J. 262, 286–294. https://doi.org/10.1016/j.cej.2014.09.100

Sowmiya, S., Gandhimathi, R., Ramesh, S.T., Nidheesh, P.V., 2016. Granular activated carbon as a particle electrode in three-dimensional electrochemical treatment of reactive black B from aqueous solution. Environ. Prog. Sustain. Energy 35, 1616–1622. https://doi.org/10.1002/ep.12396

Staehelln, J., Hoigne, J., 1985. Decomposition of Ozone in Water in the Presence of Organic Solutes Acting as Promoters and Inhibitors of Radical Chain Reactions. Environ. Sci. Technol. 19, 1206–1213. https://doi.org/10.1021/es00142a012

Stirling, R., Walker, W.S., Westerhoff, P., Garcia-Segura, S., 2020. Techno-economic analysis to identify key innovations required for electrochemical oxidation as point-of-use treatment systems. Electrochim. Acta 338, 135874. https://doi.org/10.1016/j.electacta.2020.135874

Su, P., Zhou, M., Lu, X., Yang, W., Ren, G., Cai, J., 2019. Electrochemical catalytic mechanism of N-doped graphene for enhanced H2O2 yield and in-situ degradation of organic pollutant. Appl. Catal. B Environ. 245, 583–595. https://doi.org/10.1016/j.apcatb.2018.12.075

Sun, L., Wang, L., Tian, C., Tan, T., Xie, Y., Shi, K., Li, M., Fu, H., 2012. Nitrogen-doped graphene with high nitrogen level via a one-step hydrothermal reaction of graphene oxide with urea for superior capacitive energy storage. RSC Adv. 2, 4498–4506. https://doi.org/10.1039/c2ra01367c

Taqieddin, A., Nazari, R., Rajic, L., Alshawabkeh, A., 2017. Review—Physicochemical Hydrodynamics of Gas Bubbles in Two Phase Electrochemical Systems. J. Electrochem. Soc. 164, E448–E459. https://doi.org/10.1149/2.1161713jes

Thamilselvan, A., Govindan, K., Nesaraj, A.S., Maheswari, S.U., Oren, Y., Noel, M., James, E.J., 2018. Investigation on the effect of organic dye molecules on capacitive deionization of sodium sulfate salt solution using activated carbon cloth electrodes. Electrochim. Acta 279, 24–33. https://doi.org/10.1016/j.electacta.2018.05.053

Trotochaud, L., Andrus, R.M., Tyson, K.J., Miller, G.H., Welling, C.M., Donaghy, P.E., Incardona, J.D., Evans, W.A., Smith, P.K., Oriard, T.L., Norris, I.D., Stoner, B.R., Guest, J.S., Hawkins, B.T., 2020. Laboratory Demonstration and Preliminary Techno-Economic Analysis of an Onsite Wastewater Treatment System. Environ. Sci. Technol. 54, 16147–16155. https://doi.org/10.1021/acs.est.0c02755

Tu, Y., Lv, M., Xiu, P., Huynh, T., Zhang, M., Castelli, M., Liu, Z., Huang, Q., Fan, C., Fang, H., Zhou, R., 2013. Destructive extraction of phospholipids from Escherichia coli membranes by graphene nanosheets. Nat. Nanotechnol. 8, 594–601. https://doi.org/10.1038/nnano.2013.125

Unesco, World Water Assessment Programme, 2014. The United Nations world water development report 2014. Unesco 53, 1–189.

Vaghela, N.R., Nath, K., 2020. Reduced graphene oxide coated graphite electrodes for treating Reactive Turquoise Blue 21 rinse water using an indirect electro-oxidation process. SN Appl. Sci. 2, 1–14. https://doi.org/10.1007/s42452-020-03719-6

Villanueva Martinez, B., Odier, H., Coetsier, C., Groenen Serrano, K., 2023. Recent advances in sub-stoichiometric TiO2 as reactive electrochemical membranes (REM) for bio-refractory pollutants removal: A critical review. J. Environ. Chem. Eng. 11, 110203. https://doi.org/10.1016/j.jece.2023.110203

Vinet, L., Zhedanov, A., 2011. A “missing” family of classical orthogonal polynomials, Journal of Physics A: Mathematical and Theoretical. https://doi.org/10.1088/1751-8113/44/8/085201

Von Gunten, U., 2003. Ozonation of drinking water: Part I. Oxidation kinetics and product

formation. Water Res. 37, 1443–1467. https://doi.org/10.1016/S0043-1354(02)00457-8
Wang, B., Kong, W., Ma, H., 2007. Electrochemical treatment of paper mill wastewater using three-dimensional electrodes with Ti/Co/SnO2-Sb2O5 anode. J. Hazard. Mater. 146, 295–301. https://doi.org/10.1016/j.jhazmat.2006.12.031
Wang, B., Shi, H., Habteselassie, M.Y., Deng, X., Teng, Y., Wang, Y., Huang, Q., 2021. Simultaneous removal of multidrug-resistant Salmonella enterica serotype typhimurium, antibiotics and antibiotic resistance genes from water by electrooxidation on a Magnéli phase Ti4O7 anode. Chem. Eng. J. 407, 127134. https://doi.org/10.1016/j.cej.2020.127134
Wang, H., Mi, X., Li, Y., Zhan, S., 2020. 3D Graphene-Based Macrostructures for Water Treatment. Adv. Mater. 32, 1806843. https://doi.org/10.1002/adma.201806843
Wang, L., Wang, Y., Sui, Y., Lu, J., Hu, B., Huang, Q., 2022. Formation of chlorate and perchlorate during electrochemical oxidation by Magnéli phase Ti4O7 anode: inhibitory effects of coexisting constituents. Sci. Rep. 12, 1–8. https://doi.org/10.1038/s41598-022-19310-5
Wang, S.G., Gong, W.X., Liu, X.W., Yao, Y.W., Gao, B.Y., Yue, Q.Y., 2007. Removal of lead(II) from aqueous solution by adsorption onto manganese oxide-coated carbon nanotubes. Sep. Purif. Technol. 58, 17–23. https://doi.org/10.1016/j.seppur.2007.07.006
Wang, Y., De Carvalho, N.A., Tan, S., Gilbertson, L.M., 2019. Leveraging electrochemistry to uncover the role of nitrogen in the biological reactivity of nitrogen-doped graphene. Environ. Sci. Nano 6, 3525–3538. https://doi.org/10.1039/c9en00802k
Wang, Yilei, El-Deen, A.G., Li, P., Oh, B.H.L., Guo, Z., Khin, M.M., Vikhe, Y.S., Wang, J., Hu, R.G., Boom, R.M., Kline, K.A., Becker, D.L., Duan, H., Chan-Park, M.B., 2015. High-Performance Capacitive Deionization Disinfection of Water with Graphene Oxide-graft-Quaternized Chitosan Nanohybrid Electrode Coating. ACS Nano 9, 10142–10157. https://doi.org/10.1021/acsnano.5b03763
Wang, Yan, Guan, H., Du, S., Wang, Yude, 2015. A facile hydrothermal synthesis of MnO2 nanorod-reduced graphene oxide nanocomposites possessing excellent microwave absorption properties. RSC Adv. 5, 88979–88988. https://doi.org/10.1039/c5ra15165a
Wang, Ying, Wang, C., Wang, Yijing, Liu, H., Huang, Z., 2016. Boric Acid Assisted Reduction of Graphene Oxide: A Promising Material for Sodium-Ion Batteries. ACS Appl. Mater. Interfaces 8, 18860–18866. https://doi.org/10.1021/acsami.6b04774
Wang, Z., Liu, L., Zhang, Y., Huang, Y., Liu, J., Zhang, Xu, Liu, X., Teng, H., Zhang, Xiaofang, Zhang, J., Yang, H., 2023. A Review of Graphene-Based Materials/Polymer Composite Aerogels. Polymers (Basel). 15, 1888. https://doi.org/10.3390/polym15081888
Wei, L., Guo, S., Yan, G., Chen, C., Jiang, X., 2010. Electrochemical pretreatment of heavy oil refinery wastewater using a three-dimensional electrode reactor. Electrochim. Acta 55, 8615–8620. https://doi.org/10.1016/j.electacta.2010.08.011
Wenderich, K., Nieuweweme, B.A.M., Mul, G., Mei, B.T., 2021. Selective Electrochemical Oxidation of H2O to H2O2Using Boron-Doped Diamond: An Experimental and Techno-Economic Evaluation. ACS Sustain. Chem. Eng. 9, 7803–7812. https://doi.org/10.1021/acssuschemeng.1c01244
WHO/UNICEF, 2017. Progress on drinking water, sanitation and hygiene: 2017 update and SDG baselines. Available at: https://apps.who.int/iris/bitstream/handle/10665/258617/9789241512893-eng.pdf.
WHO, 2019. Safe Water, Better Health, World Health Organization.
World Health Organization, 2017. UN-Water global analysis and assessment of sanitation and drinking-water (GLAAS) 2017 report: financing universal water, sanitation and hygiene under the sustainable development goals, Who.
World Health Organization, 2014. UN-Water global analysis and assessment of sanitation and drinking-water (GLAAS) 2014 report: Investing in Water and Sanitation - Increasing access, reducing inequalities, World Health Organization. World Health Organization, Geneva PP - Geneva.
Xavier, J.R., Vinodhini, S.P., 2023. Fabrication of reduced graphene oxide encapsulated MnO2/MnS2 nanocomposite for high performance electrochemical devices. J. Porous

Mater. 30, 1897–1910. https://doi.org/10.1007/s10934-023-01473-9
Xiao, Y., Hill, J.M., 2019. Mechanistic insights for the electro-Fenton regeneration of carbon materials saturated with methyl orange: Dominance of electrodesorption. J. Hazard. Mater. 367, 59–67. https://doi.org/10.1016/j.jhazmat.2018.12.066
Xie, X., Zhou, J., Wang, T., 2020. Locally Enhanced Electric Field Treatment (LEEFT) promotes the performance of ozonation for bacteria inactivation by disrupting the cell membrane. Environ. Sci. Technol. 54, 14017–14025. https://doi.org/10.1021/acs.est.0c03968
Xie, Y., Chen, L., Liu, R., Tian, J., 2018. Reduction of AOX in pharmaceutical wastewater in the cathode chamber of bio-electrochemical reactor. Bioresour. Technol. 265, 437–442. https://doi.org/10.1016/j.biortech.2018.06.034
Xing, W., Liang, J., Tang, W., Zeng, G., Wang, X., Li, Xiaodong, Jiang, L., Luo, Y., Li, Xin, Tang, N., Huang, M., 2019. Perchlorate removal from brackish water by capacitive deionization: Experimental and theoretical investigations. Chem. Eng. J. 361, 209–218. https://doi.org/10.1016/j.cej.2018.12.074
Xiong, Y., He, C., An, T., Zhu, X., Karlsson, H.T., 2003. Removal of formic acid from wastewater using three-phase three-dimensional electrode reactor. Water. Air. Soil Pollut. 144, 67–79. https://doi.org/10.1023/A:1022931618033
Xu, B., Yue, S., Sui, Z., Zhang, X., Hou, S., Cao, G., Yang, Y., 2011. What is the choice for supercapacitors: Graphene or graphene oxide? Energy Environ. Sci. 4, 2826–2830. https://doi.org/10.1039/c1ee01198g
Xue, W., Hong, X., Du, Y., Chen, B., 2023. Electro-Fenton mineralization of real textile wastewater by micron-sized ZVI powder anode. Water Sci. Technol. 87, 924–937. https://doi.org/10.2166/wst.2023.032
Yadav, N., Dubey, A., Shukla, S., Saini, C.P., Gupta, G., Priyadarshini, R., Lochab, B., 2017. Graphene Oxide-Coated Surface: Inhibition of Bacterial Biofilm Formation due to Specific Surface-Interface Interactions. ACS Omega 2, 3070–3082. https://doi.org/10.1021/acsomega.7b00371
Yang, C., Fan, Y., Li, P., Gu, Q., Li, X., 2021. Freestanding 3-dimensional macro-porous SnO2 electrodes for efficient electrochemical degradation of antibiotics in wastewater. Chem. Eng. J. 422, 130032. https://doi.org/10.1016/j.cej.2021.130032
Yang, Y., Liu, T., Zhu, X., Zhang, F., Ye, D., Liao, Q., Li, Y., 2016. Boosting Power Density of Microbial Fuel Cells with 3D Nitrogen-Doped Graphene Aerogel Electrode. Adv. Sci. 3, 1600097. https://doi.org/10.1002/advs.201600097
Yu, F., Zhou, M., Yu, X., 2015. Cost-effective electro-Fenton using modified graphite felt that dramatically enhanced on H 2 O 2 electro-generation without external aeration. Electrochim. Acta 163, 182–189. https://doi.org/10.1016/j.electacta.2015.02.166
Yusufu Mohammed I., 2012. Chlorine adsorption kinetics of activated carbon from selected local raw materials. J. Chem. Eng. Mater. Sci. 3. https://doi.org/10.5897/jcems11.067
Zaky, A.M., Chaplin, B.P., 2013. Porous substoichiometric TiO2 anodes as reactive electrochemical membranes for water treatment. Environ. Sci. Technol. 47, 6554–6563. https://doi.org/10.1021/es401287e
Zang, X.J., Tong, S.P., Ma, C.A., 2009. Kinetic and mechanism of ozonation of terephthalic acid. Huanjing Kexue/Environmental Sci. 30, 1658–1662.
Zeng, X., Wang, G., Liu, Y., Zhang, X., 2017. Graphene-based antimicrobial nanomaterials: rational design and applications for water disinfection and microbial control. Environ. Sci. Nano 4, 2248–2266. https://doi.org/10.1039/c7en00583k
Zhan, J., Li, Z., Yu, G., Pan, X., Wang, J., Zhu, W., Han, X., Wang, Y., 2019. Enhanced treatment of pharmaceutical wastewater by combining three-dimensional electrochemical process with ozonation to in situ regenerate granular activated carbon particle electrodes. Sep. Purif. Technol. 208, 12–18. https://doi.org/10.1016/j.seppur.2018.06.030
Zhang, C., Jiang, Y., Li, Y., Hu, Z., Zhou, L., Zhou, M., 2013. Three-dimensional electrochemical process for wastewater treatment: A general review. Chem. Eng. J. 228, 455–467. https://doi.org/10.1016/j.cej.2013.05.033

Zhang, W., Yang, Y., Ziemann, E., Be'Er, A., Bashouti, M.Y., Elimelech, M., Bernstein, R., 2019. One-step sonochemical synthesis of a reduced graphene oxide-ZnO nanocomposite with antibacterial and antibiofouling properties. Environ. Sci. Nano 6, 3080–3090. https://doi.org/10.1039/c9en00753a

Zhang, Y., Song, Y., Zhao, J., Li, S., Li, Y., 2020. Ultrahigh electrocatalytic activity and durability of bimetallic Au@Ni core-shell nanoparticles supported on rGO for methanol oxidation reaction in alkaline electrolyte. J. Alloys Compd. 822, 153322. https://doi.org/10.1016/j.jallcom.2019.153322

Zhang, Y., Zhang, D., Zhou, L., Zhao, Y., Chen, J., Chen, Z., Wang, F., 2018. Polypyrrole/reduced graphene oxide aerogel particle electrodes for high-efficiency electro-catalytic synergistic removal of Cr(VI) and bisphenol A. Chem. Eng. J. 336, 690–700. https://doi.org/10.1016/j.cej.2017.11.109

Zhao, B., Liu, P., Jiang, Y., Pan, D., Tao, H., Song, J., Fang, T., Xu, W., 2012. Supercapacitor performances of thermally reduced graphene oxide. J. Power Sources 198, 423–427. https://doi.org/10.1016/j.jpowsour.2011.09.074

Zhao, C., Pandit, S., Fu, Y., Mijakovic, I., Jesorka, A., Liu, J., 2016. Graphene oxide based coatings on nitinol for biomedical implant applications: Effectively promote mammalian cell growth but kill bacteria. RSC Adv. 6, 38124–38134. https://doi.org/10.1039/c6ra06026a

Zhou, W., Meng, X., Gao, J., Zhao, H., Zhao, G., Ma, J., 2021. Electrochemical regeneration of carbon-based adsorbents: a review of regeneration mechanisms, reactors, and future prospects. Chem. Eng. J. Adv. 5, 100083. https://doi.org/10.1016/j.ceja.2020.100083

Zhou, W., Rajic, L., Zhao, Y., Gao, J., Qin, Y., Alshawabkeh, A.N., 2018. Rates of H2O2 electrogeneration by reduction of anodic O2 at RVC foam cathodes in batch and flow-through cells. Electrochim. Acta 277, 185–196. https://doi.org/10.1016/j.electacta.2018.04.174

Zhu, J., Xu, Y., Wang, J., Lin, J., Sun, X., Mao, S., 2015. The effect of various electrolyte cations on electrochemical performance of polypyrrole/RGO based supercapacitors. Phys. Chem. Chem. Phys. 17, 28666–28673. https://doi.org/10.1039/c5cp04080a

Zhu, X., Ni, J., Xing, X., Li, H., Jiang, Y., 2011. Synergies between electrochemical oxidation and activated carbon adsorption in three-dimensional boron-doped diamond anode system. Electrochim. Acta 56, 1270–1274. https://doi.org/10.1016/j.electacta.2010.10.073

[1] Carballa, M., Fink, G., Omil, F., Lema, J.M., Ternes, T., 2008. Determination of the solid-water distribution coefficient (Kd) for pharmaceuticals, estrogens and musk fragrances in digested sludge. Water Res. 42, 287–295. https://doi.org/10.1016/j.watres.2007.07.012.

[2] Röhricht, M., Krisam, J., Weise, U., Kraus, U.R., Düring, R.A., 2009. Elimination of carbamazepine, diclofenac and naproxen from treated wastewater by nanofiltration. Clean - Soil, Air, Water 37, 638–641. https://doi.org/10.1002/clen.200900040

[3] Hennebel, T., De Corte, S., Vanhaecke, L., Vanherck, K., Forrez, I., De Gusseme, B., Verhagen, P., Verbeken, K., Van der Bruggen, B., Vankelecom, I., Boon, N., Verstraete, W., 2010. Removal of diatrizoate with catalytically active membranes incorporating microbially produced palladium nanoparticles. Water Res. 44, 1498–1506. https://doi.org/10.1016/j.watres.2009.10.041

[4] Yang, X., Flowers, R.C., Weinberg, H.S., Singer, P.C., 2011. Occurrence and removal of pharmaceuticals and personal care products (PPCPs) in an advanced wastewater reclamation plant. Water Res. 45, 5218–5228. https://doi.org/10.1016/j.watres.2011.07.026

[5] Mandal, S., 2018. Reaction Rate Constants of Hydroxyl Radicals with Micropollutants and Their Significance in Advanced Oxidation Processes. J. Adv. Oxid. Technol 21, 178-195. https://doi.org/10.26802/jaots.2017.0075

[6] Ning, B., Graham, N.J., 2008. Ozone Degradation of Iodinated Pharmaceutical Compounds. J. Environ. Eng. 134, 944–953. https://doi.org/10.1061/(asce)0733-9372(2008)134:12(944)

[7] Huber, M.M., Canonica, S., Park, G.Y., Von Gunten, U., 2003. Oxidation of pharmaceuticals during ozonation and advanced oxidation processes. Environ. Sci. Technol. 37, 1016–1024. https://doi.org/10.1021/es025896h
[8] Benitez, F.J., Acero, J.L., Garcia-Reyes, J.F., Real, F.J., Roldan, G., Rodriguez, E., Molina-Díaz, A., 2013. Determination of the reaction rate constants and decomposition mechanisms of ozone with two model emerging contaminants: DEET and nortriptyline. Ind. Eng. Chem. Res. https://doi.org/10.1021/ie402916u
[9] Wendel, F.M., Lütke Eversloh, C., Machek, E.J., Duirk, S.E., Plewa, M.J., Richardson, S.D., Ternes, T.A., 2014. Transformation of iopamidol during chlorination. Environ. Sci. Technol. 48, 12689–12697. https://doi.org/10.1021/es503609s
[10] Lee, Y., von Gunten, U., 2010. Oxidative transformation of micropollutants during municipal wastewater treatment: Comparison of kinetic aspects of selective (chlorine, chlorine dioxide, ferrateVI, and ozone) and non-selective oxidants (hydroxyl radical). Water Res. 44, 555–566. https://doi.org/10.1016/j.watres.2009.11.045
[11] Acero, J.L., Benitez, F.J., Real, F.J., Roldan, G., Rodriguez, E., 2013. Chlorination and bromination kinetics of emerging contaminants in aqueous systems. Chem. Eng. J. 219, 43–50. https://doi.org/10.1016/j.cej.2012.12.067